Universitat Autònoma de Barcelona

The value of using chitosan based implant with microfractures for treatment of acetabular cartilage lesions associated with femoroacetabular impingement

MAHMOUD FATHY TAHOUN

Universitat Autònoma de Barcelona

The value of using chitosan based implant with microfractures for treatment of acetabular cartilage lesions associated with femoroacetabular impingement

Thesis

Submitted for fulfillment of Doctorate Degree

By

MAHMOUD FATHY TAHOUN

Supervisors

Dr. *Marc Tey Pons*

Dr. *Hatem Galal Said*

Tutor

Dr. *Joan Carles Monllau Garcia*

FACULTAT DE MEDICINA

DEPARTAMANT DE CIRURGIA

Programa de Doctorat: CIRURGIA I CIÈNCIES MORFOLÒGIQUES

2020

This doctoral thesis entitled:

The value of using Chitoasn based implant with microfracture for treatment of acetabular cartilage lesions associated with femoroacetabular impingement (in English*),*
*El valor de la utilització d'implants basats en Chitosan combinats amb microfractures per el tractament de lesions del cartílag de la còtila associats amb el xoc femoroacetabular (*en català*),*
*El valor de la utilización de implantes basados en Chitosan con microfracturas para el tratamiento de lesiones del cartílago acetabular asociados con el choque femoroacetabular (*en castellano*);*

has been presented in the form of compendium of articles under the regulations of Universitat Autònoma de Barcelona and fulfillment of the requirements of the Surgery and Morphological Sciences PhD Academic Board including the following two publications:

Tahoun MF, Tey M, Mas J, Abd-Elsattar Eid T, Monllau JC. Arthroscopic Repair of Acetabular Cartilage Lesions by Chitosan-Based Scaffold: Clinical Evaluation at Minimum 2 Years Follow-up. Arthroscopy. 2018; 34(10).
Journal Title: Arthroscopy: The Journal of Arthroscopic & Related Surgery
DOI: https://doi.org/10.1016/j.arthro.2018.06.037

and

Tahoun MF, Tey M, Ormazabal I, ElSayed AS, Said HG, Monllau JC. Promising radiological outcome after repair of acetabular chondral defects by microfracture augmented with chitosan-based scaffold: mid-term T2 mapping evaluation. Knee Surgery, Sport Traumatol Arthrosc. 2020
Journal Title: Knee Surgery, Sports Traumatology, Arthroscopy
DOI: https://doi.org/10.1007/s00167-020-06068-4

ACKNOWLEDGMENT

I am greatly indebted and sincerely felt gratitude to my mentor; *Dr. Joan Carles Monllau* for his guidance, help and sincere supervision. He offered me much of his experience that constituted the corner stone in the building up of this thesis.

I am grateful and deeply thankful to *Dr. Marc Tey* for offering me his knowledge and experience so generously; step-by-step and hand-by-hand, refining my skills of the clinical practice as well as the scientific research.

Special thanks go to *Dr. Jesus Mas* and *Dr. Inmacolada Ormazabal*, for their valuable role in collecting the material and data of this study. Their contributions are greatly appreciated.

I would like to express my great appreciation to *Dr. Hatem Said*, for his constructive suggestions during the planning and development of this research work.

My grateful thanks are also extended to all the staff members, residents, and nurses of orthopedic departments in *Parc De Salut Mar* Hospitals for the unlimited help and the enthusiastic encouragement.

CONTENTS

INTRODUCTION

Femoroacetabular impingement (FAI) is a clinical syndrome recognized as a source of mechanical hip pain and a cause of secondary osteoarthritis[1]. There are 2 types of FAI, as described by *Ganz et al* [2], based on bone morphology patterns. The Cam-type is characterized by an alteration at the femoral head-neck junction, while the Pincer-type occurs with acetabular alteration, which leads to an abnormal overcoverage of the femoral head. However, in most of the cases there is a combination of both conditions, known as mixed-type FAI [2].

Acetabular cartilage damage occurs in association with FAI due to the abnormal contact throughout the range of motion of the hip, mostly in the anterosuperior area, leading to chondral delamination and labral tears [3,4]

The articular cartilage has a poor intrinsic healing capacity, so several techniques have been developed to potentiate the cartilage healing and reproduce a new tissue with structural and biomechanical properties similar to the normal cartilage [5,6]. Debridement and microfracture , as easily performed and cost-effective techniques, are considered standard methods for small full-thickness defect [7].

Scaffold augmentation techniques have emerged to enhance the biomechanical and biochemical properties of cartilage repair tissue after microfracture [8–10]. Chitosan-based scaffold material has been introduced to the clinical application after extensive animal studies which showed promising results regarding the histological and biomechanical properties of the cartilage repair tissue compared to the native cartilage [8–11].

MORPHOLOGY OF THE NORMAL HIP JOINT

Depending on the types of joints, the hip represents a “ball and socket” synovial joint with the femoral head is a ball which fits into the acetabulum as a deep socket.[12]

Acetabulum

The pediatric acetabulum is formed by the confluence of the ilium, ischium, and pubis with the triradiate cartilage complex, a Y-shaped synchondrosis, at the center of these bones. according to this pattern of development, a wide variation and complexity in the acetabular morphology may occur[13].

In normal hips, the acetabulum is anteverted and inclined in abduction [14,15]. Different studies showed torsional change of anteversion in the caudal part of the acetabulum to retroversion of the cranial part [16, 17,18].

The acetabular cavity is a horse shoe-like articular surface (lunate surface), incompletely surrounding a quadrangular non-articular area referred to as the acetabular (Cotyloid) fossa which occupies the inferior portion of the acetabulum. The lower third of the fossa is filled with adipose tissue rich in capillaries. At the inferior border of the acetabular fossa, the acetabular rim forms the acetabular notch which is covered by the transverse acetabular ligament [19,20].

Proximal femur

The femoral head makes up approximately two-thirds of a sphere, and is oriented medially, superiorly and anteriorly. On the articular surface, where the lower third joins the upper thirds, there is a small wrinkled depression called the fovea capitis femoris that holds the round ligament of the femur (ligamentum teres) which extends to the inferior acetabular rim [12].

Labrum

The acetabular labrum is a horseshoe-shaped fibrocartilaginous structure attached to the peripheral bony margin of the acetabulum, with the anterior and posterior horns are connected inferiorly to the transverse acetabular ligament which

completes the ring shape [21]. The shape and size of the labrum varies gently throughout its circumference being widest anteriorly with average width measured 5.4-7.4 mm, relatively higher than the other points (4.0 to 6.8 mm), while thickness is maximum superiorly (4.9-5.5 mm) , where maximum weight bearing occurs [22,23].

Most of the labrum is composed of thick, type I collagen fiber bundles principally arranged parallel to the acetabular rim[24]. Histological examination by *Seldes et al* [22] demonstrated that the labrum merged with the articular hyaline cartilage through a transition zone of 1 to 2 mm. A consistent thin tongue of bone extended from the edge of the bony acetabulum into the substance of the labrum with firm attachment via a zone of calcified cartilage and a well-defined tidemark at the articular side, not the outer side.

Capsular-ligamentous structures of the hip joint

Proximally, the capsule is attached at a mean 5.1 mm proximal to the bony acetabular rim, just beyond the labrum, continuous with the periosteum [25]. Distally, the anterior fibers of the capsule were firmly attached to the femur at the intertrochanteric line. The posterior fibers of the capsule did not have a direct osseous distal insertion on the femur; instead, the arcuate fibers of the zona orbicularis form an arched free border [25,26].

Cadaveric studies showed that the capsule can be differentiated into two layers, internal and external fibers. The internal fibers run in a circular fashion and are tightly organized in the middle area to form the zona orbicularis which appears grossly a collar around the femoral neck, and they are lined by the synovium that touches the femoral head. The external fibers run longitudinally and are defined anatomically as the iliofemoral, pubofemoral and ischiofemoral ligaments [27,28]

Blood supply to the hip joint

Collectively, the blood supply to the hip joint comes from internal iliac artery and femoral artery; however there are specific patterns of vascularization to each structure in the hip joint [12,29,30,31].

The pelvic surface of the acetabulum receives branches of the iliolumbar artery which arises from the posterior trunk of the internal iliac artery. From outside the pelvis, the acetabulum receives the main nutrient branch of the superior gluteal artery, and multiple nutrient vessels around the margins of the acetabulum form a complete vascular circle from the obturator, superior gluteal and inferior gluteal artery. The cotyloid fossa is perforated by a number of small vessels from the acetabular branch of the obturator artery [32,33]

The blood supply to the femoral head and neck derives from three main arterial systems: retinacular, foveolar and intraosseous communication with the femoral shaft ; however it is well accepted that the retinacular arteries are the major source in all ages [34,35,36]. There are two constant groups of retinacular arteries arise from the deep branch of medial femoral circumflex artery (MFCA): the superior, or the posterosuperior, group of arteries which dominantly supply most of the head including the lateral weight bearing portion and the inferior, or posteroinferior, group which constantly contribute in vascularity of the head [37–41]. One or, less frequently, two small arteries of the ligamentum teres “Foveolar vessels” usually spring from branches of the obturator artery, or from the medial femoral circumflex artery or from both[31,34–36,39,42,43].

STRUCTURE OF ARTICULAR CARTILAGE

Unlike most tissues, articular cartilage does not have blood vessels, nerves, or lymphatics. It is composed of a dense extracellular matrix (ECM) with a sparse distribution of highly specialized cells called chondrocytes.

Extracellular Matrix (ECM)

The ECM is principally composed of water, collagen, and proteoglycans, with other noncollagenous proteins and glycoproteins present in lesser amounts. Water is the most abundant component of articular cartilage, contributing to 60-80% of its wet weight [44,45]. Inorganic ions such as sodium, calcium, chloride, and potassium are dissolved in the tissue water [46,47].

Collagen is the most abundant structural macromolecule in ECM, and it makes up about 15-22% of the wet weight and about 50-80% of the dry weight of cartilage. Type II collagen represents 90% to 95% of the collagen in ECM, and other collagen types are also present with a minor proportion [48–50]. Proteoglycans are heavily glycosylated protein monomers, represent the second-largest group of macromolecules in the ECM [49,50,51].

Chondrocytes

The chondrocyte is the resident cell type in articular cartilage functioning in the development, maintenance, and repair of the ECM. Chondrocytes originate from mesenchymal stem cells and constitute about 1-2% of the total volume of articular cartilage [48,52]. Each chondrocyte is entrapped in the chondron, a complex microanatomical unit containing a heterogeneous mixture of matrix macromolecules. The pericellular microenvironment produced around each chondron essentially prevents any migration of the chondrocyte to adjacent areas of cartilage, so rarely to find cell-to-cell chondrocytes contact. Chondrocytes have limited potential for replication, a factor that contributes to the limited intrinsic healing capacity of cartilage in response to injury[52,53].

Organization of the Articular Cartilage

Four different zones have been identified, located from the articular surface to subchondral bone: superficial zone, transitional (middle) zone, deep zone, and the calcified cartilage zone [52].

Superficial (Tangential) zone

The superficial zone is the thinnest (10–20% thickness) and consists of two layers: the first layer, closest to the articular surface, is acellular and is comprised of a sheet of fine fibrous material; the second layer consists of flat chondrocytes with their long axis parallel to the cartilage surface. The collagen fibers are aligned parallel to the joint surface [54,52,55].

This zone is in contact with synovial fluid and is responsible for most of the tensile properties of cartilage, which enable it to resist the sheer, tensile, and compressive forces. The integrity of this layer is essential in the protection and maintenance of deeper layers [56].

Middle (Transitional) zone

The middle zone provides an anatomic and functional bridge (transitional) between the superficial and deep zones. The middle zone represents 40% to 60% of the total cartilage volume, and it contains higher concentration of proteoglycans and larger diameter of collagen fibrils. In this layer, the collagen is organized obliquely, and the chondrocytes are spherical and show more synthetic organelles, endoplasmic reticulum and Golgi membrane than the superficial zone [50,52,55].

Deep zone

The deep zone represents approximately 30% of articular cartilage volume. It contains the largest diameter collagen fibrils, the highest proteoglycan content, and the lowest water concentration. The collagen fibrils are arranged perpendicular to the articular surface. The chondrocytes are typically more round in shape, arranged in columnar orientation, parallel to the collagen fibers and perpendicular to the joint line. The deep zone is responsible for providing the greatest amount of resistance to compressive forces because of the high proteoglycan content and the perpendicular

orientation of collagen fibrils to the articular surface. The tide mark distinguishes the deep zone from the calcified cartilage [50,52,55].

A wavy tidemark of basophilic matrix separates the deep zone from the calcified cartilage zone. Thick collagen bundles of the deep zone cross the tidemark and insert into the calcified cartilage providing a strong anchoring system for the cartilage on to the subchondral bone [50,57].

Calcified cartilage zone

The calcified zone marks the transition from a soft layer to a stiff layer, and plays an integral role in securing the cartilage to bone. Chondrocytes in this zone are surrounded by a calcified matrix and have a small volume and a small amount of intracellular organelles suggesting that they have an extremely low metabolic activity. Mineral content and thickness of calcified cartilage increase with age and in osteoarthritis. This zone transfers joint forces from the cartilage to the underlying subchondral bone through the vertically oriented collagen fibrils [50,52,57,58].

The subchondral bone is interdigitated with calcified cartilage, except that the fibers do not extend from the calcified zone to the bone. Subchondral bone can be classified into two types: the subchondral bone plate, cortical bone; immediately located below the cartilage with low porosity and vascularity, followed by the subchondral trabecular bone further beneath, which contains trabeculae oriented in random directions [58].

FEMOROACETABULAR IMPINGEMENT (FAI)

The concept of femoroacetabular impingement (FAI) has been clearly formulated by professor *Ganz* and colleagues. they described FAI occurring in the native hip as a precursor to the development of osteoarthritis [2].

Bony Morphology of FAI

The Femur: Cam FAI

The general character of cam-type deformity is loss of normal sphericity and obliteration of the normal concavity at the head-neck junction leading to premature contact with the acetabular rim [59].

Although the exact etiology of a cam-type deformity is not well understood, suggested causes are bone remodeling, a growth abnormality of the epiphysis, and consequences of childhood diseases [60–62]. The idiopathic cam type deformity has been thought to occur as an extension of the epiphysis towards the anterosuperior portion of the femoral neck triggered by environmental factors such as high-level sports activity during childhood and around the time of closure of the capital growth plate [60,63,64].

Malunion following femoral neck fracture, particularly subcapital and transcervical, may produce retroversion of the femoral neck potentially giving rise to a cam-type deformity[65,66]. Slipped capital femoral epiphysis (SCFE) is a common adolescent hip disorder which predisposes to development of cam-type deformity [67,68]. Legg-Calve-Perthes Disease leads to femoral head asphericity and hip joint incongruence.

The Acetabulum: Pincer FAI

Pincer-type FAI is an abnormal acetabular morphology producing encroachment of the acetabular rim beyond the motion area of the femoral head. This acetabular abnormality leads to either a focal or a generalized overcoverage of the femoral head [2]. Retroversion of the cranial part of the acetabulum represents the simple form of focal anterior overcoverage as the anterior acetabular rim appears more

prominently lateral to the posterior rim [69,70]. Global retroversion may involve the whole acetabulum in the form of dysplasia with deficiency in the posterior wall [71].

Generalized overcoverage occurs in the sever form of pincer-type FAI associated with coxa profunda and protrusio acetabula. In these conditions, the femoral head is deeply located in the deepened acetabular socket, and the acetabular rim circumferentially contact the head-neck junction producing global pincer FAI [69,72,73]. Os acetabuli is an intra-articular osseous fragment originating from the anterolateral acetabular rim, and it has been reported as a source of pincer-type FAI [74–76].

Patterns of damage associated with FAI

As the Cam lesion rotates within the acetabular rim, compressive forces and shear stress at the cartilage-bone interface increase, resulting in delamination of the chondral surface from the underlying bone and producing the so called 'wave sign' visible at arthroscopy. The injury progresses when the cartilage fails at the chondro-labral junction. Loss of continuity at the chondro-labral junction exposes the edge of the chondral surface to the advancing 'front' of the femoral cam lesion, and result in the creation of chondral flap tears. As this acetabular cartilage injury enlarges, reciprocal damage to the femoral head may be induced by contact with the irregular acetabular surface leading to the end result of an osteoarthritic hip [77,78](**Figure 1**).

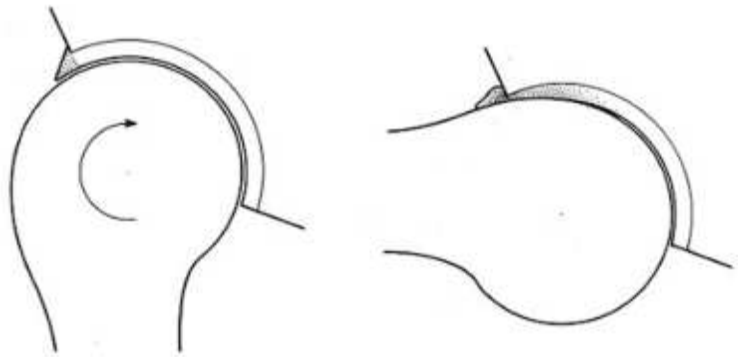

Figure 1: Diagram of the mechanism of damage in cam impingement (*Republished with permission of British Editorial Society of Bone & Joint Surgery from Beck M, Kalhor M, Leunig M, Ganz R. Hip morphology influences the pattern of damage to the acetabular cartilage. Femoroacetabular Impingement As A Cause Of Early Osteoarthritis Of The Hip. J Bone Jt Surg [Br]. 2005;87(7):1012-1018; permission conveyed through Copyright Clearance Center,Inc.)*.

Hips with pincer-type deformities exhibit a different pattern of cartilage injury. The area of abutment between the femoral neck and acetabular rim is more circumferential and peripheral; so the compressive forces are limited to a narrow streak along the acetabular rim only. Frequent impactions during flexion produce a narrow band of malacia along the anterosuperior rim. The point of anterosuperior contact serves as a fulcrum by which the head of the femur is elevated out of the acetabulum and impacts against posteroinferior region of the acetabulum producing a contre-coup cartilage lesion [79,80](**Figure 2**).

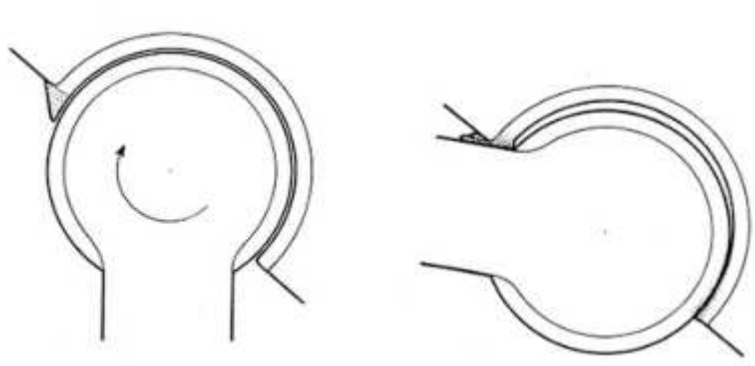

Figure 2: Diagram of the mechanism of damage in pincer impingement (*Republished with permission of British Editorial Society of Bone & Joint Surgery from Beck M, Kalhor M, Leunig M, Ganz R. Hip morphology influences the pattern of damage to the acetabular cartilage. Femoroacetabular Impingement As A Cause Of Early Osteoarthritis Of The Hip. J Bone Jt Surg [Br]. 2005;87(7):1012-1018; permission conveyed through Copyright Clearance Center,Inc.)*.

When impingement occurs at the anterosuperior rim and further flexion is enforced, the femoral head begins to translate posteriorly and, because of the constrained nature of the hip, increased pressure between the posteromedial aspect of the femoral head and the posteroinferior acetabulum occurs. This “contre-coup” lesion was observed in the cartilage of femoral head in 62% and in the posteroinferior acetabulum in 31% [4,69].

Grading systems

The *Outerbridge* [81,82] **(Table 1)** and *Beck et al* [79] (**Table 2**)[69,83], grading systems have been established to introduce a quantitative and qualitative evaluation for the actual condition of the articular cartilage at a certain time, providing a guide for management and proper method for follow-up [84].

Table 1: The Outerbridge classification system

Grade	Description
Grade 1	Cartilage softening and swelling
Grade 2	Fragmentation and fissuring in an area ≤ ½ an inch in diameter
Grade 3	Fragmentation and fissuring in an area > ½ an inch in diameter
Grade 4	Erosion of cartilage down to bone

Table 2: Beck's modified classification system of acetabular chondral defects

Grade	Description	Criteria
Grade 0	Normal	Macroscopically sound cartilage
Grade 1	Malacia	Roughening of surface, fibrillation
Grade 2	Debonding	Loss of fixation to the subchondral bone, macroscopically sound cartilage; carpet phenomenon
Grade 3	Cleavage	Loss of fixation to the subchondral bone; frayed edges, thinning of the cartilage, flap
Grade 4	Defect	Full-thickness defect

Localizing the site of the injury

The clock-face method has long been used as the standard for describing the anatomical features and, later, for the intra-articular hip pathology on the acetabulum and the acetabular rim[20,85,86]. When used adequately, it places the 6-o'clock position at the center of the transvers acetabular ligament and the 12-o'clock position on the most lateral aspect of the rim opposite to the 6-o'clock position [69,79,87,88]. In the case of a right hip, the anterior acetabulum is located between 1 and 5 o'clock; while for a left hip, the anterior acetabulum is located between 7 and 11 o'clock.

Ilizaliturri et al.[89] developed an alternative method to divide the acetabulum into 6 different zones based on anatomic landmark, the acetabular fossa, clearly visible during arthroscopy. Two vertical imaginary lines that follow the anterior and posterior limits of the acetabular fossa divide the acetabulum into 3 sections. A horizontal line perpendicular to the previous lines is placed at the superior limit of the fossa dividing the acetabulum into a superior and inferior half. The resulting 6 zones are given numbers as shown in **Figure 3**. They applied same system to the femoral head with considering the area around the ligamentum teres corresponds to the acetabular fossa, and the same imaginary lines are then positioned on the femoral head following the same pattern used for the acetabulum. On the head, zones 2, 3, and 4 are subdivided into medial, superior, and lateral referring to the covering of the

femoral head in a neutral position (**Figure 3**). The numbers assigned for acetabular and head zones are the same for right as well as left hip.

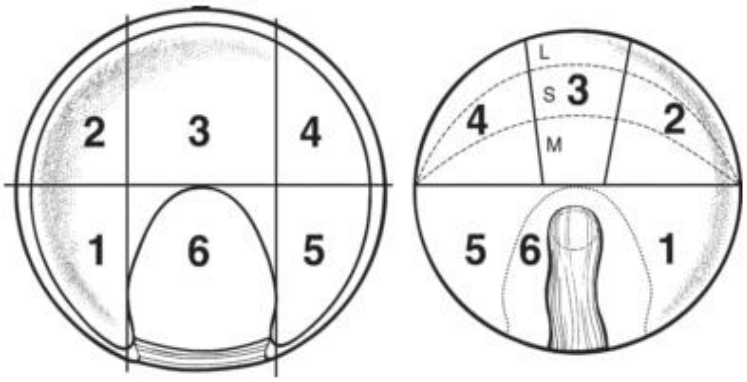

Figure 3: The acetabular zones are to the left and the femoral head is to the right of the picture (*Reprinted from Ilizaliturri VM, Byrd JWTT, Sampson TG, et al. A Geographic Zone Method to Describe Intra-articular Pathology in Hip Arthroscopy: Cadaveric Study and Preliminary Report. Arthroscopy.2008;24(5):534-539.,Copyright 2008 ,with permission from Elsevier).*

Cartilage imaging

Detection of chondral defects in the hip joint is particularly difficult on MRI due to the curved, tightly opposed surfaces of the acetabulum and head, and the relatively thin cartilage over both surfaces [90,91].

Intra-articular injection of contrast fluid distends the joint, and then acetabular chondral delamination can be clearly seen as elongated high signal interposed between the subchondral plate and the overlying cartilage. Cartilage flap can also appear as inverted “Oreo” cookie sign when low signal cartilage flap is “sandwiched” between two high signals, the deep contrast high signal and the superficial joint fluid[91].

The biochemical imaging of dGEMRIC is specified for quantitative analysis of the articular cartilage, it allows measuring the GAG concentration indirectly in cartilage, however the long imaging time needed by the technique and the contrast-related systemic side effects limit its clinical applicability [92]. T2 mapping offers another quantitative method to detect subtle cartilage changes without applying contrast

material. This imaging technique can detect any alteration of cartilage water content and collagen fiber orientation. T2 mapping assesses the degree of loss of collagen fiber orientation and subsequent increased mobility of water in the matrix[93–95]. Beside the safety of avoiding contrast injection and the advantage of faster scanning time, T2 mapping has been recommended for evaluation of cartilage repair because of its ability to estimate the restoration of articular zonal structure [96,97].

Arthroscopic Treatment of FAI

The goals of FAI surgery are to eliminate the pathologic contact between the femoral head and neck and the acetabular rim, to alleviate impingement symptoms, and to prevent further damage to the labrum and cartilage [87].

Rim trimming for pincer impingement: Acetabuloplasty

The goal should be to remove excessive overcoverage and leave a Wiberg angle of at least 25°. On the other hand, if there is acetabular retroversion, resection of too much anterior rim to eliminate a crossover sign could result in iatrogenic instability [87,98,99].

Preservation of the labrum is preferred whenever possible, but if labral degeneration is extensive or labral damage is not salvageable, then it should be managed with simple debridement [98,100–102]. If a large resection is planned such that the articular cartilage becomes redundant, a labral takedown should be performed to remove cartilage overlying the rim. If the planned resection is small, the rim trimming is performed without labral takedown[87].

Treatment of associated cartilage damage

The management of damage to articular cartilage is a significant challenge owing to the very limited ability of the cartilage to heal. Various methods of treatment have been described, but the first step is the proper assessment of the extent and depth of the lesion [103–105].

Chondroplasty:

Partial-thickness defects are generally treated with chondroplasty, involving debridement of the defect to remove any damaged cartilage and create a smooth

surface. The chondroplasty should be performed carefully with a full radius shaver with or without arthroscopic biters [7,105]. Thermal chondroplasty has been described to have advantages of sealing of the fibrillation, and stabilizing the edges of lesions and decreasing the risk of propagation to a full-thickness lesion [106,107].

Microfracture:

Microfracture technique depends on bone marrow stimulation by penetration of the subchondral bone plate within the cartilage defect which leads to bleeding and subsequent fibrin clot formation, filling the defect and covering the exposed bony surface. Pluripotent, marrow-derived mesenchymal stem cells then migrate into the clot and promote the formation of a fibrocartilaginous repair tissue [5,52,108]. The calcified cartilage layer should be adequately removed while maintaining the integrity of the subchondral plate to make a rough, raw surface that can hold the clot [109].

Scaffold augmentation:

The resulting repair of microfracture is typically fibrocartilaginous or fibrous tissue types with weak biomechanical properties and reduced wear capacity compared to hyaline cartilage, which contains high levels of collagen type II and glycosaminoglycans (GAGs). When the defect is large in size, the fibrocartilage repair patch tends to shrink over time and separates from the surrounding [9,110].

Different scaffold materials, such as poly-glycolic acid (PGA)/ hyaluronan, chitosan-glycerol phosphate blood and chondroitin sulfate/hydrogel composites, have been studied in animal trials and showed a significant improvement in the mechanical properties of repair tissue [8–11]. Clinical trials of chitosan-based scaffold for treating chondral defects in the femoral condyle of human knees demonstrated adequate safety for clinical practice, and presented favorable histological and functional results [111,112].

The surgical technique of application of chitosan-based scaffold in the hip has been described by *Tey et al* [113]. The authors recommend the technique for isolated full-thickness acetabular defects larger than 2cm^2 after adequate debridement and microfracture based on *Steadmann's* method.

Treatment of Cam Impingement: Femoroplasty

Adequate visualization of the cam lesion within the peripheral compartment is essential, therefore a T-shaped capsulotomy is recommended, and the fluoroscopy is frequently used during the procedure [98,114,115].

The lateral and medial synovial folds should be identified as the arthroscopic landmarks for the retinacular vessels, approximately at 12 and 5:30 o'clock position respectively , and care must be taken to preserve these structures which are considered the limits during resection [98,99,114,116].

AIM OF THE WORK

The purpose of this work was to evaluate the mid-term results of using the chitosan-based scaffold material with bone marrow stimulation for treatment of large full-thickness acetabular chondral defects associated with femoroacetabular impingement (FAI) in young active patients.

The plan was to perform a full correction of the FAI components, and specifically treat the large full-thickness acetabular chondral defects by chitosan based scaffold material after microfracture through a single-stage arthroscopic surgery. The quality of cartilage repair was evaluated by specific biochemical techniques of magnetic resonance imaging (MRI) after minimum 2 years.

We hypothesized that the performed procedures can achieve the following:

- Correction of the Cam and Pincer morphologies and consequently restoration of the normal biomechanics of the hip joint can improve the patients' symptoms and hip functions over the early postoperative period.
- Proper treatment of the cartilage defects will be reflected on the clinical outcomes after 2 years, so the patient reported outcome scores will maintain increased over the baseline at the mid-term follow-up.
- MRI studies will show favorable interpretation of the cartilage-specific T2 values of the repair tissue in comparison to the native articular cartilage of the same joint.

MATERIAL AND METHODS

This work was conducted in the orthopedic department of university hospitals of Universitat Autònoma de Barcelona (Parc de Salut Mar and Hospital Universitari Dexeus) during the period from April 2015 to April 2018.

Population of the study

This study was concerned in the young active patients who were diagnosed to have femoroacetabular impingement (FAI) associated with acetabular chondral lesion. Diagnosis of the condition was performed clinically and confirmed by radiological investigation.

Clinical diagnosis

Groin pain during hip motion was considered the primary presentation for FAI. The C-sign for localizing the pain around the affected hip was considered the main symptom, however lateral and posterior locations were not excluded. Other mechanical symptoms, such as clicking or catching of the hip, were suggestive for unstable intra-articular injury as labral or chondral lesion.

Physical examination included gait testing to detect abnormal gait patterns such as the abductor-deficient gait or antalgic gait, excessive internal or external rotation, short leg limp, and abnormal foot progression. Trendelenburg test and measurements of the limb length were performed

Range of motion (ROM) was examined actively then passively with comparison between both sides. Internal and external rotation ROM were performed passively in a supine position with the hip flexed at 90° and with the hip extended, performed in a prone position.

The following Provocative Tests were performed: Impingement test, Decompression test, Flexion/Adduction/Internal Rotation (FADIR), Flexion/Abduction/External Rotation (FABER), Dynamic Internal Rotatory Impingement Test (DIRI), Dynamic External Rotatory Impingement Test (DEXRI), and Dial Test.

Radiological diagnosis:

<u>Plain X-ray:</u>

Views**:**

- Standard anteroposterior (AP) view of the pelvis and both hips
- Dunn lateral view of both hips (performed with hip flexion of 45° and abduction of 20°). Cross-table or frog-leg lateral views were also used.

Cam deformity was diagnosed by:

- Measuring the alpha angle > 55° in the Dunn lateral view (**Figure 4A**).
- Head-Neck offset < 10mm in the Dunn lateral view (**Figure 4B**).

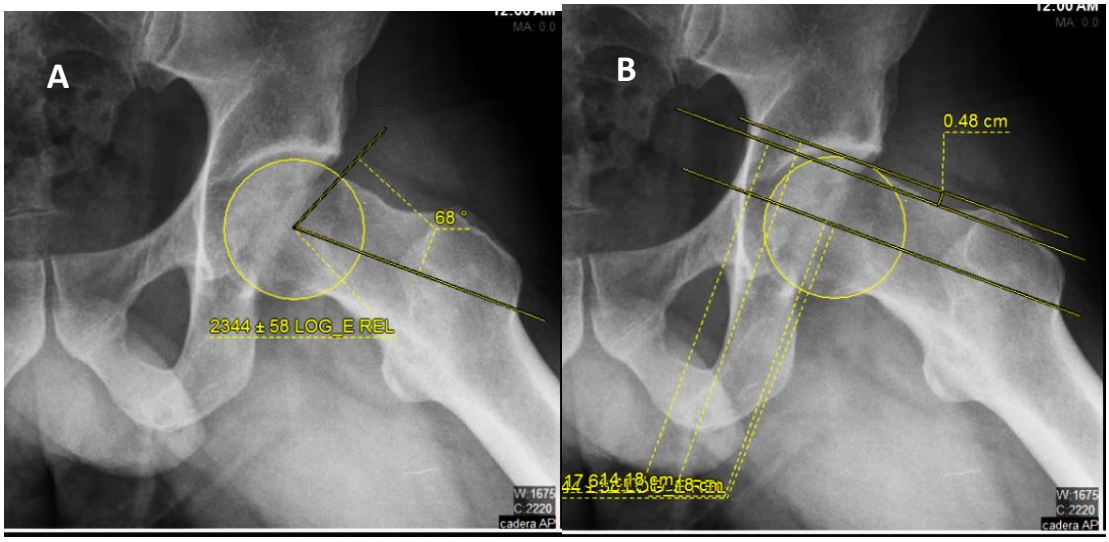

Figure 4: detailed radiograph of left hip in Dunn 45° view showing, A. measurement of the alpha angle (68°), and B. measurement of the H-N offset (4.8mm)

Pincer deformity was diagnosed by:

- Cross-over sign: (**Figure 5A)**.
- Posterior wall sign (**Figure 5 C)**.
- Ischial spine sign (**Figure 5 C)**.
- Os acetabuli: (**Figure 5 D)**.
- Coxa profunda, (**Figure 5 B**) or protrusio acetabuli

➢ Acetabular dysplasia was excluded if :

- Lateral Center edge (LCE) angle of Wiberg < 25° (**Figure 6 A**)
- Acetabular index of Tönnis > 10° (**Figure 6 B**)

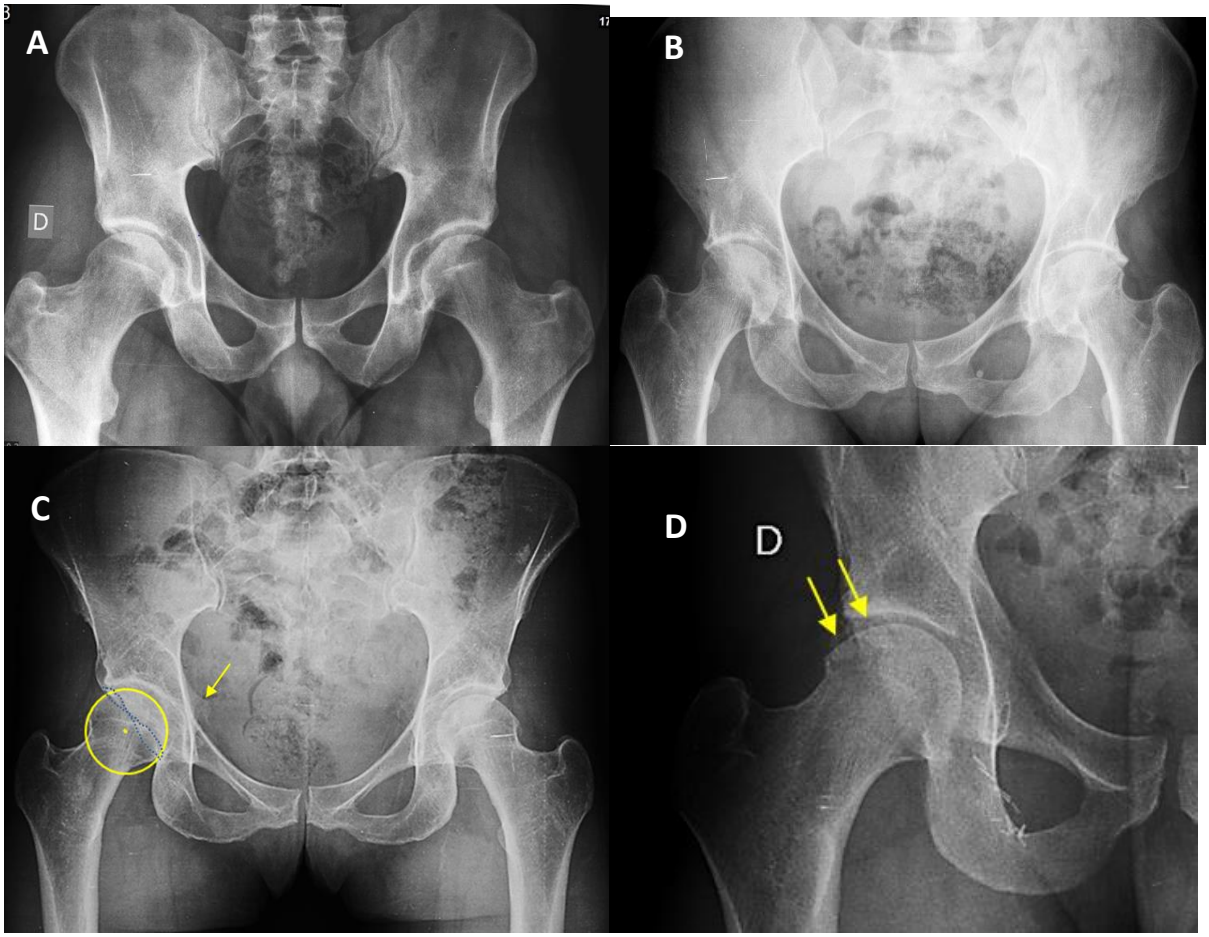

Figure 5: plain X-rays of AP views of pelvis and both hips showing; A. cross-over sign in both sides, B. bilateral coxa profunda, C. posterior wall sign and ischial spine sign, and D. os acetabuli in the right hip.

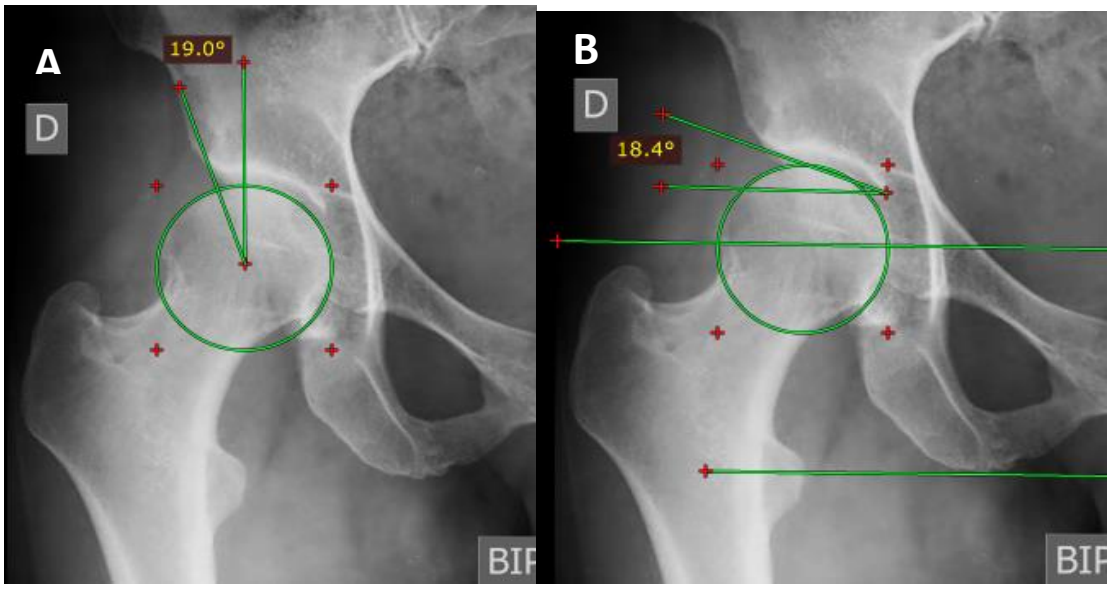

Figure 6: detailed radiograph of right hip in AP view of the pelvis showing; A. LCE angle 19°, B. acetabular index angle 18.4°

- Osteoarthritis (OA) was excluded according to Tönnis classification:
  - Tönnis Grade 0: No signs of OA
  - Grade 1: Increased sclerosis, slight narrowing of the joint space (**Figure 7**)
  - Grade 2: Small cysts, moderate narrowing of the joint space, loss of head sphericity
  - Grade 3: Large cysts, severe narrowing or obliteration of the joint space, severe deformity of the head

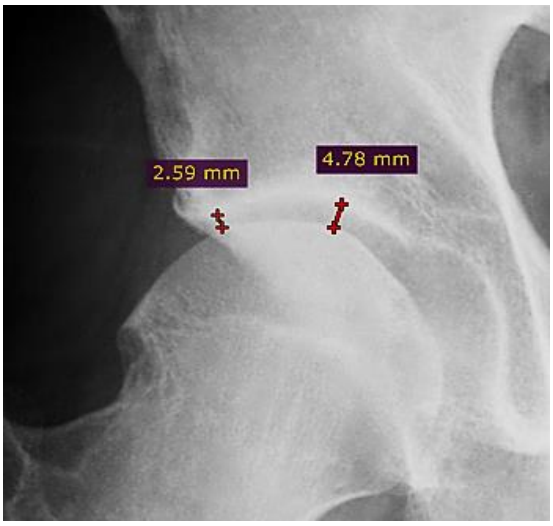

Figure 7: detailed radiograph of right hip in AP view of the pelvis showing Tonnis grade 1; narrowing of the lateral joint space

Magnetic Resonance Arthrography (MRA):

All cases were investigated by MRA for

- Detection of labral lesion (**Figure 8 A**)
- Detection of chondral lesion identifying its location (**Figure 8 B**).
- Excluding other pathologies such as AVN of femoral head or intra-articular loose bodies.

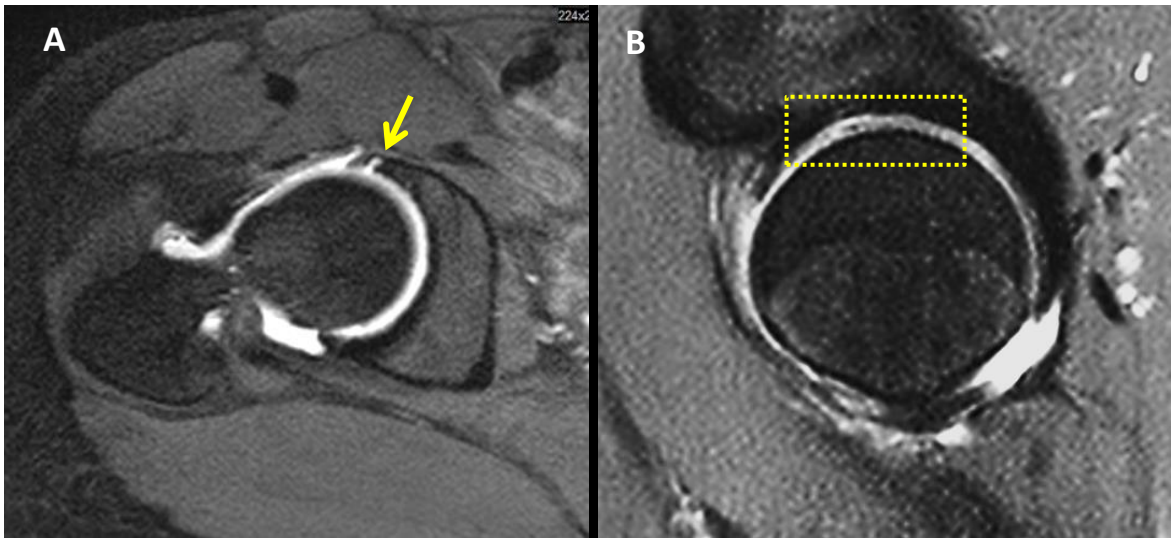

Figure 8: MRA images of the right hip; A. axial cut illustrating labral tear in the anterior zone, B. sagittal cut illustrating a chondral defect in the anterosuperior area

Selection of subjects

Criteria of inclusion:

- Clinical and radiological evidence of FAI (Cam, pincer or mixed)
- Age between 18 and 55 years

Criteria of exclusion:

- Osteoarthritis with Tönnis grade > 1 and/or joint space < 2 mm.
- Radiological evidence of hip dysplasia
- Inflammatory joint disease
- Previous history of operation or significant trauma to the hip of interest.

Patients with FAI were included in the study according to the criteria of selection after taking a written informed consent from all participants and approval of the Ethical Committee of Clinical Research. Included patients were operated by hip arthroscopy techniques for treatment of the FAI and the associated acetabular chondral lesion and labral tear. Patients were considered as a subject after arthroscopic assessment of the acetabular cartilage which was classified according to Outerbridge system and Beck's system.

All of the patients were asked to fill the following questionnaires and functional scores before the operation (**Appendix**):

- Non Arthritic Hip Score (NAHS)
- The 33-items International Hip outcome Tool (iHOT-33)
- Hip Outcome Score of both subscales; Activities of Daily Living (HOS-ADL) and Sports Specific Scale (HOS-sports).

Surgical procedure

Anesthesia:

General anesthesia with adjuvant lumbar plexus block was standardized for all patients undergoing hip arthroscopy. Preoperative single dose of antibiotic (cefazolin 1g) was routinely given to the patients.

Position and preparation:

After anesthesia, the patient was placed in supine position with both feet securely mounted on the traction table and a large well-padded perineal post was fixed medial to the operated hip. Maximal traction was applied to the operated side in abduction then adduction against the large perineal post produces effective separation of the joint distally and laterally (**Figure 9 A**).

When the ability to distract the hip joint was confirmed, the traction was released, the hip was then prepped and draped, and traction was reapplied when ready to begin arthroscopy. The operating site, from the iliac crest to the mid-thigh, anteriorly, laterally, and posteriorly, was sterilized and draped (**Figure 9 B**) and then setup of the arthroscopy equipment and fluoroscopy were prepared. The hip is adducted, internally rotated and flexed up to 20° to relax the iliofemoral ligament and facilitate distraction.

Portals placement and joint access:

The main difference among available techniques is the sequence of hip compartment access, which governs the choice of portals. As preferred in our work, central compartment (CC) was accessed first for management of the intraarticular lesions then the peripheral compartment (PC) for femoroplasty.

The anterolateral portal (ALP):

An 18-gauge arthroscopy needle (cannulated needle) was placed on the skin of the patient to approximate the trajectory into the joint under fluoroscopic guidance. The anterolateral portal was established by inserting the needle 1 cm anterior and 1 cm superior to the tip of the greater trochanter towards the articular space until the capsule resistance passed, then nitinol wire was inserted through the needle hole till the acetabular fossa is touched and confirmed by fluoroscopic image. Air was injected to separate the labrum from the capsule then the needle was withdrawn and reinserted to avoid injury to the labrum (**Figure 10 A&B**).

A small entry incision was done then the portal in the capsule was progressively dilated by serial obturators with diameters 4.0, 4.5 and 5.0 mm which were advanced over the nitinol wire. Once the capsule was breached by the 5.0-mm cannula and obturator, a 70° arthroscope is inserted through the anterolateral portal. Then, with

direct visualization established, diagnostic arthroscopy and additional portal placement could be performed.

The mid-anterior portal (MAP):

The mid-anterior portal (MAP) is safe to the lateral femoral cutaneous nerve, so it was preferred in our work rather than the anterior portal (AP). Placement of the needle into the joint was guided by direct arthroscopic vision from the anterolateral portal (**Figure 11 A&B**). The third portal, the distal anterolateral accessory portal (DALP), was occasionally established to facilitate the management of the peripheral compartment. The ALP and MAP were connected together by sharp arthroscopy knife making an interportal capsulotomy (parallel and within 5 mm distal to the labrum) which facilitated the manipulation of instruments.

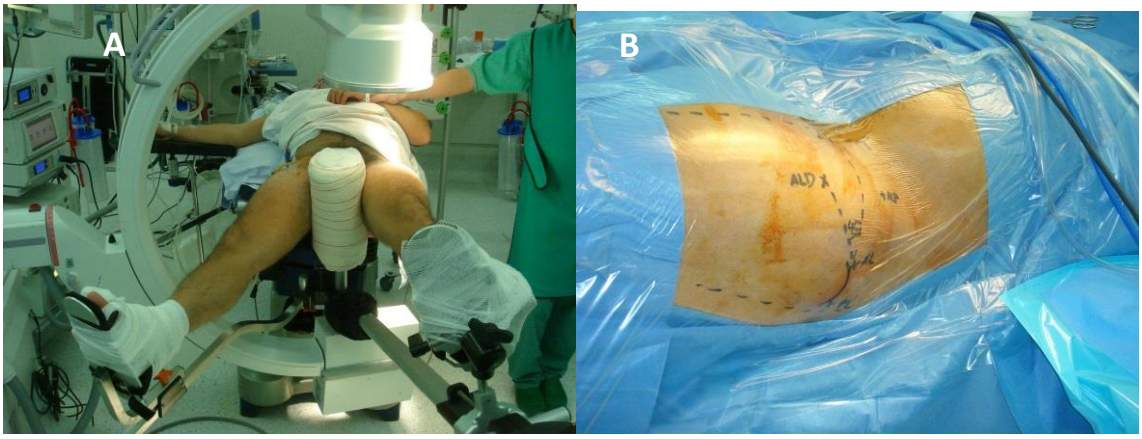

Figure 9: A, position of the patient and operating room equipment. B, sterilization and draping of the operating site on the left hip

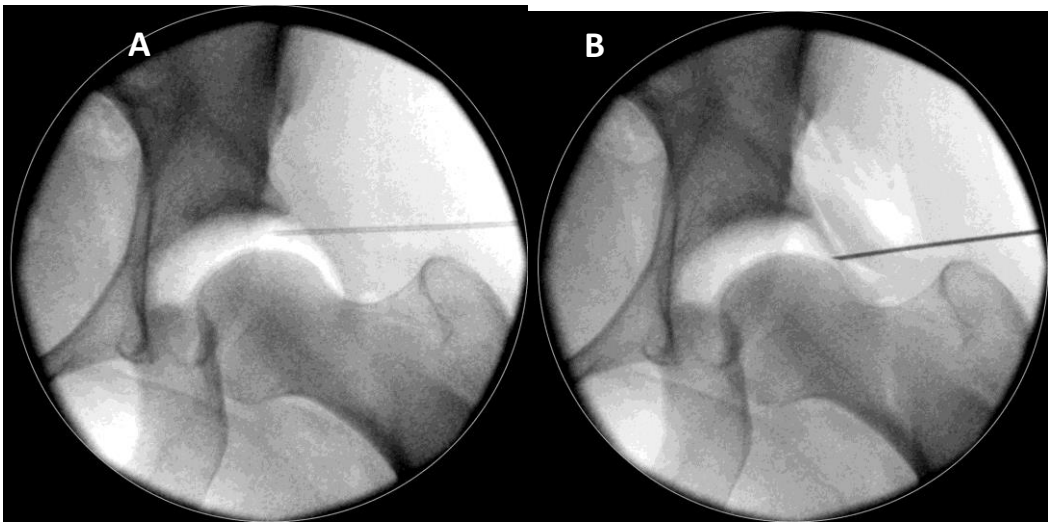

Figure 10: fluoroscopic pictures of the left hip. A, air was injected to separate the capsule from the labrum. B, the needle was withdrawn and reinserted to minimize injury to the labrum.

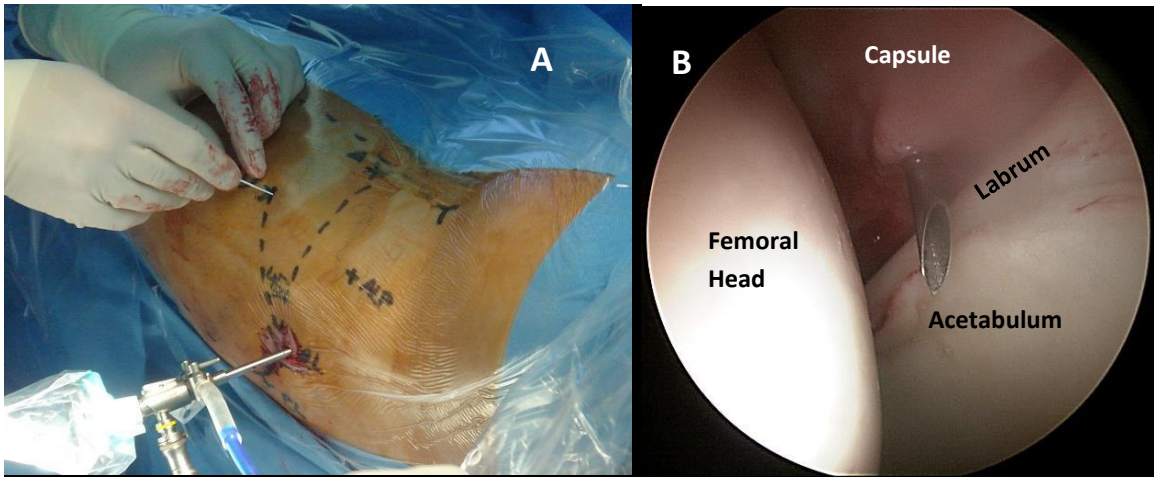

Figure 11: A, picture of left hip showing placement of the MAP from the skin. B, arthroscopic view of the left hip from the ALP showing the needle passing between the labrum and the femoral head

Diagnostic Arthroscopy:

Inspection began from the anterolateral portal by using the 70°scope, which provided the best view of the anterior portion of the joint. Next, the arthroscope was placed in the mid-anterior portal. Viewing laterally, the entry site of the anterolateral portal was checked, because this portal was placed with only fluoroscopic guidance, so there was a risk of labral penetration. Viewing medially from the mid-anterior portal, the most inferior limit of the anterior labrum could be seen.

Management of the labrum:

The labrum was evaluated to determine the appropriate treatment considering the size and condition of the labral tissue (**Figure 12 A**). For a bruised labrum without tear, treatment of the impingement by femoroplasty was thought to prevent further damage. When the labrum was detached, repair was required. The labrum was debrided of fraying and unhealthy tissue, leaving as much viable tissue as possible for secure repair and preservation of the function.

Once the decision was made to repair the labrum, the acetabular rim had to be prepared. The acetabular rim was exposed using a mechanical shaver and thermal ablator between the capsule and the labrum (opening the capsule-labral space), and then the rim was trimmed using a 4.5 or 5 mm bone burr (**Figure 12 B**). The rim trimming was completed using both portals (ALP and MAP).

Following adequate rim resection for mixed cases or just trimming for cam cases, the labrum was reattached to the acetabular bone using 1.4-1.7 mm suture anchors. The distance between anchors was 5-10 mm depending on the size of the torn segment. The anchors were placed 2 to 3 mm beyond the cartilage margin with an angle of placement adjusted to avoid penetrating the articular surface inside or the outer cortex on the acetabulum on the other side. Sutures were placed around the labrum in a loop fashion or passed through the labrum in a piercing (translabral) fashion based on the quality of the labral tissue. Translabral sutures were the standard in our work but when the labrum was hypotrophic or seriously damaged, sutures were placed around the labrum in a loop fashion. The knots were fastened on the capsular side to avoid friction with the adjacent cartilage (**Figure 12 C**).

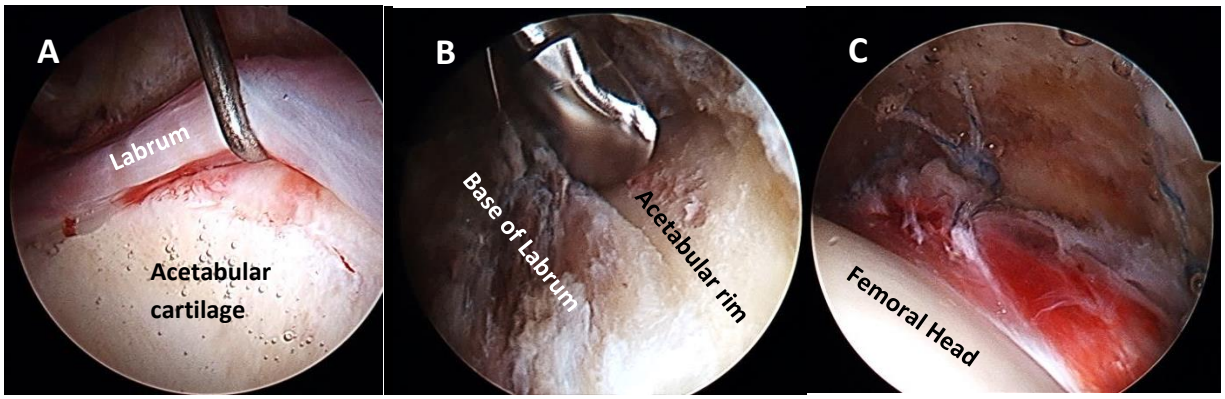

Figure 12: Arthroscopic views of the left hip from the AL portal showing: A. labral tear in the anterolateral area, B. preparation of the acetabular rim, C. reinsertion of the labrum by translabral sutures and restoration of the labral sealing on the head.

Acetabuloplasty:

Acetabuloplasty was required in patients with pincer impingement. The size of the burred-down area from the acetabular rim, both in length and in depth, depended on the degree of anterosuperior bony coverage. Acetabuloplasty was performed by estimating that 1 mm of bone resection results in about 1° of correction and by taking care not to decrease the lateral center edge angle of Wiberg below 25°.

The area of bone resection was exposed by using the mechanical shaver and thermal ablator taking into account three reference points: the psoas valley (most medial point) as the medial limit of resection, the lateral edge of the acetabulum, and the anterior inferior iliac spine as the superior limit of bone resection (**Figure 13 A&B**). Fluoroscopy was used frequently to control the acetabuloplasty. The 30°

arthroscope was utilized to obtain a direct tunnel view during the stage of rim resection. After bone resection, the labrum was reattached as mentioned before.

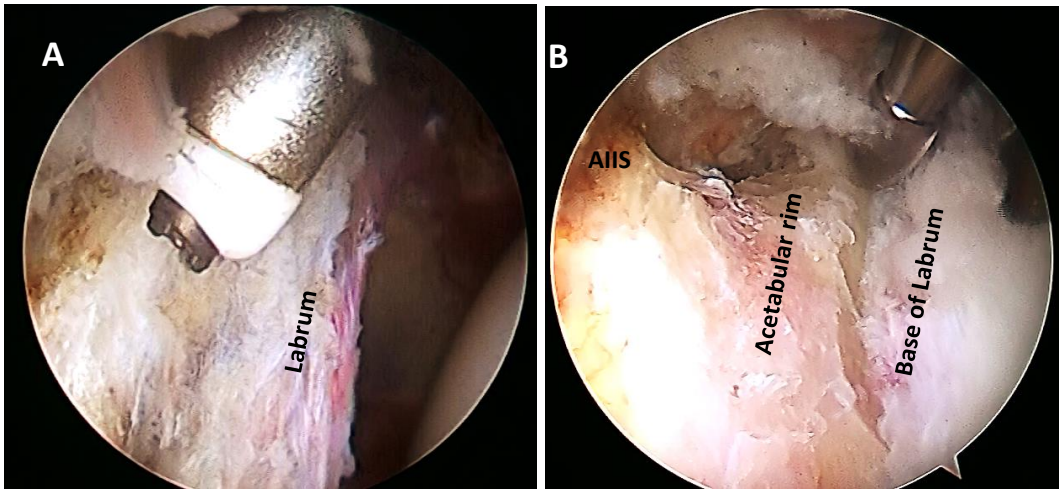

Figure 13: Arthroscopic view of the right hip from the AL portal using the 30° scope showing: A. exposure of the acetabular bone by thermal ablation, B. resection of the acetabular rim by 4.5mm bone burr. (AIIS: anterior inferior iliac spine)

Management of the cartilage lesion:

The acetabular cartilage was classified according to Outerbridge and the Beck's systems. While considering the condition of the acetabular cartilage and size of the lesion, the method of treatment was specified as following (**Figure 14 A-D**):

- Patients with normal acetabular cartilage (Outerbridge 0 and Beck's 0) did not require specific cartilage treatment.
- Patients with partial thickness acetabular cartilage lesion (Outerbridge I-III and Beck's I, II) required superficial debridement to the fibrillated or unstable parts without exposure of the subchondral bone.
- Patients with small full-thickness acetabular cartilage defect < 2 cm^2 (Outerbridge Grade IV and Beck's III, IV) were treated by full debridement and microfracture only.
- Patients with large full-thickness acetabular cartilage defects ≥ 2 cm^2 after debridement received augmentation of the microfracture by chitosan-based scaffold material (BST CarGel®; from Piramal Life Sciences, Quebec, Canada , provided by Smith & Nephew).

Visualization was predominantly obtained from the anterolateral portal with the mid-anterior portal being used for instrument passage and performing the microfracture. For more superolateral lesions of the acetabulum, the portals were exchanged.

Full debridement of the full-thickness defects was performed using the shaver; loose flaps and portions of delaminated cartilage were removed. A ring curette was then used to create stable borders and to remove the calcified layer. Arthroscopic microfracture awls with 40°, 60° and 90° tips were used perpendicular to the exposed subchondral bone and advanced with a mallet. Multiple holes were made with depth of 2-3mm and interval of 3-4 mm distance until covering the entire defect (**Figure 16**). The size of the lesion was measured using a calibrated probe in cm^2 and the location was identified according to the geographic description based on the 6 anatomical zones done by *Ilizaliturri et al* (**Figure 15**)[89].

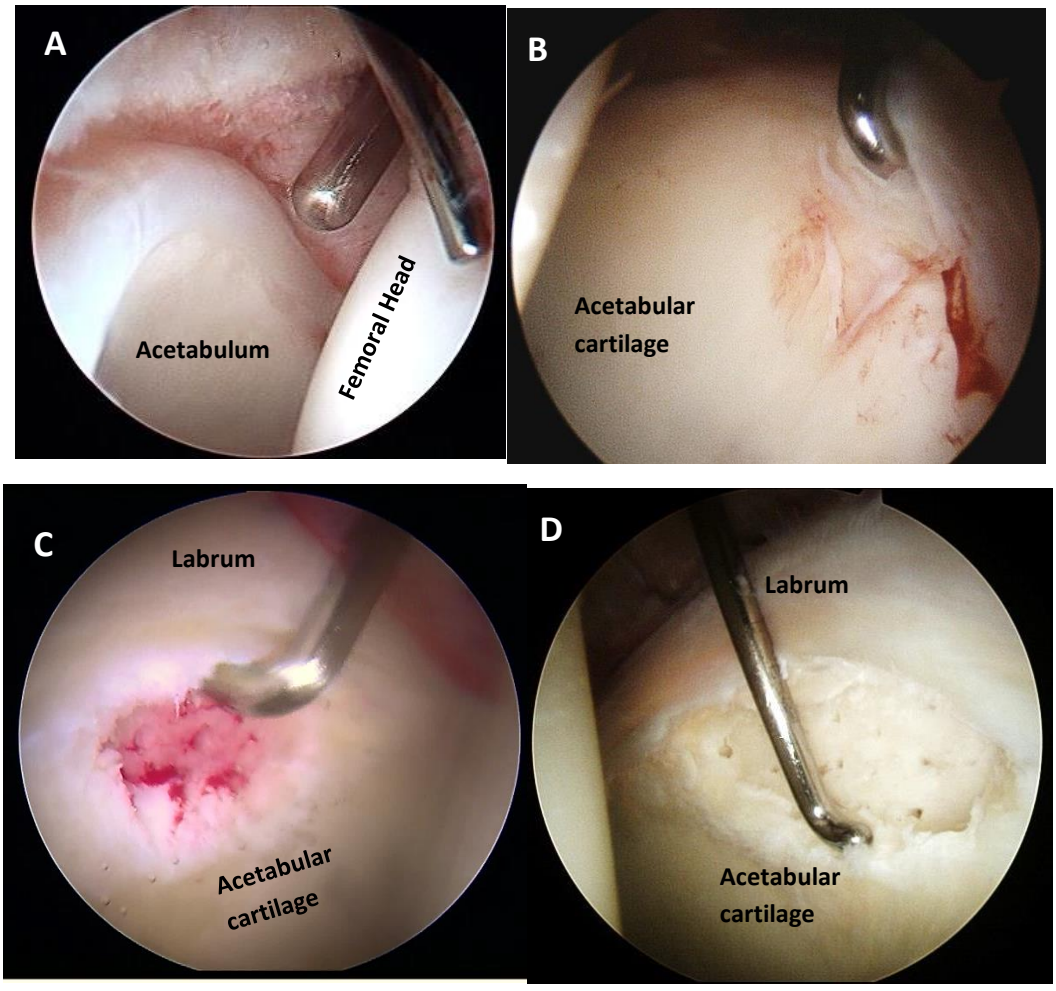

Figure 14: Arthroscopic views of different grades of the acetabular cartilage; A. right hip with normal cartilage, B. left hip with partial thickness lesion, C. right hip with small full-thickness lesion, D. left hip with large full-thickness lesion after debridement and microfracture.

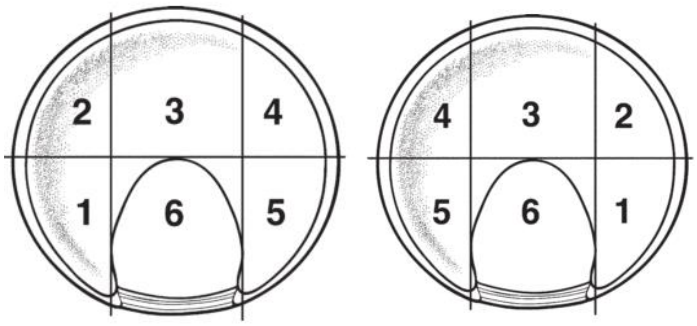

Figure 15: The geographic acetabular zones (*Reprinted from Ilizaliturri VM, Byrd JWTT, Sampson TG, et al. A Geographic Zone Method to Describe Intra-articular Pathology in Hip Arthroscopy: Cadaveric Study and Preliminary Report. Arthroscopy.2008;24(5):534-539., Copyright 2008, with permission from Elsevier).*

In case of cartilage defect ≥ 2 $cm^{2,}$ the defect was covered with the chitosan-based scaffold (BST CarGel®) for augmentation of the repair tissue. According to the sequence of work, application of the BST CarGel® material was the final step before closure of the capsule, so after performing the microfracture the traction of the limb is released then access to the peripheral compartment was done for management of the Cam deformity. Then traction was reapplied again and all fluid inside the joint was drained and the lesion surface was dried using swabs. BST CarGel® was prepared according to the manufacturer's instructions, the mixture was then delivered in a drop-wise manner using large bent 18-gauge needle making layer by layer until the defect was covered (**Figure 17**). The implant was left in place for 15 minutes for consolidation then traction was released.

Access to the peripheral compartment:

After management of the intraarticular lesions, traction of the limb is released and the hip is flexed to 40 degrees to relax the anterior capsule and facilitate management of the peripheral compartment. For better visualization and easier manipulation, the capsulotomy is extended from the middle of the interportal incision distally parallel to the neck until the zona orbicularis (T-capsulotomy) with application of two stay sutures at the angles of the capsular flaps, then sutures were retrieved outside the portals then traction is applied on them for enhanced visualization (**Figure 18 A&B**). The distal anterolateral accessory portal (DALP) is commonly used for working in the peripheral compartment.

Resection of the Cam deformity (Femoroplasty):

Once the lesion was identified, resection of this lesion was carried out using a 5.5 mm high-speed arthroscopic burr until the cam lesion was adequately resected

(**Figure 18 C**). To achieve adequate evaluation of the procedure, we used both direct visualization and fluoroscopy.

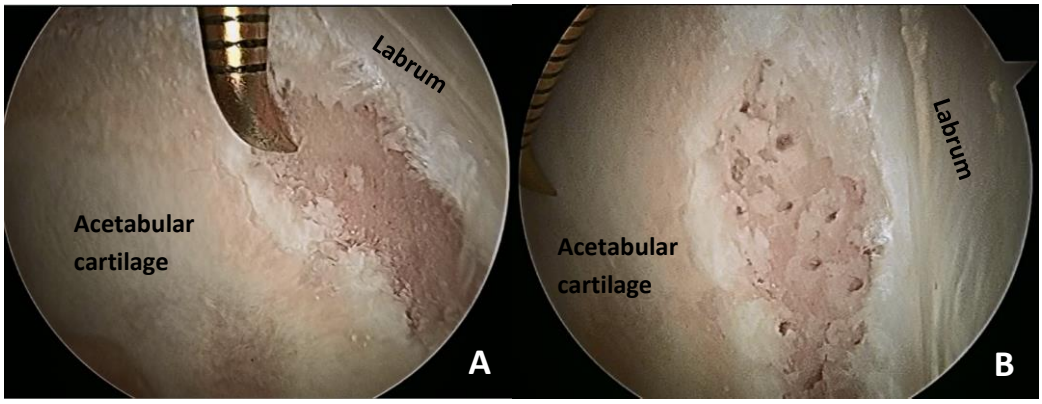

Figure 16: arthroscopic views of the left hip showing the technique of microfracture; A. the 60° awl is directed perpendicular to the surface, B. the defect is covered with holes.

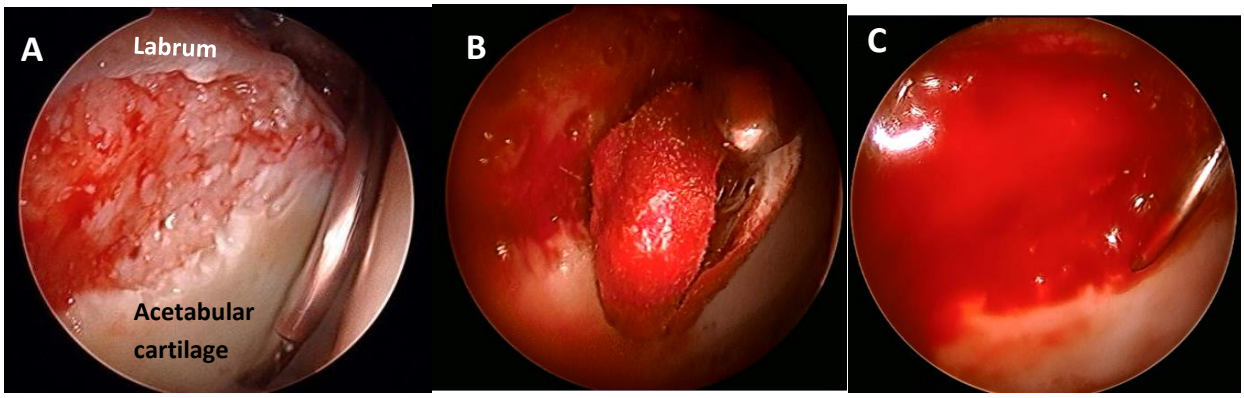

Figure 17: arthroscopic views of the right hip from the AL portal showing the technique of scaffold augmentation; A. the acetabular defect after debridement and microfracture, B. the surface is dried with swabs, C. the BST CarGel mixture is delivered by a needle in a drop-wise manner to fill the defect.

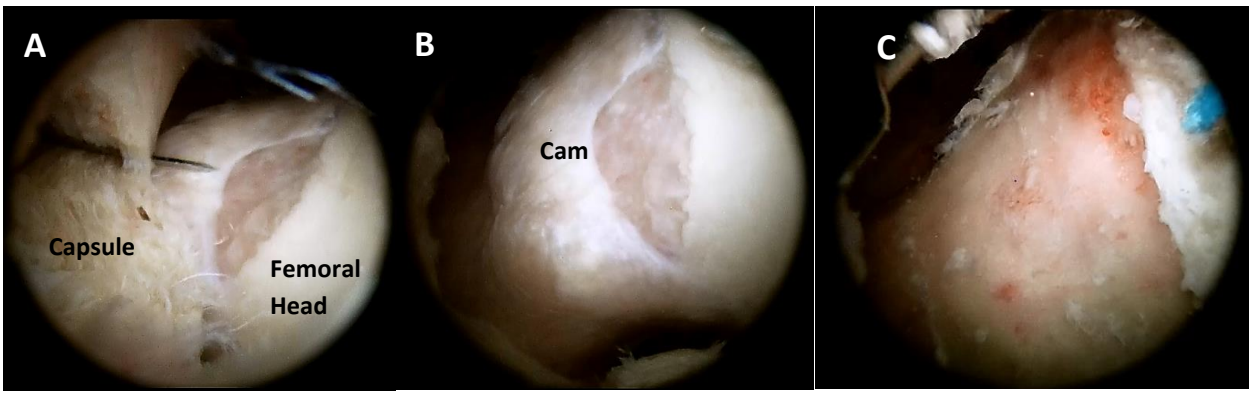

Figure 18: arthroscopic views of the left hip from the AL portal showing, A. a knife making the longitudinal incision of T-capsulotomy, B. open peripheral compartmant exposing the Cam deformity, C. restoration of the normal contour of the head-neck junction after femoroplasty.

The hip was held in neutral rotation and 40° of flexion to reproduce a Dunn lateral view. The position allowed some degrees of hip external and internal rotation for circumferential imaging of the head-neck junction. The femoroplasty began with the scope in the mid-anterior portal and the burr in the anterolateral portal. This technique was preferred for the portions of the cam lesion that extend very laterally, then the burr can be placed in the distal anterolateral accessory portal (DALP) with the scope placed in either the mid-anterior portal or the anterolateral portal for final configuration. The medial and lateral synovial folds were considered the anatomical limits for femoroplasty to preserve the medial and lateral retinacular vessels and protect the vascularity of femoral head (**Figure 19 A**). A dynamic examination was performed to assess any residual impingement through the hip motion with viewing from different planes, and then the capsule was closed by 2-4 sutures with attempt to repair both the longitudinal and the interportal incisions for complete closure as much as possible (**Figure 19 B**). Finally, skin portals were closed by simple stitches.

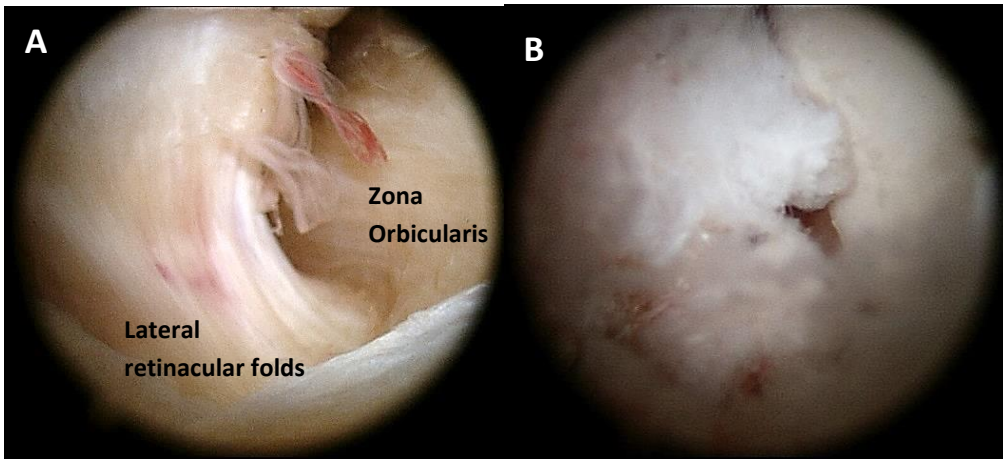

Figure 19: arthroscopic views of the left hip from the M-A Portal showing, A. the lateral synovial fold and retinacular arteries, B. closure of the capsulotomy incisions

Postoperative Rehabilitation

From the first day, the patients were encouraged to do continuous passive motion through a limited arc aided by simple analgesics to avoid the formation of adhesions. Patients were asked to ambulate with partial weight-bearing assisted by crutches for 3 weeks to avoid the risk of neck fracture after femoroplasty, and this period was prolonged to 6 weeks if the patient was treated for full thickness cartilage lesion

(microfracture ± BST CarGel®). The main objective during the first 6 weeks was restoration of full range of movement then activity was allowed to be increased gradually as patients tolerated. Patients with full-thickness chondral defects received a protective rehabilitation protocol; low-contact physical activities could be allowed in the third month, whereas high-impact and twisting movements were avoided during the first 6 months after surgery. It wasn't feasible to ensure applying a formal physiotherapy protocol for all patients; however the previous points were precisely followed.

Postoperative follow-up

The follow up visits were scheduled at 6 weeks, 3, 6 and 12 months, then every year. The patients were evaluated regarding the pain, ROM and signs of impingement. Postoperative radiographs were obtained at 3 months for assessment of correction in alpha angle and the acetabular resection. Non Arthritic Hip Score (NAHS), International Hip outcome Tool 33 (iHOT-33), Hip Outcome Score of both subscales; Activities of Daily Living (HOS-ADL) and Sports Specific Scale (HOS-sports) were collected during the visits before and after the procedure. We planned to assess the mid-term functional outcomes of cartilage management, so the scores were collected at 12 and 24 months follow-up. Clinical outcomes were collected by direct visits (hard copies), emails, and telephone contact applications.

Radiological evaluation has been performed by obtaining the plain X-ray images after 3 months of surgery to re-measure the radiographic parameters of FAI. Alpha angle and Head-Neck offset were measured to assess the correction of Cam deformity, while LCE angle and Tönnis angle were measured for pincer correction.

After 24 months of the surgery, the patients have been referred for MRI investigation of the cartilage repair. MRI studies were performed with a 1.5-T magnet (Achieva; Philips; Netherland) including the following sequences: Axial fast-spin-echo (FSE) T2-weighted with fat saturation, Axial oblique FSE T1-weighted with fat saturation, coronal FSE T2-weighted, sagittal FSE T2-weighted with fat saturation and sagittal fast spin-echo T1-weighted. MRI follow-up consisted of the T2 mapping and recording the T2 values of the cartilage repair tissue in comparison to the values of the healthy articular cartilage from the same joint. For every patient, 9 regions of

interest (ROIs) were localized manually at the acetabular articular cartilage of 3 consecutive sagittal slices including the area of repair. In each sagittal slice, two ROIs have been carefully drawn at different sites in the repair area anteriorly guided by reviewing the previously obtained preoperative MRA images and arthroscopic pictures, one of them close to the chondrolabral junction and the second one was more central. The third ROI was located at the apparently healthy posterior cartilage as a control for comparison with the repair area. The T2 values from these ROIs were recorded and statistically analyzed.

RESULTS

Twenty three patients fulfilled the criteria of inclusion and minimum 2 years of follow up in this study; 18 male and 5 female. Demographic data including age, BMI, Tegner sports level, and duration of symptoms are summarized in the **Table 3**.

	Age (years)	**BMI** (kg/m^2)	**Tegner level**	**Symptom Period** (months)
Mean±SD	40.9 ± 7	23.8 ± 2	6±1.5	32±10.4
Range	25-54	20-27	3-10	10-38

Table 3: Demographic data

Radiological measures (preoperative):

Assessment of the preoperative plain radiographs is presented in the following table **(Table 4).**

	Alpha angle preop	**H-N Offset preop**	**Acetab. Index preop**	**LCE angle preop**
Mean± SD	70.6±6.9	5.7±1.4	9.4±1.9	30.2±3.6
Range	58-80	3-9	5-13	25-38

Table 4: Preoperative radiographic measures of the total population

Positive cross-over sign was observed in 8 cases (32%). Also the radiographic features of osteoarthritis were studied; 12 cases (48%) had Tönnis grade 0 and 13 cases (52%) had Tönnis grade 1. Magnetic resonance arthrography (MRA) studies demonstrated findings suggestive of labral tear in all cases (100%) and chondral damage in 18 cases (72%) of the total population. The parameters were recorded as positive or negative based on the report of the radiologist.

Intraoperative findings:

The clinical study included 15 cases (65 %) of Cam-Type FAI, 8 cases (35%) of Mixed-Type FAI. All patients were included with acetabular chondral lesion and had a defect size 3.5±1 cm^2 (mean ± SD). Zone 2 was involved in all of the cases; 13

cases extended to zone 3, two cases extended to zone 1, and 8 cases confined to zone 2. Labrum was torn in all of the patients in the same zones corresponding to the cartilage lesion. Three patients had associated chondral lesion in the femoral head; one of them had Outerbridge grade II lesion in zone 2 and has been treated by debridement only, while the other two cases had grade VI lesions in zone 2 and 3, and have been treated by microfracture and filling with the same preparation of chitosan-based scaffold.

Clinical outcomes:

According to the preoperative evaluation, the values of the preoperative PROs (mean± SD) were 55.2 ±13.4 for NAHS, 43.1 ±14 for iHOT33, 59.7 ±14.1 for HOS-ADL, and 30.9 ±13.9 for HOS-SSS.

The immediate postoperative period showed normal recovery for all of the patients without important clinical incidents. For the patients who improved with the intervention, we observed satisfactory rehabilitation progress; disappearance of the preoperative pain, full ROM, and negative tests of impingement until the last visit. One patient developed periarticular muscular pain and stiffness which improved after 6 months of continuous physiotherapy. Three patients had had postoperative perineal hypoesthesia which recovered spontaneously within 2-6 weeks. One patient needed total hip arthroplasty after 2 years of the intervention.

The mean follow up of the patients was 38.4±7 months. Twenty one patients reported improvement in the functional scores within first 12 months and maintained their achieved scores through the subsequent period of follow up. Two patients showed no significant change from their baseline levels; one of them was 54 years old with radiological image of mild osteoarthritis (Tönnis 1), with associated chondral lesion (grade IV) in the femoral head and finally needed total hip arthroplasty because of the limiting pain. The other one was 38 years old, Tönnis 1, with acetabular chondral defect 6 cm^2. At 12th month, postoperative functional scores, and the functional scores obtained at the endpoint of the study (**Table 5**)

Interestingly, there were two male patients who had associated chondral defect (grade IV) in the femoral head and radiological image of mild osteoarthritis (Tönnis

1); one of them, 54 years old, had 24-months post- versus preoperative NAHS 41.3 vs 39, iHOT33 34 vs 30, HOS-ADL 45.8 vs 47, and HOS-SSS 5.5 vs 7 and finally needed total hip arthroplasty at 2 years because of limiting pain. The other patient, 49 years old; had 24-months post- versus preoperative NAHS 87 vs 53, iHOT33 93 vs 61, HOS-ADL 100 vs 72, and HOS-SSS 95 vs 24.

	Preoperative	12 months follow-up		End-point follow-up	
NAHS :					
mean± SD	55.2±13.4	81.9±13.6	p=0.00001	85.6±14.5	p=0.13
range	23.7-78.7	41.3-98.7		41.3-100	
iHOT 33 :					
mean± SD	43.1±14	72.6±16.6	p=0.00004	78.5±15.6	p=0.02
range	10.8-65.4	34-96.7		34-97.6	
HOS-ADL :					
mean± SD	59.8±14.1	82.6±16.7	p=0.00005	86.7±15.9	p=0.21
range	24.3-89.5	45.8-100		45.8-100	
HOS-SSS :					
mean± SD	30.9±13.9	64.8±26.3	p=0.0002	70.8±26.2	p=0.29
range	2.8-55.5	5.5-100		5.5-100	

Table 5: Preoperative and postoperative PROs

The published values MCID were used for interpretation of the individual outcomes on each one of the used PROs[117]. At the first year follow up, 91% of the patients met or exceeded the MCID for NAHS, iHOT33 and HOS-ADL, and 82% for HOS-SSS. At the end point of the follow up, the proportions were 87% for NAHS, 91% for iHOT33 and HOS-SSS, and 82% for HOS-ADL. By comparing the final scores to the corresponding first year values, 13% achieved further improvement on the NAHS, 48% on the iHOT33, and 8% on the HOS-ADL and HOS-SSS (**Table 6**).

	MCID[117]	1st year Postop	End point Postop	
			overall change	2nd year change
NAHS	10	21 (91%)	20 (87%)	3 (13%)
iHOT33	6.1	21 (91%)	21 (91%)	11 (48%)
HOS-ADL	9	21 (91%)	19 (82%)	2 (8%)
HOS-SSS	6	19 (82%)	21 (91%)	2 (8%)

Table 6: the subjects met or exceeded the minimal clinically important difference (MCID) are shown in numbers and proportions for the first year and the end point of the follow up.

Radiological outcomes:

The postoperative x-ray showed alpha angle 44.3±4.9° **(Table 7, Figure 20)**.

		Preop	Postop	test of significance	p-value
Alpha angle	Mean± SD Range	70.5±6.3 56-80	44.3±4.9 34-52	Z= -8.553	<0.0001
H-N offset	Mean± SD Range	5.6±1.8 0-9	8.9±1.5 5-13	Z= -8.479	<0.0001
LCEA	Mean± SD Range	33.1±3.9 25-42	31.6±3.6 25-38	Z= -9.231	<0.0001

Wilcoxon Signed Ranks Test

Table 7: Comparison between the pre- and postoperative alpha angles in the patients with Cam deformity

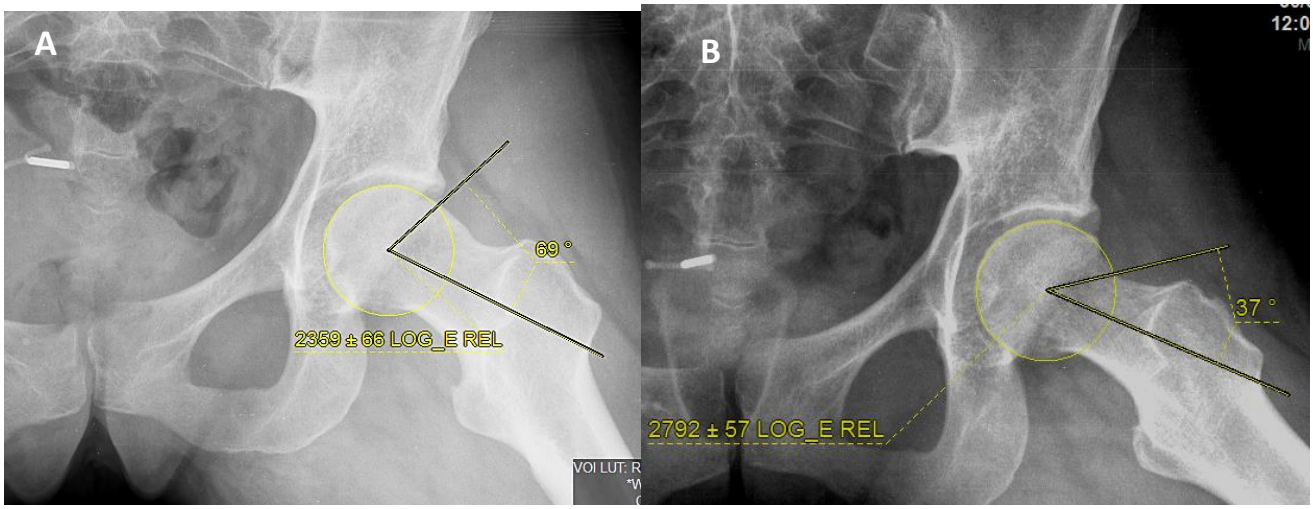

Figure 20: Plain X-ray Dunn view of both hips of a patient showing; A. preoperative alpha angle 69°, and B. postoperative alpha angle 37°

Twenty-one of the included patients were investigated by the T2 mapping technique. There is one patient reported unsatisfactory results at 1 year postoperative and underwent total tip replacement. Another patient had had revision surgery for labral reattachment. T2 relaxation values were collected from 189 ROIs for quantitative analysis. Within the peripheral repair area, the mean quantitative T2 value was 49.1± 7.2 milliseconds (ms), while ROIs of the central repair area had mean relaxation T2 values of 50.2 ± 7.1 ms. The native posterior cartilage showed mean T2 value of 46.2 ± 7.6 ms (

Table 8).

	Normal posterior cartilage	Repair cartilage		
		Peripheral	**Central**	**Global**
Mean (ms)	47.1	49.1	50.2	49.8
SD	7.6	7.3	7.2	7.0
Range	36.6 - 69.2	38.5 - 60	37.8 - 64.7	38.2 - 60.8
p-value		0.27	0.14	0.19

Table 8: T2 values (ms=milliseconds) obtained from the normal posterior cartilage and the areas of repair tissue (peripheral, central and global

DISCUSSION

The study at hand demonstrates the efficacy of the arthroscopic treatment of FAI and associated large full-thickness acetabular chondral lesions by microfracture augmented with chitosan-based scaffold. Short and mid-term follow-up of the patients exhibited satisfactory clinical outcomes in terms of improved hip function and low rate of complications. Radiological outcomes showed good quality of the repair tissue produced in the defect area resembling the native healthy cartilage of the same joint.

Using four different reliable patient-reported outcomes is considered a strength point in our work because this method covered multiple aspects of clinical and functional results. Significant improvement of the NAHS score in our patients indicates adequate improvement of their symptoms; mainly pain relief. The iHOT-33 uniquely evaluates recreational physical activities, job-related concerns, and social, emotional, and lifestyle concerns [118–120]. We can speculate that the significant improvement in iHOT-33 reported by our patients reflects marked satisfaction, as the results met their psycho-social expectations.

The HOS contains two separately scored subscales; activities of daily living (ADL) and sports, both of them are pure functional measures without any item related to symptoms [118,121], so using a combination of the NAHS and the HOS is recommended for patients undergoing hip arthroscopy [122]. We preferred to use the HOS-sports, rather than simply reporting whether the patient returned to sports or not, to obtain a quantitative description of the change occurred after surgical intervention.

Our results are enforced by calculating the minimal clinically important difference (MCID) for each PRO score used in the present study. MCID is a commonly used measure to define thresholds of patient perception of “meaningful” or “relevant” change[117]. The MCID is a metric for “within-individual” change. It is a value that represents a change in a single patient over time and is intended to reflect the threshold for a clinically meaningful difference within an individual. The proportion of patients in each treatment group whose change in score crossed the threshold of the MCID should be compared rather than the mean change in score for each group[117].

Microfracture technique has been used extensively in the knee and provided excellent early results and significant improvement in the quality of life, however the long-term follow up showed decline in the outcomes and failed to maintain patient's satisfaction [123,124]. Similarly, microfracture as an adjunct to hip arthroscopy for FAI has, in general, positive outcomes in short to midterm follow-up[125], but long-term follow-up isn't yet available. Comparing the results of microfracture only versus chitosan-augmented microfracture (the study at hand); studies of microfracture in the hip have reported lesions with mean size smaller than the minimal size in our study, in addition to the variable outcomes. *Philippon et al* [126] reported results of revision arthroscopy after 20 months of treatment by microfracture for acetabular chondral lesions with average size 163 mm^2; 8 out of 9 patients had 95% to 100% coverage of the chondral lesion and one patient had only 25% coverage. Similarly, *Karthikeyan et al* [127] performed second-look arthroscopies after an average 17 months of initial treatment with microfracture, and found a mean fill of 96% in 19 out of 20 patients who had had acetabular chondral defects with average size of 154 mm^2, and furthermore, histological analysis of full-thickness biopsy revealed that the tissue was primarily fibrocartilage with some staining for type II collagen in the region closest to the bone.

On the other hand, *Domb et al* [128] compared microfractures in a group of 79 patients with full-thickness acetabular chondral lesions to a control group of 158 patients with partial-thickness lesions who didn't receive a specific cartilage treatment. The mean age was 44 years and the mean size of the chondral defect was 189±98 mm^2; the results revealed no statistically significant difference in postoperative mHHS, HOS-ADL, HOS-SSS, and NAHS between the microfracture and control groups, except for the visual analog scale (VAS) score at 2 years which were significantly superior in the control group.

The systematic review by *Marquez-Lara et al* [129] showed that arthroscopic debridement, microfracture, and autologous chondrocyte transplantation (ACT) are associated with equivalent improvement in clinical outcomes in patients with high-grade acetabular chondral defects at short- and midterm follow-up. There were no differences in patient characteristics and demographics, but lesion size varied significantly between arthroscopic techniques (149.5 mm^2 for microfracture, 357.3 mm^2 for ACT, and 260 mm^2 for debridement). Finally it was concluded that the

decision to use one technique over another may be determined by the size of the defect [129].

Preservative treatment of a hip joint with large full-thickness acetabular defect is a great challenge. *Fontana et al* [130] compared the effectiveness of ACT versus simple debridement for management of acetabular chondral defects in 30 patients with Outerbridge grade 3 or 4 lesions. The area of involvement was >2 cm^2 in size and all patients had radiographic evidence of Tönnis grade 2. Both stages of the ACT procedure were performed arthroscopically. In both treatment groups, the mean size of the defect was 2.6 cm^2. The authors reported better clinical outcomes on the Harris Hip Score with ACT than with simple chondroplasty at final follow-up[130]. Another study by *Mancini and Fontana* [131] compared the clinical outcomes of the arthroscopic matrix-induced autologous chondrocyte implant (MACI) and autologous matrix-induced chondrogenesis (AMIC) techniques for the treatment of acetabular defects 2-4 cm^2 consequent to FAI. Mean defect size of MACI and AMIC groups were 2.8 and 2.9 cm^2, respectively. Significant improvements were observed in both treatment groups, as assessed by mHHS, up to five years follow-up[131].

Using the chitosan-based scaffold for augmentation of standard microfracture technique provided another successful, single-stage method for treatment of such large chondral defects. The results of the current study are supported by similar studies conducted on patients with chondral lesions in the knee joint. In an extended multicenter randomized controlled trial, the treatment by chitosan-based scaffold has shown superior results over the microfracture technique for chondral lesions in the knee joint regarding the clinical outcome, MRI, and histologic analysis[112,132,133]. T2 relaxation time and filling% have been considered as comparing variables. T2 values obtained at 5 years from joints treated with chitosan-based material and microfracture only treated joints showed significant difference. The authors noted that T2 values in the chitosan-based group were always closer to the ipsilateral native cartilage T2 value (mean 51.5 ± 7.5 ms) measured in the same session of analysis[112,132].

In the group of patients who underwent the MRI analysis of the current study, treatment with microfracture and chitosan-based scaffold resulted in a repair tissue with radiological features similar to the native hyaline articular cartilage over mid-

term follow up. Quantitative T2 relaxation analysis showed a non-significant difference between the area of repair (peripheral and central parts) and the native acetabular cartilage posteriorly. Specific evaluation of the peripheral area of the repair tissue is of great importance because it is more susceptible to shear forces during hip motions. Therefore, the normal appearance of the repair tissue on MRI images reflects a sound structure that can withstand the biomechanical demands of the hip joint.

The value of T2 mapping for assessment of the acetabular cartilage in symptomatic FAI patients has been proved in different studies. According to Hesper et al[134], T2 values obtained from arthroscopically normal cartilage were significantly higher than the values of regions with cartilage degeneration. These results are consistent with Ellermann et al [135] who found a strong correlation between acetabular cartilage damage and decreased T2 values in patients with FAI symptoms.

In the present study, all adverse events were recorded up to 24 months after treatment. The surgical techniques in our study showed adequate safety for subsequent use, based on the rate and severity of reported complications. It worth noting that significant postoperative complications, such as DVT, infection, instability, AVN of femoral head and fracture neck of femur, have not occurred in any patient of our study.

Results of the current study reported one patient developed periarticular muscular pain and stiffness which improved after 6 months of continuous physiotherapy. Three patients had had postoperative perineal hypoesthesia which recovered spontaneously within 2-6 weeks. These postoperative complications can be attributed to the prolonged traction time during the procedure rather than to the scaffold material used for treatment. The systematic review by *Harris et al* [136] found that the most commonly affected nerve is the pudendal (40%), followed by lateral femoral cutaneous (21%), sciatic (17%), common peroneal (17%), and femoral (4.7%). According to the studies of *Telleria et al* [137] and *Dippmann et al* [138], total traction force, rather than total traction time, is a more significant predictor of nerve dysfunction during hip arthroscopy

A very similar study has been conducted by *Rhee et al* [139] who concluded a satisfactory safety profile and short-term clinical outcomes of patients treated arthroscopically with BST-CarGel for acetabular chondral defects in conjunction with microfracture. They reported a mean defect size of 5.8 ± 2.6 cm^2. There were 2 (5.4%) patients presented with significant hip pain within 2 days of surgery, with C-reactive protein levels above 200 mg/L. This was believed to be caused by an exaggerated inflammatory response to BST-CarGel. They also observed a statistically significant improvement in iHOT, HOS-ADL, and HOS-sport scores at short-term follow-up (1 year) [139].

Important limitations to our work are the lack of control group to compare the results and the wide range of follow up period (24-50 months) at the endpoint of the study. Also the cases were operated by two senior surgeons, and this may be a source of bias even though both of them strictly followed the same technique and steps. Priori power analysis was not performed, so there is a risk of statistical type 2 error with the small sample size of our study. Because of the small number of patients, we couldn't definitely conclude the safety of chitosan implant for use in the hip joint. The good results can be attributed to several factors such as the non-extensive chondral defects (maximally involving 2 zones), the short preoperative period of symptoms (mean 32 ±10.4 months) and the initial improvement after Cam resection and labral repair, so it is difficult to conclude the specific contribution of the chitosan-based material to the results.

The time for T2 mapping follow-up was not the same for all patients (ranged from 24 to 38 months), so the expected changes in the repair tissue may differ among patients. The study did not include normal patients without FAI symptoms for comparison. Although the apparently normal posterior cartilage has been considered as self-control for comparison, but the minimum 2 years of follow-up may render this normal cartilage pathologic as a disease progression.

CONCLUSIONS & RECOMMENDATIONS

The use of chitosan-based scaffold after microfracture for treatment of large acetabular chondral lesions associated with FAI improved the hip symptoms and function markedly in the patients over the short-term follow-up. However, this early improvement can be attributed to the proper correction of the original biomechanical FAI conflict.

Up to 91% of the patients with large (≥2cm^2) full-thickness acetabular chondral defect associated with FAI maintained satisfactory clinical outcomes at mean follow-up of 38.4 months. This mid-term improvement can reflect the adequate integrity of cartilage repair by the arthroscopic combined treatment of microfracture and chitosan-based scaffold.

Arthroscopic microfracture of large full thickness acetabular chondral defects with chitosan-based scaffold produced a homogenous repair tissue similar to the corresponding native cartilage of the same joint on quantitative T2 mapping at mid-term follow-up.

The low rate of morbidity and complications can raise the belief of safety towards using the chitosan-based scaffold material in further clinical work even though it couldn’t be definitely concluded in the current study.

Preservative treatment of a hip joint with large full-thickness acetabular defect is a great challenge. It is strongly recommended to study the long-term clinical, radiological, and histological follow-up of this cartilage treatment method to recognize its effectiveness and durability.

REFERENCES

1. Griffin DR, Dickenson EJ, O'Donnell J, et al. The Warwick Agreement on femoroacetabular impingement syndrome (FAI syndrome): An international consensus statement. *Br J Sports Med*. 2016;50(19):1169-1176. doi:10.1136/bjsports-2016-096743

2. Ganz R, Parvizi J, Beck M, Leunig M, Notzliv H, Siebenrock KA. Femoroacetabular Impingement A Cause for Osteoarthritis of the Hip. *Clin Orthop Relat Res*. 2003;417:112-120. doi:10.1097/01.blo.0000096804.78689.c2

3. Beck M, Kalhor M, Leunig M, Ganz R. Hip morphology influences the pattern of damage to the acetabular cartilage. Femoroacetabular impingement as a cause of early osteoarthritis of the hip. *J Bone Jt Surg - Ser B*. 2005;87(7):1012-1018. doi:10.1302/0301-620X.87B7.15203

4. Pfirrmann CW a, Mengiardi B, Dora C, Kalberer F, Zanetti M, Hodler J. Cam and pincer femoroacetabular impingement: characteristic MR arthrographic findings in 50 patients. *Radiology*. 2006;240(3):778-785. doi:10.1148/radiol.2403050767

5. Buckwalter JA. Articular cartilage: injuries and potential for healing. *J Orthop Sports Phys Ther*. 1998;28(4):192-202. doi:10.2519/jospt.1998.28.4.192

6. El-Radi MA, Marin-Peña OR, Said HG, Tey-Pons M. Basics in hip chondrolabral lesions and state of the art. *Sicot-J*. 2017;3:73. doi:10.1051/sicotj/2017040

7. Yen YM, Kocher MS. Chondral Lesions of the Hip Microfracture and Chondroplasty. *Sports Med Arthrosc*. 2010;18(2):83-89. doi:10.1097/JSA.0b013e3181de1189

8. Erggelet C, Endres M, Neumann K, et al. Formation of cartilage repair tissue in articular cartilage defects pretreated with microfracture and covered with cell-free polymer-based implants. *J Orthop Res*. 2009;27(10):1353-1360. doi:10.1002/jor.20879

9. D CDHP, Sun JMD, Sc M, et al. Chitosan e glycerol phosphate / blood implants elicit hyaline cartilage repair integrated with porous subchondral bone in microdrilled rabbit defects. 2007:78-89. doi:10.1016/j.joca.2006.06.015

10. Wang D-A, Varghese S, Sharma B, et al. Multifunctional chondroitin sulphate for cartilage tissue–biomaterial integration. *Nat Mater*. 2007;6(5):385-392. doi:10.1038/nmat1890

11. Hoemann CD, Hurtig M, Rossomacha E, et al. Chitosan-Glycerol Phosphate/Blood Implants Improve Hyaline Cartilage Repair in Ovine Microfracture Defects. *J Bone Jt Surg Am*. 2005;87(12):2671-2686. doi:10.2106/JBJS.D.02536

12. Standring S, Borley NR, Collins P, et al. *Gray's Anatomy: The Anatomical Basis of Clinical Practice*.; 2008.

13. Lee MC, Eberson CP. Growth and Development of the Child's Hip. *Orthop Clin North Am*. 2006;37(2):119-132. doi:10.1016/j.ocl.2005.12.001

14. Vandenbussche E, Saffarini M, Taillieu F, Mutschler C. The asymmetric profile of the acetabulum. *Clin Orthop Relat Res*. 2008;466(2):417-423. doi:10.1007/s11999-007-0062-x

15. Murray DW. The Definition and Orientation Measurement of. *Br Editor Soc Bone Jt Surg*. 1993;75:228-232.

16. Bs ACP, Hunter JC, Laird T, Jamali AA. Multilevel Measurement of Acetabular Version Using 3-D CT-generated Models Implications for Hip Preservation Surgery. 2011:552-561. doi:10.1007/s11999-010-1567-2

17. Zilber S, Lazennec JY, Gorin M, Saillant G. Variations of caudal, central, and cranial

acetabular anteversion according to the tilt of the pelvis. *Surg Radiol Anat*. 2004;26(6):462-465. doi:10.1007/s00276-004-0254-y

18. Kopydlowski NJ, Tannenbaum EP, Bedi A, Smith M V., Sekiya JK. An increase in cranial acetabular version with age: Implications for femoroacetabular impingement. *J Arthroplasty*. 2014;29(9):1741-1744. doi:10.1016/j.arth.2014.03.042

19. Rissech C, Sañudo JR, Malgosa a. The acetabular point: a morphological and ontogenetic study. *J Anat*. 2001;198(Pt 6):743-748. doi:10.1046/j.1469-7580.2001.19860743.x

20. Philippon MJ, Michalski MP, Campbell KJ, et al. An Anatomical Study of the Acetabulum with Clinical Applications to Hip Arthroscopy. *J Bone Jt Surg*. 2014;96(20):1673-1682. doi:10.2106/JBJS.M.01502

21. Petersen W, Petersen F, Tillmann B. Structure and vascularization of the acetabular labrum with regard to the pathogenesis and healing of labral lesions. *Arch Orthop Trauma Surg*. 2003;123:283-288. doi:10.1007/s00402-003-0527-7

22. Seldes RM, Tan V, Hunt J, Katz M, Winiarsky R, Fitzgerald RHJ. Anatomy, histologic features, and vascularity of the adult acetabular labrum. *Clin Orthop Relat Res*. 2001;(382):232-240.

23. Won YY, Chung IH, Chung NS SK. Morphological study on the acetabular labrum. *Yonsei Med J*. 2003;44(5):855-862.

24. Narvani a a, Tsiridis E, Tai CC, Thomas P. Acetabular labrum and its tears. *Br J Sports Med*. 2003;37(May 2005):207-211. doi:10.1136/bjsm.37.3.207

25. John Cooper H, Walters BL, Rodriguez JA. Anatomy of the hip capsule and pericapsular structures: A cadaveric study. *Clin Anat*. 2015;28(5):665-671. doi:10.1002/ca.22539

26. Wagner FV, Negrão JR, Campos J, Ward SR, Haghighi P, Trudell DJ RD. Capsular ligaments of the hip: anatomic, histologic, and positional study in cadaveric specimens with MR arthrography. *Radiology*. 2012;263(1):189-198. doi:10.1148/radiol.

27. Walters BL, Cooper JH, Rodriguez JA. New findings in hip capsular anatomy: Dimensions of capsular thickness and pericapsular contributions. *Arthroscopy*. 2014;30(10):1235-1245. doi:10.1016/j.arthro.2014.05.012

28. Ito H, Song Y, Lindsey DP, Safran MR, Giori NJ. The proximal hip joint capsule and the zona orbicularis contribute to hip joint stability in distraction. *J Orthop Res*. 2009;27(8):989-995. doi:10.1002/jor.20852

29. Kalhor M, Beck M, Huff TW, Ganz R. Capsular and pericapsular contributions to acetabular and femoral head perfusion. *J Bone Jt Surg Am*. 2009;91(2):409-418. doi:10.2106/JBJS.G.01679

30. Kasai T, Takao Suzuki, Tomoaki Fukushi, Masashi K, Chiba S. Peripheral Distribution of the Medial Circumflex Femoral Artery. *Okajimas Folia Anat Jpn,*. 1985;62(August):89-97.

31. S. Sevitt, Thompson RG. The Distribution and Anastomoses of Arteries Supplying The Head and Neck of The Femur. *J Bone Jt Surg Br*. 1965;47(3):560-573.

32. Letournel E, Judet R. *Fractures of the Acetabulum, 2nd Edn. Springer, Berlin Heidelberg New York*.; 1993.

33. Beck M, Leunig M, Ellis T, Sledge JB, Ganz R. The acetabular blood supply: Implications for periacetabular osteotomies. *Surg Radiol Anat*. 2003;25(5-6):361-367. doi:10.1007/s00276-003-0149-3

34. Tucker FR. Arterial supply to the femoral head and its clinical importance. *J Bone Jt Surg Br*. 1949;3(1):82-93.

35. Ogden JA. Changing patterns of proximal femoral vascularity. *J Bone Joint Surg Am*. 1974;56(5):941-950.

36. Ogden JA. Trauma, Hip Development, and Vascularity. In: *Surgery of the Hip Joint*. Vol I. ; 1984:145-180. doi:10.1007/978-1-4612-5224-5

37. Zlotorowicz M, Szczodry M, Czubak J, Ciszek B. Anatomy of the medial femoral circumflex artery with respect to the vascularity of the femoral head. *J Bone Jt Surg - Br Vol*. 2011;93-B(11):1471-1474. doi:10.1302/0301-620X.93B11.26993

38. Gautier E, Ganz K, Krügel N, Ganz R. Anatomy of the medial femoral circumfle artery and its surgical implications. *J Bone Jt Surg Br*. 2000;82:679-683.

39. Kalhor M, Horowitz K, Gharehdaghi J, Beck M, Ganz R. Anatomic variations in femoral head circulation. *HIP Int*. 2012;22(3):307-312. doi:10.5301/HIP.2012.9242

40. Boraiah S, Dyke JP, Hettrich C, et al. Assessment of vascularity of the femoral head using gadolinium (Gd-DTPA)-enhanced magnetic resonance imaging: a cadaver study. *J Bone Joint Surg Br*. 2009;91(1):131-137. doi:10.1302/0301-620X.91B1.21275

41. Gautier E, Ganz K, Krügel N, Ganz R. Anatomy of the medial femoral circumflex artery and its surgical implications. *J Bone Jt Surg*. 2000;82(5):679-683.

42. Crock H V. A revision of the anatomy of the arteries supplying the upper end of the human femur. *J Anat*. 1965;99:77-88.

43. Zlotorowicz M, Czubak J. Vascular Anatomy and Blood Supply to the Femoral Head. In: *Osteonecrosis. Springer-Verlag Berlin Heidelberg*. ; 2014:19-26. doi:10.1007/978-3-642-35767-1

44. Maroudas A, Wachtel E, Grushko G, Katz EP, Weinberg P. The effect of osmotic and mechanical pressures on water partitioning in articular cartilage. *BBA - Gen Subj*. 1991;1073(2):285-294. doi:10.1016/0304-4165(91)90133-2

45. Torzilli PA. Influence of cartilage conformation on its equilibrium water partition. *J Orthop Res*. 1985;3(4):473-483. doi:10.1002/jor.1100030410

46. Lai WM, Hou JS, Mow VC. A triphasic theory for the swelling and deformation behaviors of articular cartilage. *J Biomech Eng*. 1991;113(3):245-258. doi:10.1115/1.2894880

47. Linn FC, Sokoloff L. Movement and composition of interstitial fluid of cartilage. *Arthritis Rheum*. 1965;8(4):481-494. doi:10.1002/art.1780080402

48. Buckwalter J a., Mankin H j. Articular cartilage Part I: Tissue design and chondrocyte-matix interactions. *J Bone Jt Surgury*. 1997;79(4):600-611.

49. Goldring MB, Marcu KB. Cartilage homeostasis in health and rheumatic diseases. *Arthritis Res Ther*. 2009;11(3):224. doi:10.1186/ar2592

50. Mow VC, Ratcliffe A, Robin Poole A. Cartilage and diarthrodial joints as paradigms for hierarchical materials and structures. *Biomaterials*. 1992;13(2):67-97. doi:10.1016/0142-9612(92)90001-5

51. Las Heras F, Gahunia HK, Pritzker KPH. Articular Cartilage Development: A Molecular Perspective. *Orthop Clin North Am*. 2012;43(2):155-171. doi:10.1016/j.ocl.2012.01.003

52. Doherty M, Buckwalter J a, Mankin HJ, Grodzinsky AJ. Articular cartilage and osteoarthritis. *Instr Course Lect*. 2005;54(9):465-480. doi:10.1136/ard.51.9.1028-a

53. Poole CA. Articular cartilage chondrons: form, function and failure. *J Anat*. 1997;191 (Pt 1:1-13. doi:10.1046/j.1469-7580.1997.19110001.x

54. Sophia Fox AJ, Bedi A, Rodeo SA. The Basic Science of Articular Cartilage: Structure, Composition and Function. *Orthopaedics*. 2009;1(6):461-468. doi:10.1177/1941738109350438

55. Schuurman W, Klein TJ, Dhert WJA, VanWeeren PR, Hutmacher DW, Malda J. Cartilage regeneration using zonal chondrocyte subpopulations: a promising approach or an overcomplicated strategy? *J Tissue Eng Regen Med*. 2012;9(6):669-678. doi:10.1002/term

56. Setton LA, Zhu W, Mow VC. The biphasic poroviscoelastic behavior of articular cartilage: Role of the surface zone in governing the compressive behavior. *J Biomech*. 1993;26(4-5):581-592. doi:10.1016/0021-9290(93)90019-B

57. Bullough PG, Jagannath A. The morphology of the calcification front in articular cartilage. Its significance in joint function. *J Bone Jt Surg Br*. 1983;65(1):72-78.

58. Burr DB. Anatomy and physiology of the mineralized tissues: Role in the pathogenesis of osteoarthrosis. *Osteoarthr Cartil*. 2004;12(SUPLL.):20-30. doi:10.1016/j.joca.2003.09.016

59. Bs PAT, Skalak A, Cooperman DR. Proximal Femoral Anatomy in the Normal Human Population. 2009:876-885. doi:10.1007/s11999-008-0473-3

60. Siebenrock KA, Ferner F, Noble PC, Santore RF, Werlen S, Mamisch TC. The cam-type deformity of the proximal femur arises in childhood in response to vigorous sporting activity. *Clin Orthop Relat Res*. 2011;469(11):3229-3240. doi:10.1007/s11999-011-1945-4

61. Pollard TCB, Batra RN, Judge A, et al. The hereditary predisposition to hip osteoarthritis and its association with abnormal joint morphology. *Osteoarthr Cartil*. 2013;21(2):314-321. doi:10.1016/j.joca.2012.10.015

62. Goodman D, Feighan J, Smith A, Latimer, Buly R, Cooperman D. Subclinical slipped capital femoral epiphysis. Relationship to osteoarthrosis of the hip. *J Bone Jt Surg Am*. 1997;79(10):1489-1497.

63. Agricola R, Bessems JHJM, Ginai a. Z, et al. The Development of Cam-Type Deformity in Adolescent and Young Male Soccer Players. *Am J Sports Med*. 2012;40(5):1099-1106. doi:10.1177/0363546512438381

64. Kapron AL, Anderson AE, Aoki SK, et al. Radiographic prevalence of femoroacetabular impingement in collegiate football players: AAOS Exhibit Selection. *J bone Jt surgery*. 2011;93-A(19):e111(1-10). doi:10.2106/JBJS.K.00544

65. Mathew G, Kowalczuk M, Hetaimish B, et al. Radiographic prevalence of CAM-type femoroacetabular impingement after open reduction and internal fixation of femoral neck fractures. *Knee Surgery, Sport Traumatol Arthrosc*. 2014;22(4):793-800. doi:10.1007/s00167-014-2835-6

66. Wendt MC, Cass JR, Trousdale RR. Incidence of Radiographic Cam-Type Impingement in Young Patients (<50) After Femoral Neck Fracture Treated with Reduction and Internal Fixation. *HSS J*. 2013;9(2):113-117. doi:10.1007/s11420-012-9325-5

67. Leunig M, Casillas MM, Hamlet M, et al. Slipped capital femoral epiphysis: early mechanical damage to the acetabular cartilage by a prominent femoral metaphysis. *Acta Orthop Scand*. 2000;71(4):370-375. doi:10.1080/000164700317393367

68. Klit J, Gosvig K, Magnussen E, et al. Cam deformity and hip degeneration are common after

fixation of a slipped capital femoral epiphysis. *Acta Orthop*. 2014;85(6):585-591. doi:10.3109/17453674.2014.957078

69. Beck M, Kalhor M, Leunig M, Ganz R. Hip morphology influences the pattern of damage to the acetabular cartilage: femoroacetabular impingement as a cause of early osteoarthritis of the hip. *J Bone Joint Surg Br*. 2005;87(7):1012-1018. doi:10.1302/0301-620X.87B7.15203

70. Jamali AA, Mladenov K, Meyer DC, et al. Anteroposterior Pelvic Radiographs to Assess Acetabular Retroversion: High Validity of the "'Cross-over-Sign."' *J Orthop Res*. 2007;25(6):758-65. doi:10.1002/jor

71. Li P, Ganz R. Morphologic Features of Congenital Acetabular Dysplasia. *Clin Orthop Relat Res*. 2003;(416):245-253. doi:10.1097/01.blo.0000081934.75404.36

72. Leunig PL, Schoenecker MB, Millis JC, et al. A Systematic Approach to the Plain Radiographic Evaluation of the Young Adult Hip. *J Bone Jt Surg Am*. 2008;90(4):47-66. doi:10.2106/JBJS.H.00756

73. Fadul D, Carrino J. Imaging of femoroacetabular impingement. *J Bone Joint Surg Am*. 2009;91(1):138-143. doi:10.2106/JBJS.H.01449

74. Pascual-Garrido C, Schrock JB, Mitchell JJ, Camino Willhuber G, Mei-Dan O, Chahla J. Arthroscopic Fixation of Os Acetabuli Technique: When to Resect and When to Fix. *Arthrosc Tech*. 2016;5(5):e1155-e1160. doi:10.1016/j.eats.2016.07.001

75. Klaue K, Durnin C, Ganz R. The acetabular rim syndrome. A clinical presentation of dysplasia of the hip. *J Bone Jt Surg Br*. 1991;73(3):423-429.

76. Thomas Byrd JW. Femoroacetabular impingement in athletes, part 1: cause and assessment. *Sports Health*. 2010;2(4):321-333. doi:10.1177/1941738110368392

77. Johnston TL, Schenker ML, Briggs KK, Philippon MJ. Relationship Between Offset Angle Alpha and Hip Chondral Injury in Femoroacetabular Impingement. *Arthroscopy*. 2008;24(6):669-675. doi:10.1016/j.arthro.2008.01.010

78. Henak CR, Ateshian G a, Weiss JA. Finite element prediction of transchondral stress and strain in the human hip. *J Biomech Eng*. 2014;136(2):021021. doi:10.1115/1.4026101

79. Beck M, Leunig M, Parvizi J, Vincent B, Daniel W, Ganz R. Anterior Femoroacetabular Impingement Part II. Midterm Results of Surgical Treatment. *Clin Orthop Relat Res*. 2004;418(1):67-73. doi:10.1097/00003086-200401000-00012

80. Martin DE, Tashman S. The biomechanics of femoroacetabular impingement. *Oper Tech Orthop*. 2010;20(4):248-254. doi:10.1053/j.oto.2010.09.015

81. Outerbridge RE. Etiology of chondromalacia patellae. *J Bone Jt Surg Br*. 1961;43:752-757.

82. Amenabar T, Piriz J, Mella C, Hetaimish BM, O'Donnell J. Reliability of 3 Different Arthroscopic Classifications for Chondral Damage of the Acetabulum. *Arthroscopy*. 2015;31(8):1492-1496. doi:10.1016/j.arthro.2015.02.029

83. Nepple JJ, Larson CM, Smith M V., et al. The reliability of arthroscopic classification of acetabular rim labrochondral disease. *Am J Sports Med*. 2012;40(10):2224-2229. doi:10.1177/0363546512457157

84. Konan S, Rayan F, Meermans G, Witt J, Haddad FS. Validation of the classification system for acetabular chondral lesions identified at arthroscopy in patients with femoroacetabular impingement. *J Bone Joint Surg Br*. 2011;93(3):332-336. doi:10.1302/0301-620X.93B3.25322

85. Telleria JJM, Lindsey DP, Giori NJ, Safran MR. An anatomic arthroscopic description of the hip capsular ligaments for the hip arthroscopist. *Arthroscopy*. 2011;27(5):628-636. doi:10.1016/j.arthro.2011.01.007

86. Harris-Hayes M, Commean PK, Patterson JD, Clohisy JC, Hillen TJ. Bony abnormalities of the hip joint: a new comprehensive, reliable and radiation-free measurement method using magnetic resonance imaging. *J Hip Press Surg*. 2014;1(2):62-70. doi:10.1093/jhps/hnu009

87. Jackson TJ, Stake CE, Trenga AP, Morgan J, Domb BG. Arthroscopic Technique for Treatment of Femoroacetabular Impingement. *Arthrosc Tech*. 2013;2(1):e55-e59. doi:10.1016/j.eats.2012.10.005

88. Byrd JWWT, Philippon M, Stubbs A, et al. Arthroscopic Management of Femoroacetabular Impingement. *Oper Tech Sports Med*. 2011;19(9):81-94. doi:10.1053/j.otsm.2010.10.006

89. Ilizaliturri VM, Byrd JWTT, Sampson TG, et al. A Geographic Zone Method to Describe Intra-articular Pathology in Hip Arthroscopy: Cadaveric Study and Preliminary Report. *Arthroscopy*. 2008;24(5):534-539. doi:10.1016/j.arthro.2007.11.019

90. Schmid MR, Nötzli HP, Zanetti M, Wyss TF, Hodler J. Cartilage Lesions in the Hip: Diagnostic Effectiveness of MR Arthrography. *Radiology*. 2003;226(2):382-386. doi:10.1148/radiol.2262020019

91. Anderson LA, Peters CL, Park BB, Stoddard GJ, Erickson JA, Crim JR. Acetabular Cartilage Delamination in Femoroacetabular Impingement. *J Bone Jt Surgery-American Vol*. 2009;91(2):305-313. doi:10.2106/JBJS.G.01198

92. Hesper T, Bulat E, Bixby S, et al. Both 3-T dGEMRIC and Acetabular-Femoral T2 Difference May Detect Cartilage Damage at the Chondrolabral Junction. *Clin Orthop Relat Res*. 2017;475(4):1058-1065. doi:10.1007/s11999-016-5136-1

93. Lattanzi R, Petchprapa C, Ascani D, et al. Detection of cartilage damage in femoroacetabular impingement with standardized dGEMRIC at 3T. *Osteoarthr Cartil*. 2014;22(3):447-456. doi:10.1016/j.joca.2013.12.022

94. Jazrawi LM, Alaia MJ, Chang G, Fitzgerald EF, Recht MP. Advances in magnetic resonance imaging of articular cartilage. *J Am Acad Orthop Surg*. 2011;19(7):420-429. doi:19/7/420 [pii]

95. Surowiec RK, Lucas EP, Ho CP. Quantitative MRI in the evaluation of articular cartilage health: Reproducibility and variability with a focus on T2 mapping. *Knee Surgery, Sport Traumatol Arthrosc*. 2014;22(6):1385-1395. doi:10.1007/s00167-013-2714-6

96. Rehnitz C, Kupfer J, Streich NA, et al. Comparison of biochemical cartilage imaging techniques at 3T MRI. *Osteoarthr Cartil*. 2014;22(10):1732-1742. doi:10.1016/j.joca.2014.04.020

97. Imaging H, Zanetti M, Pfirrmann CW a., Sutter R, Zanetti M, Pfirrmann CW a. New Developments in Hip Imaging. *Radiology*. 2012;264(3):651-667. doi:10.1148/radiol.12110357

98. Byrd JWWT. Arthroscopic Management of Femoroacetabular Impingement. *Oper Tech Sports Med*. 2011;19(2):81-94. doi:10.1053/j.otsm.2010.10.006

99. Larson CM, Wulf CA. Intraoperative Fluoroscopy for Evaluation of Bony Resection During Arthroscopic Management of Femoroacetabular Impingement in the Supine Position. *Arthrosc - J Arthrosc Relat Surg*. 2009;25(10):1183-1192. doi:10.1016/j.arthro.2009.07.020

100. Larson CM, Giveans MR. Arthroscopic Debridement Versus Refixation of the Acetabular Labrum Associated With Femoroacetabular Impingement. *Arthrosc J Arthrosc Relat Surg*. 2011;27(5):e49. doi:10.1016/j.arthro.2011.03.040

101. Philippon MJ, Stubbs AJ, Schenker ML, Maxwell RB, Ganz R, Leunig M. Arthroscopic Management of Femoroacetabular Impingement. *Am J Sports Med*. 2007;35(9):1571-1580. doi:10.1177/0363546507300258

102. Espinosa N, Rothenfluh D, Beck M, Ganz R, Leunig M. Treatment of femoroacetabular impingement: preliminary results of labral refixation. *J Bone Jt Surg*. 2006;88:925-935.

103. McCarthy JC, Lee J-A. Arthroscopic intervention in early hip disease. *Clin Orthop Relat Res*. 2004;429:157-162. doi:10.1097/01.blo.0000150118.42360.1d

104. Logan ZS, Redmond JM, Spelsberg SC, Jackson TJ, Domb BG. Chondral Lesions of the Hip. *Clin Sports Med*. 2016;35(3):361-372. doi:10.1016/j.csm.2016.02.005

105. Sampson TG. Arthroscopic Treatment for Chondral Lesions of the Hip. *Clin Sports Med*. 2011;30(2):331-348. doi:10.1016/j.csm.2010.12.012

106. Suarez-Ahedo C, Pavan Vemula S, Stake CE, et al. What are the current indications for use of radiofrequency devices in Hip arthroscopy? A systematic review: Table I. *J Hip Preserv Surg*. 2015;2(4):323–331. doi:10.1093/jhps/hnv055

107. Barber FA, Uribe JW, Weber SC. Current applications for arthroscopic thermal surgery. *Arthrosc J Arthrosc Relat Surg*. 2002;18(2):40-50. doi:10.1053/JARS.2002.31794

108. Gill TJ, Asnis PD, Berkson EM. The Treatment of Articular Cartilage Defects Using the Microfracture Technique. *J Orthop Sport Phys Ther*. 2006;36(10):728-738. doi:10.2519/jospt.2006.2444

109. Frisbie DD, Morisset S, Ho CP, Rodkey WG, Steadman JR, McIlwraith CW. Effects of calcified cartilage on healing of chondral defects treated with microfracture in horses. *Am J Sports Med*. 2006;34(11):1824-1831. doi:10.1177/0363546506289882

110. Williams GM, Chan EF, Temple-Wong MM, et al. Shape, loading, and motion in the bioengineering design, fabrication, and testing of personalized synovial joints. *J Biomech*. 2010;43(1):156-165. doi:10.1016/j.jbiomech.2009.09.021

111. Stanish WD, McCormack R, Forriol F, Mohtadi N, Pelet S, Desnoyers J et al. Novel scaffold-based BST-CarGel® treatment results in superior cartilage repair compared with microfracture in a randomized controlled trial. *J Bone Jt Surg Am*. 2013;95:1640-1650.

112. Shive MS, Stanish WD, McCormack R, et al. BST-CarGel® Treatment Maintains Cartilage Repair Superiority over Microfracture at 5 Years in a Multicenter Randomized Controlled Trial. *Cartilage*. 2015;6(2):62-72. doi:10.1177/1947603514562064

113. Tey M, Mas J, Pelfort X, Monllau JC. Arthroscopic treatment of hip chondral defects with bone marrow stimulation and BST-CarGel. *Arthrosc Tech*. 2015;4(1):e29-e33. doi:10.1016/j.eats.2014.10.002

114. Mauro CS, Voos JE, Kelly BT. Femoroacetabular impingement surgical techniques. *Oper Tech Orthop*. 2010;20(4):223-230. doi:10.1053/j.oto.2010.10.004

115. Ross JR, Bedi A, Stone RM, et al. Intraoperative Fluoroscopic Imaging to Treat Cam Deformities. *Am J Sports Med*. 2014;42(6):1370-1376. doi:10.1177/0363546514529515

116. Gédouin J-E. Arthroscopic treatment of femoroacetabular impingement: Technical review. *Orthop Traumatol Surg Res*. 2012;98(5):583-596. doi:10.1016/j.otsr.2012.06.001

117. Harris JD, Brand JC, Cote MP, Faucett SC, Dhawan A. The Significance of Statistics and Perils of Pooling. Part 1 : Clinical Versus Statistical Significance. *Arthrosc J Arthrosc Relat Surg*. 2017;33(6):1102-1112. doi:10.1016/j.arthro.2017.01.053

118. Ramisetty N, Kwon Y, Mohtadi N. Patient-reported outcome measures for hip preservation surgery-a systematic review of the literature. *J hip Preserv Surg*. 2015;2(1):15-27. doi:10.1302/2046-3758.47.2000380

119. Harris-Hayes M, McDonough CM, Leunig M, Lee CB, Callaghan JJ, Roos EM. Clinical outcomes assessment in clinical trials to assess treatment of femoroacetabular impingement: use of patient-reported outcome measures. *J Am Acad Orthop Surg*. 2013;21(1):S39-S46. http://www.ncbi.nlm.nih.gov/pubmed/23818190.

120. Kemp JL, Collins NJ, Roos EM, Crossley KM. Psychometric properties of patient-reported outcome measures for hip arthroscopic surgery. *Am J Sports Med*. 2013;41(9):2065-2073. doi:10.1177/0363546513494173

121. Lodhia P, Slobogean GP, Noonan VK, Gilbart MK. Patient-reported outcome instruments for femoroacetabular impingement and hip labral pathology: A systematic review of the clinimetric evidence. *Arthroscopy*. 2011;27(2):279-286. doi:10.1016/j.arthro.2010.08.002

122. Tijssen M, Van Cingel R, Van Melick N, De Visser E. Patient-reported Outcome questionnaires for hip arthroscopy: A systematic review of the psychometric evidence. *BMC Musculoskelet Disord*. 2011;12:117-124. doi:10.1186/1471-2474-12-117

123. Strauss EJ, Barker JU, Kercher JS, et al. Augmentation Strategies following the Microfracture Technique for Repair of Focal Chondral Defects. *Cartilage*. 2010;1(2):145-152. doi:10.1177/1947603510366718

124. Mithoefer K, Williams RJ, Warren RF, et al. The Microfracture Technique for the Treatment of Articular Cartilage Lesions in the Knee. *J Bone Jt Surg Am*. 2005;87:1911-1920. doi:10.2106/JBJS.D.02846

125. MacDonald AE, Bedi A, Horner NS, et al. Indications and Outcomes for Microfracture as an Adjunct to Hip Arthroscopy for Treatment of Chondral Defects in Patients With Femoroacetabular Impingement: A Systematic Review. *Arthroscopy*. 2016;32(1):190-200. doi:10.1016/j.arthro.2015.06.041

126. Philippon MJ, Schenker ML, Briggs KK, Maxwell RB. Can Microfracture Produce Repair Tissue in Acetabular Chondral Defects? *Arthrosc J Arthrosc Relat Surg*. 2008;24(1):46-50. doi:10.1016/j.arthro.2007.07.027

127. Karthikeyan S, Roberts S, Griffin D. The American Journal of Sports Medicine Microfracture for Acetabular Chondral Defects in Patients With Femoroacetabular Impingement. 2012. doi:10.1177/0363546512465400

128. Domb BG, Gupta A, Dunne KF, Gui C, Chandrasekaran S, Lodhia P. Microfracture in the Hip. *Am J Sports Med*. 2015;43(8):1865-1874. doi:10.1177/0363546515588174

129. Marquez-Lara A, Mannava S, Howse EA, Stone A V., Stubbs AJ. Arthroscopic Management of Hip Chondral Defects: A Systematic Review of the Literature. *Arthrosc J Arthrosc Relat Surg*. 2016;32(7):1435-1443. doi:10.1016/j.arthro.2016.01.058

130. Fontana A, Bistolfi A, Crova M, Rosso F, Massazza G. Arthroscopic treatment of hip chondral defects: Autologous chondrocyte transplantation versus simple debridement-A pilot study. *Arthrosc - J Arthrosc Relat Surg*. 2012;28(3):322-329. doi:10.1016/j.arthro.2011.08.304

131. Mancini D, Fontana A. Five-year results of arthroscopic techniques for the treatment of acetabular chondral lesions in femoroacetabular impingement. *Int Orthop*. 2014;38(10):2057-2064. doi:10.1007/s00264-014-2403-1

132. Stanish WD, McCormack R, Forriol F, et al. Novel Scaffold-Based BST-CarGel Treatment Results in Superior Cartilage Repair Compared with Microfracture in a Randomized Controlled Trial. *J Bone Jt Surg Am*. 2013;95(18):1640-1650. doi:10.2106/JBJS.L.01345

133. Méthot S, Changoor A, Tran-Khanh N, et al. Osteochondral Biopsy Analysis Demonstrates That BST-CarGel Treatment Improves Structural and Cellular Characteristics of Cartilage Repair Tissue Compared With Microfracture. *Cartilage*. 2016;7(1):16-28. doi:10.1177/1947603515595837

134. Hesper T, Neugroda C, Schleich C, et al. T2*-Mapping of Acetabular Cartilage in Patients With Femoroacetabular Impingement at 3 Tesla: Comparative Analysis with Arthroscopic Findings. *Cartilage*. 2018;9(2):118-126.

135. Ellermann J, Ziegler C, Nissi MJ, et al. Acetabular Cartilage Assessment in Patients with Femoroacetabular Impingement by Using T2* Mapping with Arthroscopic Verification. *Radiology*. 2014;271(2):512-523. doi:10.1148/radiol.13131837

136. Harris JD, McCormick FM, Abrams GD, et al. Complications and reoperations during and after hip arthroscopy: A systematic review of 92 studies and more than 6,000 patients. *Arthrosc - J Arthrosc Relat Surg*. 2013;29(3):589-595. doi:10.1016/j.arthro.2012.11.003

137. Telleria JJ, Safran MR, Gardi JN, Harris AH, Glick JM. Risk of Sciatic Nerve Traction Injury During Hip Arthroscopy-Is It the Amount or Duration? *J Bone Jt Surgery-American Vol*. 2012;94(22):2025-2032. doi:10.2106/JBJS.K.01597

138. Complication AU, Dippmann C, Ph D, et al. Symptoms of Nerve Dysfunction After Hip Arthroscopy: An Under-Reported Complication? *Arthrosc J Arthrosc Relat Surg*. 2014;30(2):202-207. doi:10.1016/j.arthro.2013.11.014

139. Rhee C, Amar E, Glazebrook M, Coday C, Wong IH. Safety Profile and Short-term Outcomes of BST-CarGel as an Adjunct to Microfracture for the Treatment of Chondral Lesions of the Hip. *Orthop J Sport Med*. 2018;6(8):1-6. doi:10.1177/2325967118789871

Escalas de Valoración Funcional
Non Arthritic Hip Score

Paciente: [redacted]

Fecha: 07/06/2017

Escala de **Non Arthritic Hip Score: 0-100/100.** **NAHS 100 : Función Normal**

Cadera: X **DER** □ **IZQ** Meses Postoperatorio: 36

_____

Severidad durante las ultimas 48 HORAS:	**Ninguno (4)**	**Discreto (3)**	**Moderado (2)**	**Severo (1)**	**Extremo (0)**
Dolor al caminar en plano	X				
Dolor al subir y bajar escaleras	X				
Dolor nocturno en la cama	X				
Dolor cuando sentado o tumbado	X				
Dolor al estar de pie		X			
Sensación de captura o bloqueo de la cadera	X				
Sensación de inestabilidad de la cadera	X				
Sensación de rigidez de la cadera		X			
Sensación de disminución de la movilidad de la cadera		X			
Dificultad al bajar escaleras	X				
Dificultad al subir escaleras	X				
Dificultad al levantarse de sentado	X				
Dificultad al ponerse calcetines / medias	X				
Dificultad al levantarse de la cama	X				
Severidad en actividades durante el ULTIMO MES:	**Ninguno (4)**	**Discreto (3)**	**Moderado (2)**	**Severo (1)**	**Extremo (0)**
Dificultad en actividades deportivas de alta exigencia (football, balloncesto, tennis, gimnasia aeróbica)				X	
Dificultad en actividades deportivas de moderada exigencia (golf, bowling)			X		
Dificultad en jogging como entrenamiento			X		
Dificultad en caminar como entrenamiento		X			
Dificultad en labores domesticas pesadas		X			
Dificultad en labores domesticas ligeras		X			

Valoración: _____ x 1,25 = Non Arthritic Hip Score _____ %

IHOT33 INTERNATIONAL HIP OUTCOME TOOL.

(Cuestionario de calidad de vida en personas jóvenes, personas activas con problemas de cadera).

Nombre y apellidos. Día del cuestionario. / /

Fecha de nacimiento.

Cadera: Derecha __X__ Izquierda ____

Instrucciones:

- Cuestionario relativo a problemas que ha experimentado en su cadera, cómo afectan estos problemas a su vida diaria y las emociones relativas a ese problema.

- Por favor, indique la severidad del problema marcando con una cruz encima de la línea de debajo de cada pregunta.

    - Si usted marca al final de la línea a la izquierda, se siente especialmente afectado. Por ejemplo:

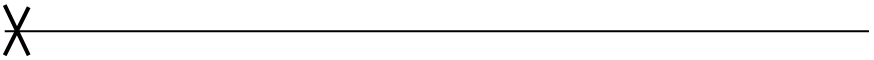

SIGNIFICATIVAMENTE AFECTADO — NINGUN PROBLEMA TODO CORRECTO

    - Si usted marca al final de la línea a la derecha, representa que no tiene el más mínimo problema en su cadera. Por ejemplo:

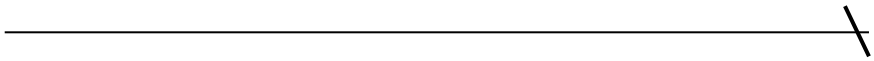

SIGNIFICATIVAMENTE AFECTADO — NINGUN PROBLEMA TODO CORRECTO

    - Si usted marca en el medio de la línea, indica que usted tiene un dolor o problema moderado, o en otras palabras, entre los extremos de “especialmente afectado” y “ningún problemas”. Es importante no marcar en los extremos de las líneas si usted no se encuentra en una situación extrema.

- Por favor, conteste a las preguntas describiendo su situación en el último mes.

SECCIÓN 1. SINTOMAS Y LIMITACIONES FUNCIONALES.

Las preguntas se refieren a síntomas que usted experimenta en su cadera y sobre la funcionalidad de ella respecto a las actividades de la vida diaria. Por favor, piense en cómo se ha sentido durante el último mes y responda las siguientes preguntas.

Q1. Con que frecuencia tiene dolor en la cadera/ingle?

CONSTANTEMENTE NUNCA

Q2. Cómo nota de rígida la cadera después de estar sentado / parado a lo largo del día?

EXTREMADAMENTE RÍGIDA NADA RÍGIDA

Q3. Cuánta dificultad tiene para andar largas distancias?

MUCHA DIFICULTAD NADA DE DIFICULTAD

Q4. Cuánto le duele la cadera al estar sentado/a?

MUCHO DOLOR NADA DE DOLOR

Q5. Cuánta dificultad tiene para estar de pie largos períodos de tiempo?

MUCHA DIFICULTAD NADA DE DIFICULTAD

Q6. Cuánta dificultad tiene para levantarse o estirarse al suelo?

MUCHA DIFICULTAD NADA DE DIFICULTAD

Q7. Cuánta dificultad tiene para andar por terreno irregular?

MUCHA DIFICULTAD NADA DE DIFICULTAD

Q8. Cuánta dificultad tiene para estar apoyado sobre la cadera afecta?

MUCHA DIFICULTAD NADA DE DIFICULTAD

Q9. Cuánta dificultad tiene para superar obstáculos?

MUCHA DIFICULTAD NADA DE DIFICULTAD

Q10. Cuánta dificultad tiene para subir o bajar escaleras?

MUCHA DIFICULTAD NADA DE DIFICULTAD

Q11. Cuánta dificultad tiene para levantarse de una silla?

MUCHA DIFICULTAD NADA DE DIFICULTAD

Q12. Cuánta dificultad le supone hacer pasos largos al andar?

MUCHA DIFICULTAD — NADA DE DIFICULTAD

Q13. Cuánta dificultad le supone subir o bajar del coche?

MUCHA DIFICULTAD — NADA DE DIFICULTAD

Q14. Cuántos problemas en relación a chasquidos o crujidos tiene en su cadera?

MUCHOS — NINGUNO

Q15. Cuánta dificultad tiene para ponerse/sacarse los calcetines, medias o zapatos?

MUCHA DIFICULTAD — NADA DE DIFICULTAD

Q16. En general, cuánto dolor tiene en su cadera/ingle?

DOLOR EXTREMO — NADA DE DOLOR

SECCIÓN 2. DEPORTES Y ACTIVIDADES RECREATIVAS.

Las siguientes preguntas son sobre su cadera cuando usted participa en deportes o actividades lúdicas. Por favor, piense en cómo se ha sentido durante el último mes y responda las siguientes preguntas.

Q17. Cómo se preocupa usted acerca de la capacidad para mantener su nivel deseado de deporte?

EXTREMADAMENTE PREOCUPADO — NADA PREOCUPADO

Q18. Cuánto dolor experimenta en su cadera después de la actividad física?

DOLOR EXTREMO — NADA DE DOLOR

Q19. Cuánto le preocupa que el dolor de la cadera incremente si usted participa en deportes / actividades recreativas?

EXTREMADAMENTE PREOCUPADO — NADA PREOCUPADO

Q20. Cuánto se le ha deteriorado la calidad de vida al no poder participar en deportes /actividades recreativas?

EXTREMADAMENTE DETERIORADA — NADA DETERIORADA

Q21. Cuánto le preocupa sobre el hecho de cambiar de dirección mientras hace deporte / actividades recreativas?

☑ Yo no realizó estas acciones en mis actividades

EXTREMADAMENTE PREOCUPADO NADA PREOCUPADO

Q22. Cuánto ha disminuido su rendimiento en el deporte /actividad lúdica?

HAN DISMINUIDO EXTREMADAMENTE NO HAN DISMINUIDO NADA

SECCIÓN 3. RELACIONADAS CON EL TRABAJO LABORAL

Las siguientes cuestiones son acerca de cómo le afecta su cadera en su actividad laboral. Por favor, piense en cómo se ha sentido durante el último mes y responda las siguientes preguntas.

Q23. Cuánto le cuesta poner, traccionar, levantar o cargar objetos pesados en el trabajo?

☐ Yo no realizó estas acciones en mis actividades

SEVERO PROBLEMA NO ES UN PROBLEMA

Q24. Cuánto le cuesta ponerse en cuclillas o agacharse?

SEVERO PROBLEMA NO ES UN PROBLEMA

Q25. Cuánto le preocupa que su cadera empeore por su trabajo?

EXTREMADAMENTE PREOCUPADO NADA PREOCUPADO

Q26. Cuánto le dificulta poder realizar su trabajo correctamente la disminución de la movilidad de la cadera?

MUCHA DIFICULTAD NADA DE DIFICULTAD

SECCIÓN 4. ASPECTOS DEL ESTILO DE VIDA, SOCIAL, EMOCIONAL.

Las siguientes cuestiones son acerca de cómo le afecta su cadera en su vida social, emocional y a su estilo de vida. Por favor, piense en cómo se ha sentido durante el último mes y responda las siguientes preguntas.

Q27. Cómo de frustrado se siente por su problema de cadera?

EXTREMADAMENTE FRUSTRADO NADA FRUSTRADO

Q28. Cuánto se ve dificultada su actividad sexual a causa de su problema de cadera?

SEVERO PROBLEMA NO ES UN PROBLEMA

Q29. Cuánta distracción le provoca su problema de cadera?

EXTREMADA DISTRACCIÓN NO LE DISTRAE NADA

Q30. Cuánto le cuesta liberar su tensión y estrés por su problema de cadera?

MUCHA DIFICULTAD NADA DE DIFICULTAD

Q31. Cómo de desanimado/a está por su problema de cadera?

EXTREMADAMENTE DESANIMADA NADA DESANIMADA

Q32. Cuánto le preocupa el hecho de coger o cargar los niños por su problema de cadera?

☐ Yo no realizó estas acciones en mis actividades

EXTREMADAMENTE PREOCUPADO NADA PREOCUPADO

Q33. Durante cuánto tiempo usted es consciente de su problema de cadera?

CONSTANTEMENTE NUNCA

ESCALA DE CADERA PARA LAS ACTIVIDADES DE LA VIDA DIARIA.

RESPONDA **TODAS LAS PREGUNTAS** CON **UNA SOLA RESPUESTA** LA QUE CORRESPONDA A SU SITUACIÓN EN LOS ÚLTIMOS DÍAS.
SI HA HABIDO ALGUNA COSA QUE NO HA PODIDO REALIZAR DEBIDO A OTRAS CAUSAS DIFERENTES A SU CADERA MARQUE **NA.**

	Ninguna dificultad	Dificultad leve	Dificultad Moderada	Dificultad extrema	Incapaz de hacerlo	No Responde
Estar de pie durante 15 minutos	**x**					
Entrar y salir de un coche normal	**x**					
Ponerse calcetines y zapatos	**x**					
Subir caminando por terrenos empinados		**x**				
Bajar caminando por terrenos empinados		**x**				
Subir un tramo de escaleras		**x**				
Bajar un tramo de escaleras		**x**				
Subir y bajar los bordillos de las aceras	**x**					
Ponerse en cuclillas agachándose lo máximo posible		**x**				
Entrar y salir de la bañera	**x**					
Estar sentado durante 15 minutos	**x**					
Empezar a caminar	**x**					
Caminar durante 10 minutos aproximadamente	**x**					
Caminar durante 15 minutos o más		**x**				

A causa de su cadera, ¿qué grado de dificultad tiene para realizar las actividades siguientes?

	Ninguna dificultad	Dificultad leve	Dificultad Moderada	Dificultad extrema	Incapaz de hacerlo	No Responde
Girar/pivotar sobre la pierna afectada		**x**				
Darse la vuelta en la cama		**x**				
Efectuar trabajos ligeros o moderados (estar de pie, caminar)		**x**				
Efectuar trabajos pesados (empujar/arrastrar, subirse a sitios, cargar pesos)			**x**			
Realizar actividades de ocio				**x**		

¿Como puntuaría usted de 0 a 100 su nivel actual de funcionamiento durante sus actividades de la vida diaria habituales (siendo 100 el nivel de funcionamiento antes de su problema de cadera y 0 la incapacidad para realizar cualquiera de sus actividades de la vida diaria habituales)?
□□□%

Subescala de deportes A causa de su cadera, ¿qué grado de dificultad tiene para realizar las
actividades siguientes?

	Ninguna dificultad	Dificultad leve	Dificultad Moderada	Dificultad extrema	Incapaz de hacerlo	No Responde
Correr 1,5 km					**x**	
Saltar				**x**		
Balancear un objeto, como un palo de golf		**x**				
Caer sobre los pies tras un salto		**x**				
Echar a correr y pararse rápidamente			**x**			
Efectuar cambios de dirección / movimientos laterales			**x**			
Efectuar actividades de bajo impacto como caminar deprisa		**x**				
Capacidad para ejecutar la actividad con su técnica habitual					**x**	
Capacidad para practicar el deporte que desee durante el tiempo que quiera					**x**	

¿Cómo puntuaría de 0 a 100 su nivel actual de funcionamiento en las actividades relacionadas con el deporte (siendo 100 su nivel de funcionamiento antes de su problema de cadera y 0 la incapacidad para realizar cualquiera de sus actividades de la vida diaria habituales)?
□□□%
¿Cómo puntuaría su nivel actual de funcionamiento?

Normal **Casi Normal** Anormal Muy anormal

Case 1

C/H: male patient 41 years old presented with left groin pain related to daily activities, duration of 2 years. BMI 24 kg/m^2, Tegner level 5 (recreational sports-Jogging)

Ex.: +ve impingement, FADIR and DIRI tests. Infiltration test positive

Preoperative X-ray: Alpha angle 75° and H-N offset 4mm (Cam).

MRA: labral tear and chondral injury in the anterosuperior zone

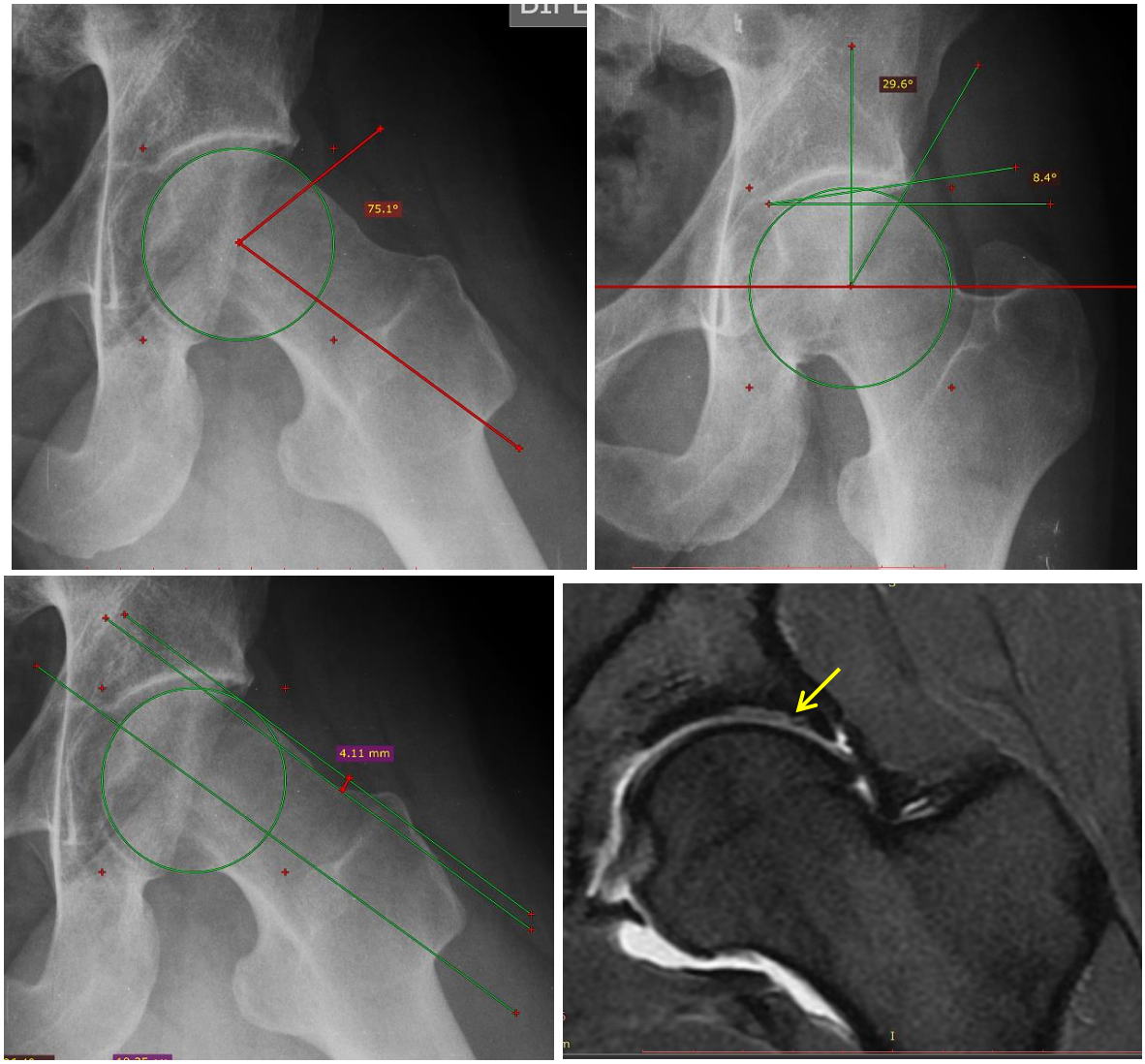

Arthroscopic finding: torn labrum between 12 and 2 o'clock. Delaminated chondral flap was found in zone 2 with exposed subchondral bone (Outerbridge & Beck Grade 4). Cam deformity was identified in the anterolateral head-neck junction.

Arthroscopic treatment: repair of the torn labrum was performed. The defect size was 3 cm^2 involving zones 2 & 3. The acetabular chondral lesion was treated by

debridement and microfracture and then it was filled by chitosan-based scaffold. The Cam deformity was resected.

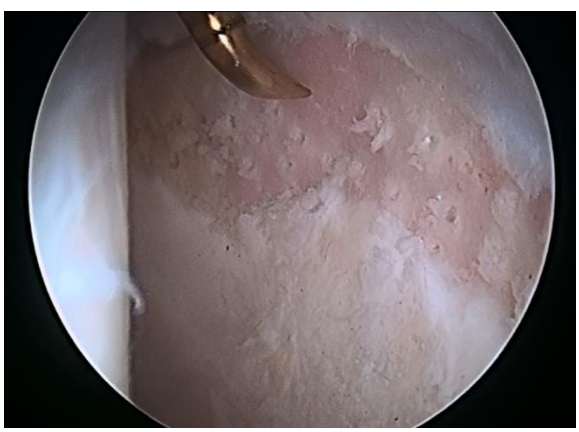

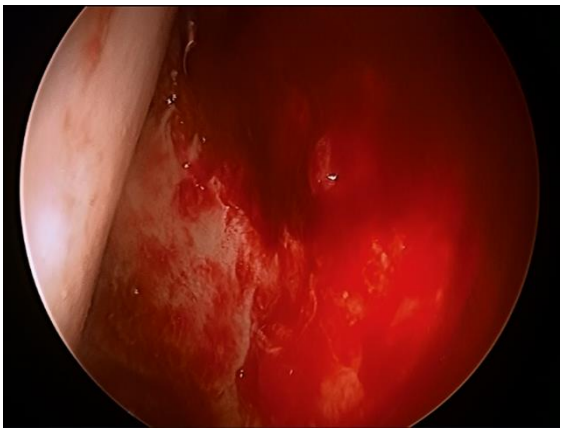

Postoperative X-ray: adequate resection of the Cam deformity (alpha angle 44° and H-N offset 7 mm)

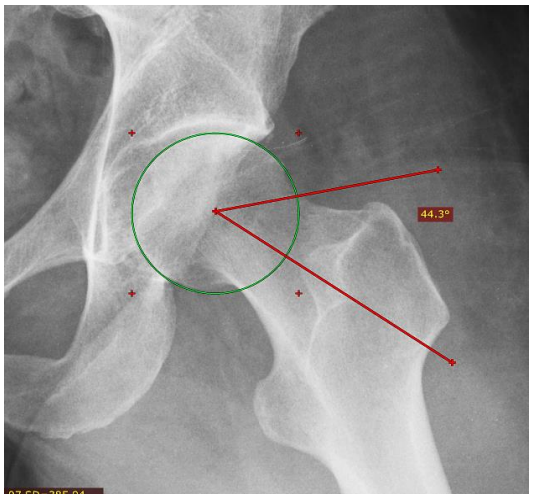

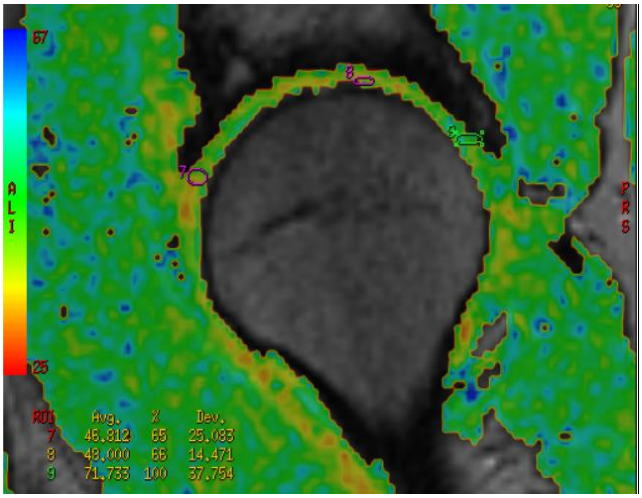

Preoperative scores:
NAHS=49, iHOT-33=37, HOS-ADL=42, and HOS-sports=29

Period of recovery:
No adverse events

Postoperative scores at 12 months:
NAHS=75, iHOT-33=68, HOS-ADL=81, and HOS-sports= 64

Case 2

C/H: male patient 35 years old presented with right groin pain related to sports activity, duration of one year. BMI 22 kg/m^2, Tegner level 5 (competitive cycling)

Ex.: +ve impingement, decompression, FADIR and DIRI tests.

Preoperative X-ray: Alpha angle 73° and H-N offset 5mm (Cam).

MRA: labral tear and chondral injury in the anterosuperior zone

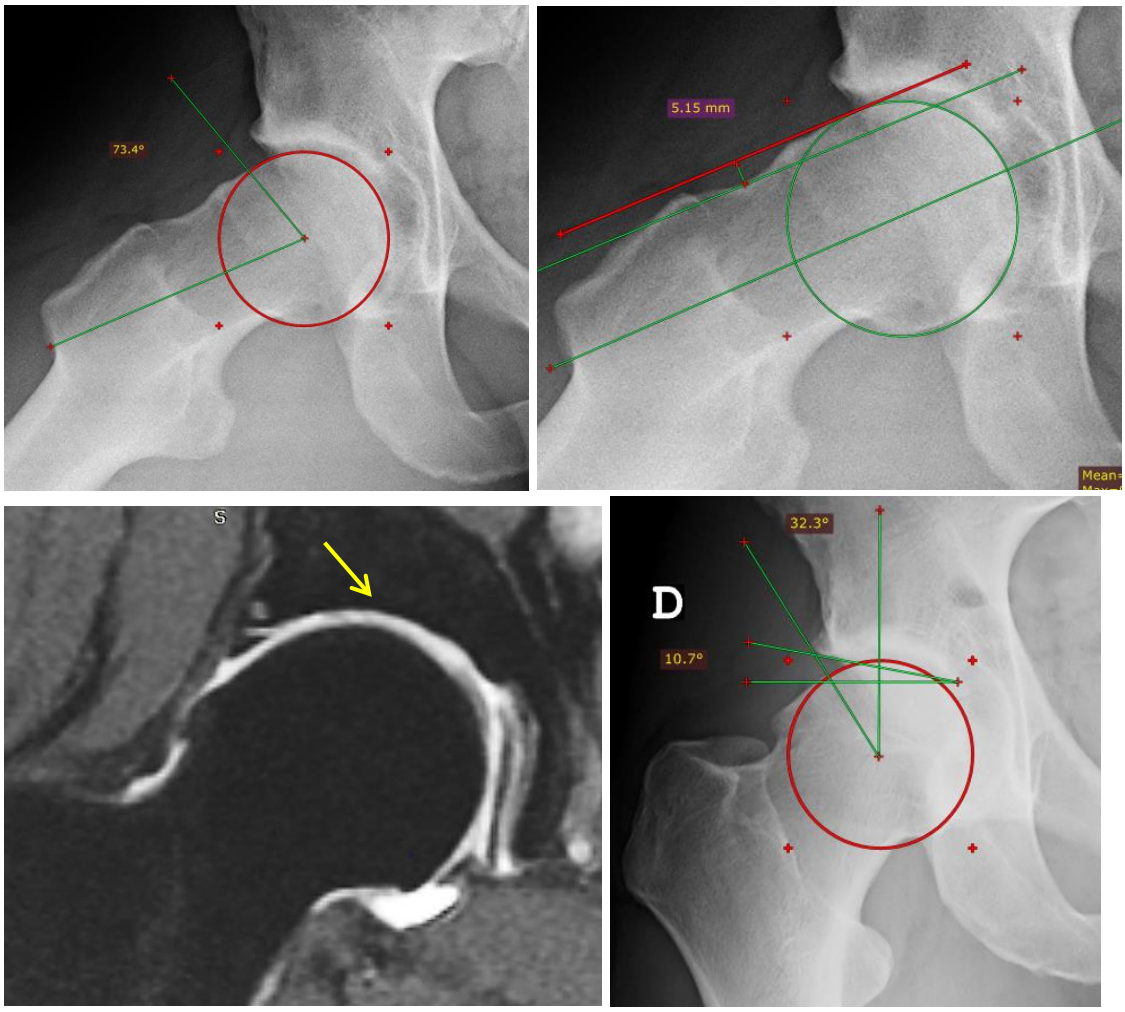

Arthroscopic finding: torn labrum between 11 and 2 o'clock. Delaminated chondral flap with exposed subchondral bone (Outerbridge & Beck Grade 4) was found. Cam deformity was identified in the anterolateral head-neck junction.

Arthroscopic treatment: repair of the torn labrum was performed. After debridement and microfracture, the defect size was 3.5 cm^2 involving zones 2 & 3. The defect was filled by chitosan-based scaffold to augment the microfracture. The Cam deformity was resected.

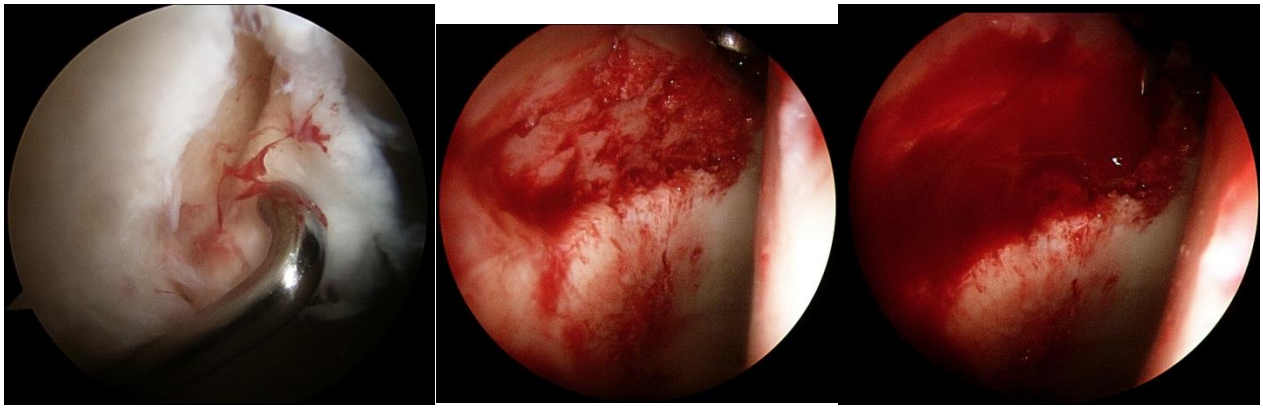

Postoperative X-ray: adequate resection of the Cam deformity (alpha angle 42° and H-N offset 8 mm)

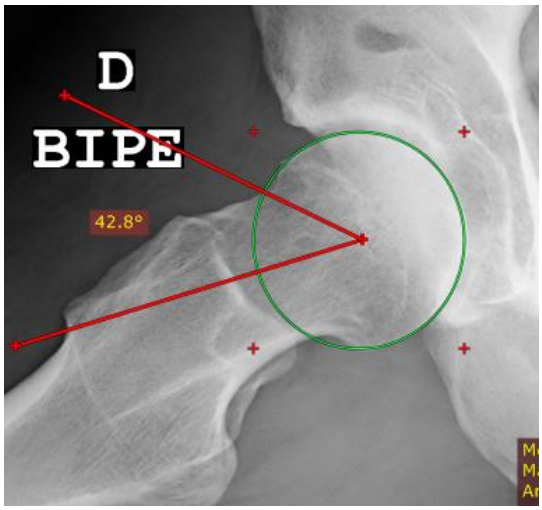

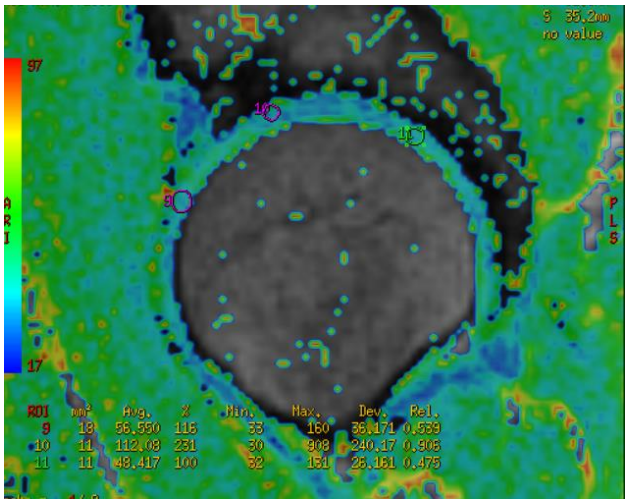

Preoperative scores:
NAHS=31, iHOT-33=28, HOS-ADL=40, and HOS-sports=49

Period of recovery:
The patient had perineal hypoesthesia which resolved spontaneously after 4 weeks

Postoperative scores at 12 months:
NAHS=82, iHOT-33=85, HOS-ADL=91, and HOS-sports=78

Case 3

C/H: male patient 39 years old, presented with right groin pain affecting his daily activities, exaggerated by sports, onset of 30 months. BMI 23 kg/m^2, Tegner level 7 (recreational sports-football)

Ex.: limited ROM mainly internal rotation, +ve impingement, FADIR and DIRI.

Preoperative X-ray: Alpha angle 81° and H-N offset 4mm (Cam), joint space preserved.

MRA: labral tear and chondral injury in the anterosuperior zone

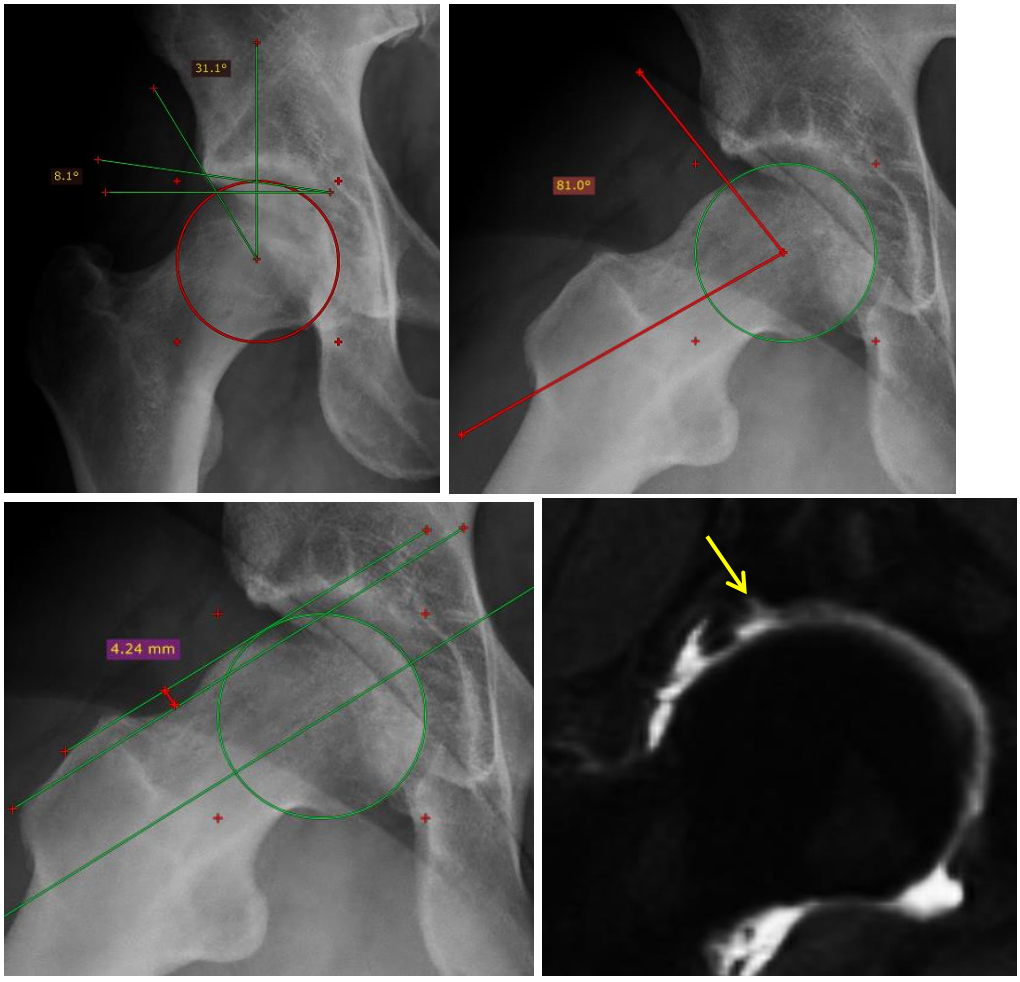

Arthroscopic finding: torn labrum between 12 and 2 o'clock. Delaminated chondral flap with exposed subchondral bone (Outerbridge & Beck Grade 4) was found. Cam deformity was identified in the anterolateral head-neck junction.

Arthroscopic treatment: repair of the torn labrum was performed. After debridement and microfracture, the defect size was 3 cm^2 involving zones 1 & 2. The defect was filled by chitosan-based scaffold to augment the microfracture. The Cam deformity was resected.

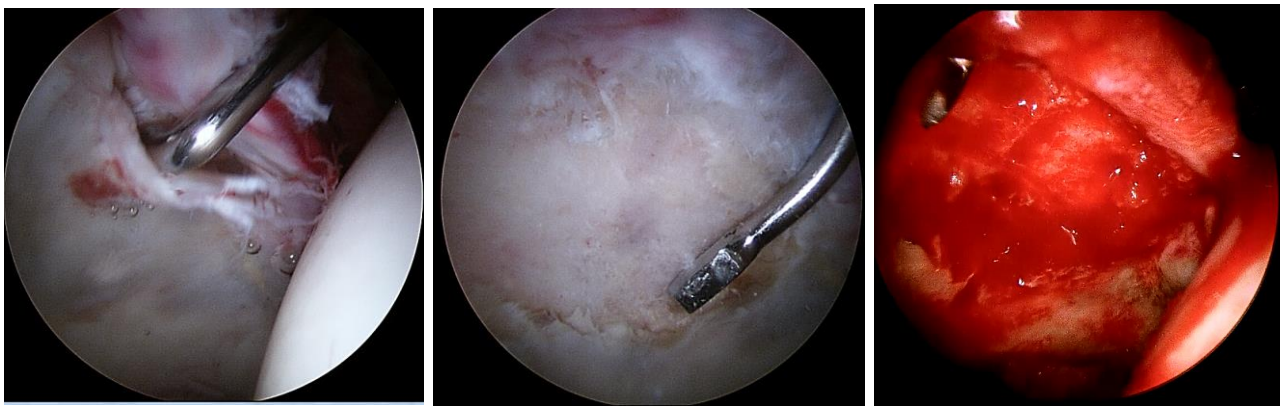

Postoperative X-ray: adequate resection of the Cam deformity (alpha angle 39° and H-N offset 10 mm)

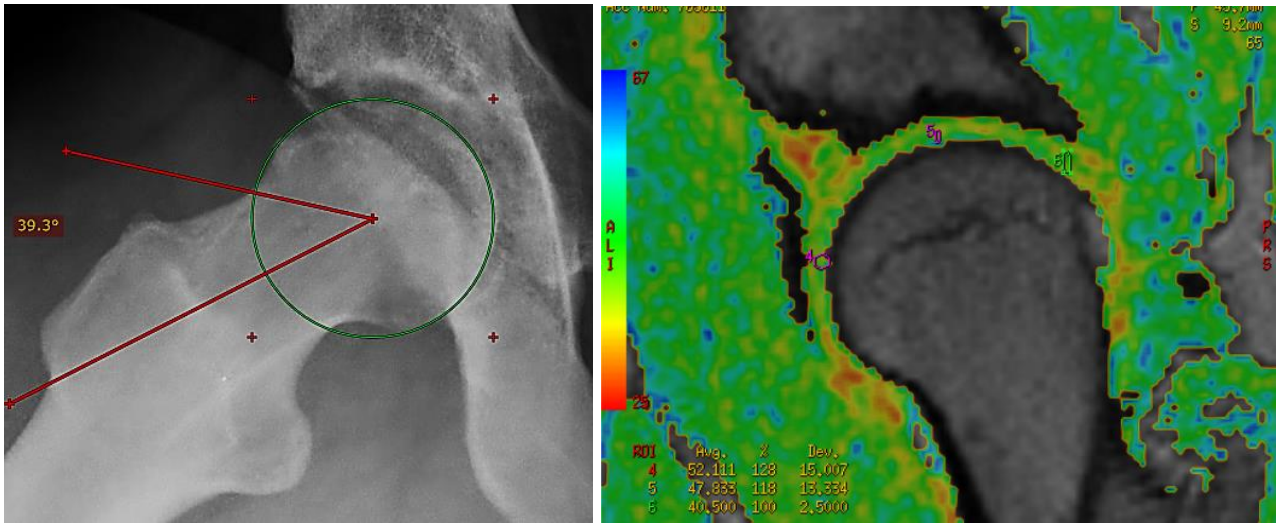

Preoperative scores:
NAHS=29, iHOT-33=22, HOS-ADL=31, and HOS-sports=18

Period of recovery:
The patient had perineal hypoesthesia which resolved spontaneously after 2 weeks

Postoperative scores at 12 months:
NAHS=88, iHOT-33=84, HOS-ADL=95, and HOS-sports=75

Arthroscopic Repair of Acetabular Cartilage Lesions by Chitosan-Based Scaffold: Clinical Evaluation at Minimum 2 Years Follow-up

Mahmoud Fathy Tahoun, M.Sc., Marc Tey, M.D., Ph.D., Jesús Mas, M.D., Taher Abd-Elsattar Eid, M.D., Ph.D., and Joan Carles Monllau, M.D., Ph.D.

Purpose: To evaluate the functional outcome of using chitosan-based material in our patients after 2 years of follow-up. **Methods:** Nonarthritic nondysplastic femoroacetabular impingement patients with an acetabular chondral lesion, 18 to 55 years of age, were included for arthroscopic repair between May 2013 and July 2015. Full-thickness chondral defects $\geq$2 cm^2 were filled with chitosan-based implant after microfractures. Follow-up consisted of alpha angle assessment and clinical outcome in the form of the Non Arthritic Hip Score (NAHS), International Hip Outcome Tool 33 (iHOT33), Hip Outcome Score of Activities of Daily Living (HOS-ADL), and Hip Outcome Score of Sports Specific Scale (HOS-SSS). **Results:** Twenty-three patients were included. The mean follow-up was 38.4 $\pm$ 7.0 months (range, 24-50 months). The mean defect size was 3.5 $\pm$ 1.0 cm^2, principally involving zone 2 and to a lesser extent in zones 1 and 3. Using femoroplasty, the alpha angle was corrected from a mean 70.5 $\pm$ 6.3° to 44.3 $\pm$ 4.9° (P = .00001). Significant improvement occurred comparing the preoperative to the first-year postoperative patient-reported outcomes: P = .00001 for the NAHS, P = .00004 for the iHOT33, P = .00005 for the HOS-ADL, and P = .0002 for the HOS-SSS. No statistically significant change has been observed in the patient-reported outcomes obtained at the endpoint when compared with the first-year values (P = .13 for the NAHS, P = .21 for the HOS-ADL, and P = .29 for the HOS-SSS), except for the iHOT33, which showed further significant improvement (P = .02). Up to 91% of the patients met or exceeded the minimal clinically important difference. One patient needed total hip arthroplasty. Perineal hypoesthesia occurred in 3 patients, who recovered within 2 to 6 weeks, and 1 patient needed a prolonged physiotherapy program for postoperative muscular stiffness. **Conclusions:** The arthroscopic combined treatment of microfractures and chitosan-based scaffold has maintained satisfactory clinical outcomes in 91% of the patients with a large ($\geq$2 cm^2) full-thickness acetabular chondral defect associated with femoroacetabular impingement at a mean follow-up of 38.4 months. The study could not definitely draw any conclusion regarding the safety of chitosan-based material for use in the hip joint. **Level of Evidence:** Level IV, case series.

See commentary on page 2829

Acetabular cartilage damage occurs in association with femoroacetabular impingement (FAI) owing to the abnormal shear stresses, mostly in the anterosuperior area, leading to chondral delamination and labral tears.[1,2] This continuous pathologic process in young active patients may lead to early osteoarthritis.[3]

Lesion size and severity are considered primary determining factors for the strategy of management and the expected prognosis.[4,5] One of the treatment procedures is the technique of microfractures, which depends on stimulation of the subchondral bone marrow through liberating the progenitor cells, and finally formation of a fibrocartilage patch that covers the defect, but this fibrocartilage tissue has poor biomechanical properties.[6,7] When the defect is large in size, the fibrocartilage repair patch tends to shrink over time and separate from the surrounding structures.[7,8]

Scaffold augmentation techniques have emerged to enhance the biomechanical and biochemical properties

From the Department of Orthopedics, Menoufia University (M.F.T., T.A-E.E.), Egypt; Department of Orthopedics, Parc de Salut Mar, Universitat Autònoma de Barcelona (M.F.T., M.T., J.C.M.), Barcelona; Department of Orthopedics, Hospital Vistahermosa (J.M.), Alicante; and Hip Unit, iMove Traumatologia, Clínica Mitrestorres (M.T.), Barcelona, Spain.

The authors report that they have no conflicts of interest in the authorship and publication of this article. Full ICMJE author disclosure forms are available for this article online, as supplementary material.

Received January 7, 2018; accepted June 10, 2018.

Address correspondence to Mahmoud Fathy Tahoun, M.Sc., Hospital de l'Esperanca, Sant Josep de la Muntanya, 12, 08024 Barcelona, Spain. E-mail: mftahoon@hotmail.com

0749-8063/1838/$36.00

https://doi.org/10.1016/j.arthro.2018.06.037

of cartilage repair tissue after microfractures. Different scaffold materials, such as polyglycolic acid/hyaluronan, chitosan-glycerol phosphate blood, and chondroitin sulfate/hydrogel composites, have been studied in experimental animal trials and have shown a significant improvement in the mechanical properties and a histologic structure similar to the native cartilage.[8-11] Clinical trials of chitosan-based scaffold for treating chondral defects in the femoral condyle of human knees showed adequate safety for clinical practice and presented favorable histologic and functional results.[12,13]

In our work, we used the technique of scaffold augmentation, using chitosan-based implant, for treatment of large full-thickness acetabular cartilage lesions associated with FAI. This study was conducted to evaluate the functional outcome of using chitosan-based material in our patients after 2 years of follow-up. Depending on the previous studies, we hypothesized that the technique will give satisfactory clinical results and improvement in the patient-reported outcome (PRO) scores.

Methods

Patient Selection

From May 2013 to July 2015, we included patients between 18 and 55 years old who had a clinical diagnosis and radiologic evidence of FAI associated with an acetabular chondral lesion. Exclusion criteria were inflammatory joint disease, radiologic signs of osteoarthritis (Tönnis grade $\geq$2), or hip dysplasia (lateral center edge angle of Wiberg $<25^\circ$, acetabular index angle of Tönnis $>10^\circ$). Final inclusion in the study was decided during the arthroscopic procedure when the patient had a full-thickness acetabular cartilage lesion $\geq$2 cm^2 after adequate debridement.

Arthroscopic treatment was indicated primarily for patients who presented with groin pain related to hip motion and a clinical examination suggestive of impingement (limited range of motion [ROM], mainly internal rotation, and tests for flexion, adduction, and internal rotation, flexion abduction external rotation, and dynamic internal rotation, as well as the dynamic external rotatory impingement test).[14,15] Diagnosis was confirmed by radiologic assessment. Initially, plain radiographs in the standard anteroposterior view and 45° Dunn lateral view were obtained. The lateral center edge angle of Wiberg and acetabular index angle were measured in the anteroposterior view to exclude dysplastic cases. The alpha angle was measured in the 45° Dunn view (which correlates with the 1:00-2:00 o'clock position) to determine the cam morphology.[16,17] All patients were investigated preoperatively by magnetic resonance angiography to evaluate the labrum and the articular cartilage.

All patients who had indications for the procedure and met the inclusion criteria received an adjuvant treatment of the acetabular chondral lesion by microfracture and chitosan-based scaffold, in addition to treatment of the underlying FAI. Primary treatment of FAI consisted of arthroscopic femoroplasty for cam deformity, acetabuloplasty for pincer impingement, and repair of associated labral tears.[18-20] All patients participating in the study provided a written informed consent after fulfilling the rules of the Ethical Committee of Clinical Research.

Surgical Technique

The technique of application of chitosan-based implant has been described by Tey et al.,[21] which provided a guide for the surgical procedure in the current study. The operations were performed by 2 senior surgeons (M.T., J.M.), who strictly followed the original technique and steps. Diagnostic hip arthroscopy began with exploration of the central compartment with the patient in the supine position, and appropriate traction was applied to the operating limb. The acetabular cartilage was classified according to the Outerbridge classification[22] (as a standard method) and Beck's system[1] (as a hip-specified system). Full-thickness acetabular cartilage lesions (Outerbridge IV or Beck's III, IV) were treated by full debridement and microfracture (Figs 1 and 2). A motorized shaver and a curette were used for removal of the damaged cartilage and exposure of subchondral bone, then microfractures were performed by 60° arthroscopic awl with a depth of 2 to 3 mm every 5 mm through the entire defect. After adequate debridement, the size of the defect was measured by a calibrated arthroscopic probe and the

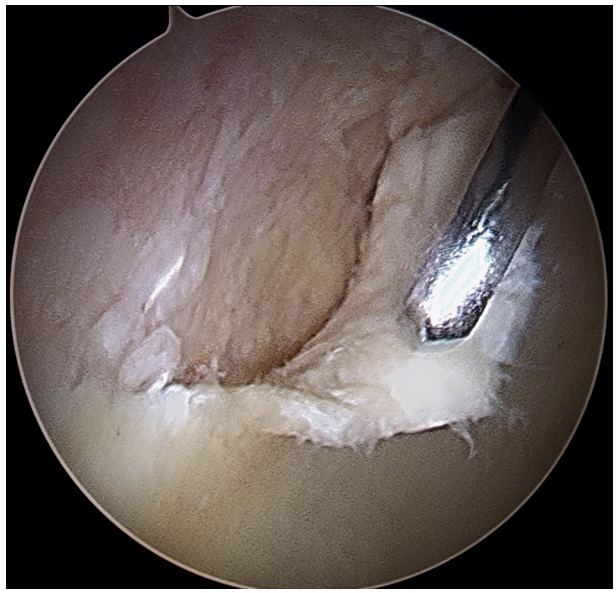

Fig 1. Arthroscopic image of a right hip (viewed from the anterolateral portal) demonstrating delaminated chondral flap in the acetabular cartilage involving zone 2. A full-thickness lesion can be seen exposing the subchondral bone.

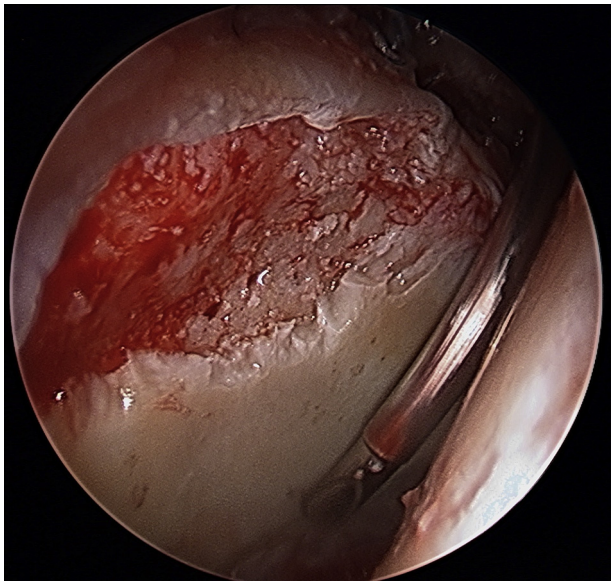

Fig 2. Arthroscopic image of a right hip (viewed from the anterolateral portal) after debridement and microfractures of the chondral defect. Stable chondral margins and bleeding base with bone punctures.

lesion was localized according to the geographic zone method.[23] Lesions $\geq$2 cm^2 were further treated by the chitosan-based scaffold material at the end of the procedure. Pincer impingement was corrected by acetabuloplasty, and labral tears were repaired by suture anchors (3-5 based on the extent of the lesion), then traction of the limb was released to access the peripheral compartment. For better visualization, the capsule was opened in a T-fashion, which facilitates proper identification and resection of the cam deformity.

The chitosan-based implant (BST-CarGel; Smith & Nephew, London, UK) material was prepared, according to manufacturer instructions, by mixing the components with the patient's blood sample to form the final product that was applied to cover the defect.[21] Traction was reapplied to the limb, and fluid was drained outside the joint space; small gauze swabs were delivered inside to dry the defect surface. Once the surface was clean and good vision was obtained, the mixture was applied using a large 18-G needle that was previously bent to direct the drops toward the sloping surface (Fig 3), covering the whole defect with successive layers that consolidate within 15 minutes. Traction was released again. Great attention was given to close the capsule completely, 2 or 3 sutures were applied first at the distal part of the T-capsulotomy, and then 1 or 2 sutures were applied to close the interportal capsulotomy.

Postoperative Rehabilitation

We asked the patients to move the hip passively and then actively from the first day and use crutches for partial weight bearing for $\leq$6 weeks, with a focus on restoration of full ROM. Activity was allowed to be increased gradually as patients tolerated. Return to full sports activities, especially impaction and twisting movements, were avoided the first year after surgery.[12,21] It was not feasible to ensure applying a formal physiotherapy protocol for all patients; however, the previous points were followed precisely.

Postoperative Evaluation

Follow-up visits were scheduled at 6 weeks; 3, 6, and 12 months; and every year. The patients were evaluated for pain, ROM, and signs of impingement (tests for flexion, adduction, and internal rotation, flexion abduction external rotation, and dynamic internal rotation impingement, as well as the dynamic external rotatory impingement test).[14] Postoperative radiographs were obtained at 3 months for assessment of correction in the alpha angle and the acetabular resection. The Non Arthritic Hip Score (NAHS), International Hip Outcome Tool 33 (iHOT33), and Hip Outcome Score of both subscales (Activities of Daily Living [HOS-ADL] and Sports Specific Scale [HOS-SSS]) were collected during the visits before and after the procedure. We planned to assess the short-term and midterm functional outcomes of cartilage management, so the PROs were collected at 12 and 24 months and then yearly until the end of the study.

Statistical Analysis

The mean value and standard deviation (SD) were calculated for each parameter. Statistical analyses were performed using SPSS software version 22 (SPSS, Chicago, IL). The Shapiro-Wilk test was used to evaluate

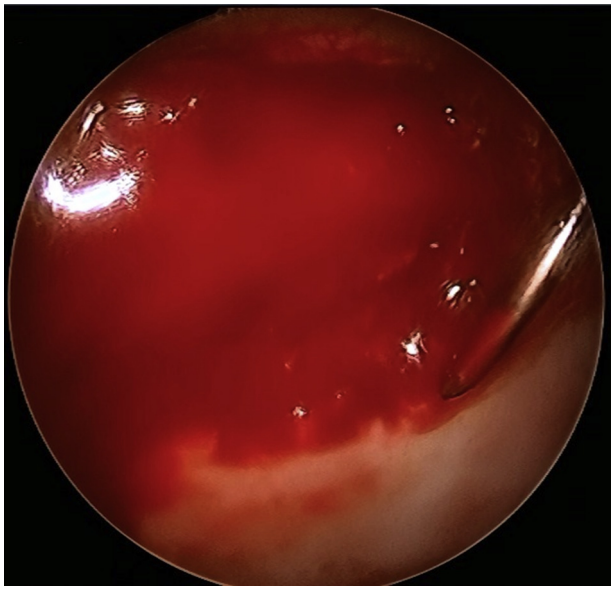

Fig 3. Arthroscopic image of a right hip (viewed from the anterolateral portal) during application of the chitosan–blood mixture by the 18-G needle. The scaffold mixture adheres to the base of the lesion and covers the entire defect.

the data with regard to normality of distribution. Data analysis was performed with the Wilcoxon signed-rank test for comparison of the preoperative and postoperative PROs; $P < .05$ was considered statistically significant.

Results

Twenty-three patients were included in this study—18 men and 5 women. Demographic data including age, body mass index, and Tegner sports level are summarized in Table 1. According to the preoperative evaluation, 15 cases (65%) had cam-type FAI, 8 cases (35%) had mixed type, and no case was diagnosed as pincer-only FAI. The mean preoperative alpha angle was 70.5 ± 6.3°, and the values of the preoperative PROs (mean ± SD) were 55.2 ± 13.4 for the NAHS, 43.1 ± 14 for the iHOT33, 59.7 ± 14.1 for the HOS-ADL, and 30.9 ± 13.9 for the HOS-SSS.

Included patients had a full-thickness acetabular chondral defect with a mean size of 3.5 ± 1 cm^2. Zone 2 was involved in all of the cases; 13 cases extended to zone 3, 2 cases extended to zone 1, and 8 cases were confined to zone 2. The labrum was torn in all patients in the same zones corresponding with the cartilage lesion. Three patients had an associated chondral lesion in the femoral head: 1 had an Outerbridge grade II lesion in zone 2 and was treated by debridement only, whereas the other 2 cases had grade IV lesions in zones 2 and 3 and were treated by microfracture and filling with the same preparation of chitosan-based scaffold.

The postoperative radiographs showed an alpha angle of 44.3 ± 4.9° (mean ± SD). The mean follow-up of the patients was 38.4 ± 7.0 months. Twenty-one patients reported improvement in functional scores within first 12 months and maintained their achieved scores through the follow-up period. Two patients showed no significant change from their baseline levels: 1 patient was 54 years old, with a radiologic image of mild osteoarthritis (Tönnis 1) and an associated chondral lesion (grade IV) in the femoral head, and ultimately required total hip arthroplasty because of the limiting pain; the other patient was 38 years old (Tönnis 1) and had an acetabular chondral defect of 6 cm^2. At month 12, postoperative functional scores (mean ± SD) were 81.9 ± 13.6 for the NAHS, 72.4 ± 16.6 for the iHOT33, 82.6 ± 16.7 for the HOS-ADL, and 64.8 ± 26.3 for the HOS-SSS, and the functional scores obtained at the endpoint of the study (mean ± SD) were 85.6 ± 14.5 for the NAHS, 78.5 ± 15.6 for the iHOT33, 86.7 ± 15.9 for the HOS-ADL, and 70.8 ± 26.2 for the HOS-SSS (Table 2).

Table 1. Demographic and Basic Patient Data

No. of Patients	23	
Male	18 (78%)	
Female	5 (22%)	
Age, yr	40.9 ± 7	(25-54)
BMI	23.8 ± 2.0	(20-27)
Tegner Level	6.0 ± 1.5	(3-10)
Follow-up, mo	38.4 ± 7.0	(24-50)
Cam-type FAI	15 (65%)	
Mixed-type FAI	8 (35%)	
Acetabular Lesions		
Size, cm^2	3.5 ± 1 cm^2	(2-6)
Zone 1	2 (8%)	
Zone 2	23 (100%)	
Zone 3	13 (54%)	
Femoral Head Lesions		
Size	0.7-1.2 cm^2	
Zone 2	2 (8%)	
Zone 3	1 (4%)	

NOTE. Values are n (%) or mean ± standard deviation (range).
BMI, body mass index; FAI, femoroacetabular impingement.

The immediate postoperative period showed normal recovery for all patients without important clinical incidents. For the patients who improved with the intervention, we observed satisfactory rehabilitation progress, namely disappearance of preoperative pain, attainment of full ROM, and negative tests of impingement at the last follow-up. One patient developed periarticular muscular pain and stiffness that improved after 6 months of continuous physiotherapy. Three patients had postoperative perineal hypoesthesia that recovered spontaneously within 2 to 6 weeks. One patient required total hip arthroplasty 2 years after the intervention.

The recently published values of a minimal clinically important difference were used for interpretation of the individual outcomes on each of the used PROs.[24] At the first-year follow-up, 91% of the patients met or exceeded the minimal clinically important difference for the NAHS, iHOT33, and HOS-ADL and 82% for the HOS-SSS. At the endpoint of the follow-up, the proportions were 87% for the NAHS, 91% for the iHOT33 and the HOS-SSS, and 82% for the HOS-ADL. By comparing the final scores with the corresponding first-year values, 13% achieved further improvement on the NAHS, 48% on the iHOT33, and 8% on the HOS-ADL and HOS-SSS (Table 3). Interestingly, 2 male patients had an associated chondral defect (grade IV) in the femoral head and a radiologic image of mild osteoarthritis (Tönnis 1). One of the patients, who was 54 years old, had 24-month postoperative versus preoperative scores as follows: NAHS, 41.3 versus 39; iHOT33, 34 versus 30; HOS-ADL, 45.8 versus 47.0; and HOS-SSS, 5.5 versus 7.0. Ultimately, this patient required total hip arthroplasty 2 years postoperatively because of limiting pain. The other patient, who was 49 years old, had 24-month postoperative versus preoperative scores as follows: NAHS, 87 versus 53; iHOT33, 93 versus 61; HOS-ADL, 100 versus 72; and HOS-SSS, 95 versus 24.

Discussion

Microfractures augmented by chitosan-based scaffold provided satisfactory short-term to midterm outcomes for treatment of large full-thickness acetabular chondral

Table 2. Alpha Angle and PRO Values

	Preoperative	12-Month Follow-up		Endpoint Follow-up	
Alpha Angle					
Mean ± SD	70.5 ± 6.3	44.3 ± 4.9	$P = .00001$		
Range	56-80	34-52			
NAHS					
Mean ± SD	55.2 ± 13.4	81.9 ± 13.6	$P = .00001$	85.6 ± 14.5	$P = .13$
Range	23.7-78.7	41.3-98.7		41.3-100	
iHOT33					
Mean ± SD	43.1 ± 14	72.6 ± 16.6	$P = .00004$	78.5 ± 15.6	$P = .02$
Range	10.8-65.4	34-96.7		34-97.6	
HOS-ADL					
Mean ± SD	59.8 ± 14.1	82.6 ± 16.7	$P = .00005$	86.7 ± 15.9	$P = .21$
Range	24.3-89.5	45.8-100		45.8-100	
HOS-SSS					
Mean ± SD	30.9 ± 13.9	64.8 ± 26.3	$P = .0002$	70.8 ± 26.2	$P = .29$
Range	2.8-55.5	5.5-100		5.5-100	

NOTE. Preoperative values (alpha angle and PROs) are compared with the corresponding 12-month postoperative values. The PROs of the endpoint are compared with the 12-month values.

HOS-ADL, Hip Outcome Score of Activities of Daily Living; HOS-SSS, Hip Outcome Score of Sports Specific Scale; iHOT33, International Hip Outcome Tool 33; NAHS, Non Arthritic Hip Score; PRO, patient-reported outcome; SD, standard deviation.

defects. The results of the current study showed a significant improvement in the 4 PROs of patients during the first year ($P = .00001$ for NAHS, $P = .00004$ for iHOT33, $P = .00005$ for HOS-ADL, and $P = .0002$ for HOS-SSS). The improvement achieved during the first year was maintained through the endpoint of the study. No changes were observed by comparing the endpoint PROs with the corresponding first-year PROs ($P = .13$ for NAHS, $P = .21$ for HOS-ADL, and $P = .29$ for HOS-SSS), except for iHOT33, which showed further significant improvement ($P = .02$). Twenty-one patients (91%) reported improvement. Two patients did not change from their baseline: 1 patient had an associated chondral lesion in the femoral head, and the other patient had an extreme lesion size (6 cm^2) in the acetabulum. The mean age of the patients at time of surgery was 40.9 ± 7.0 years, and most patients were used to performing a moderate or high level of sports activity before reporting the hip complaint (mean Tegner scale of 6.0 ± 1.5); therefore, it was important for those patients to achieve satisfactory results not only regarding the daily activities but also returning to the previous level of sports. Continuous improvement in iHOT33 scores after 2 years would be related to the emotional, social, and recreational parts of the iHOT33 test, which are not present in NAHS or HOS subscales. Thus, the further increase in iHOT33 scores, in our speculation, may reflect both physical and psychological improvement and more satisfaction over time.

Clinical studies of chondral defects of the knee and hip recommend performing microfractures for small focal well-defined lesions <4 cm^2 to obtain good results,[5,25,26] although later studies limit the indication for a lesion area <2 cm^2,[27] particularly in athletic patients seeking to return to their previous activities.[28] Considering these recommendations and the nature of our patients, we decided to apply the chitosan-based material for full-thickness defects ≥2 cm^2 after adequate debridement and a precise microfracture technique. The mean size of the acetabular cartilage defect in our results was 3.5 ± 1.0 cm^2, involving 2 zones (zones 1 and 2 or 2 and 3) or confined to zone 2 only. Consequently, these relatively nonextensive lesions may have contributed to the satisfactory results of this study; supporting this belief, we observed that 1 patient with an extreme defect size (6 cm^2) did not show significant improvement in the PROs through the entire follow-up period. The surgical procedure also may have affected the results, because we could resect the impinging cam deformity properly in all cases with a mean postoperative alpha angle of 44.93 ± 4.90° ($P = .00001$) and repaired the labrum in all of them with suture anchors, using the standard technique for microfracture described by Steadman et al.[29]

The microfracture technique has been used extensively in the knee and provides excellent early results

Table 3. Subjects Who Met or Exceeded the Minimal Clinically Important Difference

	MCID[24]	First Year Postoperatively	Endpoint Postoperatively	
			Overall Change	Year 2 Change
NAHS	10	21 (91)	20 (87)	3 (13)
iHOT33	6.1	21 (91)	21 (91)	11 (48)
HOS-ADL	9	21 (91)	19 (82)	2 (8)
HOS-SSS	6	19 (82)	21 (91)	2 (8)

NOTE. Values are n (proportions) for the PROs used in the first year and at the endpoint of follow-up.

HOS-ADL, Hip Outcome Score of Activities of Daily Living; HOS-SSS, Hip Outcome Score of Sports Specific Scale; iHOT33, International Hip Outcome Tool 33; MCID, minimal clinically important difference: NAHS, Non Arthritic Hip Score; PROs, patient-reported outcomes.

and significant improvement in quality of life; however, long-term follow-up has shown a decline in outcomes and has failed to maintain patient satisfaction.[30,31] Similarly, microfracture as an adjunct to hip arthroscopy for FAI has, in general, positive outcomes in short- to midterm follow-up,[32] but long-term follow-up is not yet available. Comparing the results of microfractures only versus chitosan-augmented microfractures (the study at hand), studies of microfractures in the hip have reported lesions with a mean size smaller than the minimal size in our study, in addition to the variable outcomes. Philippon et al.[33] published a study of 9 patients who underwent revision hip arthroscopy after an average of 20 months of initially being treated with microfracture for acetabular chondral lesions with an average size of 163 mm^2: 8 patients had 95% to 100% coverage of the chondral lesion, and 1 patient had only 25% coverage. Similarly, Karthikeyan et al.[34] performed second-look arthroscopies after an average of 17 months of initial treatment with microfracture and found a mean fill of 96% in 19 of 20 patients who had had acetabular chondral defects with an average size of 154 mm^2. Histologic analysis of full-thickness biopsy revealed that the tissue was primarily fibrocartilage with some staining for type II collagen in the region closest to the bone. In contrast, Domb et al.[35] compared microfractures in a group of 79 patients with full-thickness acetabular chondral lesions with a control group of 158 patients with partial-thickness lesions who did not receive a specific cartilage treatment. The mean age was 44 years, and the mean size of the chondral defect was 189 $\pm$ 98 mm^2; the results revealed no statistically significant difference in postoperative modified Harris Hip Score, HOS-ADL, HOS-SSS, and NAHS scores between the microfracture and control groups, except for the visual analog scale scores at 2 years, which were significantly superior in the control group.

Experimental animal studies attempted to use chitosan-based material as a scaffold to potentiate the biomechanical properties of the repair tissue after microfractures and found a significant similarity between repair tissue and native hyaline cartilage with regard to the content of glycosaminoglycan and arrangement of collagen type II, as well as proper incorporation to the surroundings.[8,10]

Previous clinical studies on chitosan-based implant, although few, support our findings. The same preparation of chitosan-based material has been used previously for treatment of full-thickness cartilage defects in the knee.[12,13] Patients treated with this technique showed significant functional improvement for $\leq$5 years and maintained quantity and quality of the repaired cartilage (percentage of filling and T2 relaxation time) more than patients treated by microfractures only.[12,13] Second-look arthroscopy after 13 months has confirmed the superior results of the chitosan-treated cartilage; better filling, surface quality, and integration to the surroundings and biopsy analysis showed more similarity to native hyaline cartilage, as measured by polarized light microscopy scoring.[36]

With regard to the application of chitosan-based implant in hip pathologies, a preliminary study[37] included quantitative magnetic resonance imaging evaluation of 10 patients after 18 months using similar methods. The results showed >90% filling of the defects with imaging properties comparable to the normal articular cartilage and significant improvement in HOS scores. This short-term and small-volume study provided a promising preliminary result, but it is not sufficient to conclude the clinical effectiveness of this method of cartilage repair.

Limitations

Important limitations to our work are the lack of a control group to compare the results and the wide range of follow-up (24-50 months) at the endpoint of the study. In addition, the cases were operated by 2 senior surgeons (M.T., J.M.), and this factor may be a source of bias, even though both surgeons strictly followed the same technique and steps. An a priori power analysis was not performed, so there is a risk of statistical type 2 error with the small sample size of our study. Because of the small number of patients, we could not definitely conclude the safety of chitosan implant for use in the hip joint. The results can be attributed to several factors, such as nonextensive chondral defects (maximally involving 2 zones), the short preoperative period of symptoms (mean 32.0 $\pm$ 10.4 months), and initial improvement after cam resection and labral repair. Thus, it is difficult to conclude the specific contribution of chitosan-based material in the results.

Conclusions

The arthroscopic combined treatment of microfractures and chitosan-based scaffold has maintained satisfactory clinical outcomes in 91% of the patients with a large ($\geq$2 cm^2) full-thickness acetabular chondral defect associated with FAI at mean follow-up of 38.4 months. However, this study could not definitely draw any conclusion regarding the safety of chitosan-based material for use in the hip joint.

References

1. Beck M, Kalhor M, Leunig M, Ganz R, Surgeon O. Hip morphology influences the pattern of damage to the acetabular cartilage. Femoroacetabular impingement as a cause of early osteoarthritis of the hip. *J Bone Joint Surg Br* 2005;87:1012-1018.
2. Pfirrmann CW, Mengiardi B, Dora C, Kalberer F, Zanetti M, Hodler J. Cam and pincer femoroacetabular impingement: Characteristic MR arthrographic findings in 50 patients. *Radiology* 2006;240:778-785.

3. Ganz R, Leunig M, Leunig-Ganz K, Harris WH. The etiology of osteoarthritis of the hip: An integrated mechanical concept. *Clin Orthop Relat Res* 2008;466:264-272.
4. Marquez-Lara A, Mannava S, Howse EA, Stone AV, Stubbs AJ. Arthroscopic management of hip chondral defects: A systematic review of the literature. *Arthroscopy* 2016;32:1435-1443.
5. Mardones R, Larrain C. Cartilage restoration technique of the hip. *J Hip Preserv Surg* 2016;3:30-36.
6. Yen YM, Kocher MS. Chondral lesions of the hip microfracture and chondroplasty. *Sports Med Arthrosc* 2010;18:83-89.
7. Williams GM, Chan EF, Temple-Wong MM, et al. Shape, loading, and motion in the bioengineering design, fabrication, and testing of personalized synovial joints. *J Biomech* 2010;43:156-165.
8. Hoemann CD, Sun J, McKee MD, et al. Chitosan-glycerol phosphate/blood implants elicit hyaline cartilage repair integrated with porous subchondral bone in microdrilled rabbit defects. *Osteoarthritis Cartilage* 2007;15:78-89.
9. Erggelet C, Endres M, Neumann K, et al. Formation of cartilage repair tissue in articular cartilage defects pretreated with microfracture and covered with cell-free polymer-based implants. *J Orthop Res* 2009;27:1353-1360.
10. Hoemann CD, Hurtig M, Rossomacha E, et al. Chitosan-glycerol phosphate/blood implants improve hyaline cartilage repair in ovine microfracture defects. *J Bone Joint Surg Am* 2005;87:2671-2686.
11. Wang D-A, Varghese S, Sharma B, et al. Multifunctional chondroitin sulphate for cartilage tissue—biomaterial integration. *Nat Mater* 2007;6:385-392.
12. Stanish WD, McCormack R, Forriol F, et al. Novel scaffold-based BST-CarGel® treatment results in superior cartilage repair compared with microfracture in a randomized controlled trial. *J Bone Joint Surg Am* 2013;95:1640-1650.
13. Shive MS, Stanish WD, McCormack R, et al. BST-CarGel® treatment maintains cartilage repair superiority over microfracture at 5 years in a multicenter randomized controlled trial. *Cartilage* 2015;6:62-72.
14. Martin HD, Palmer IJ. History and physical examination of the hip: The basics. *Curr Rev Musculoskelet Med* 2013;6:219-225.
15. Griffin DR, Dickenson EJ, Donnell JO, et al. The Warwick Agreement on femoroacetabular impingement syndrome (FAI syndrome): An international consensus statement. *Br J Sport Med* 2016;50:1169-1176.
16. Barton C, Salineros MJ, Rakhra KS, Beaulé PE. Validity of the alpha angle measurement on plain radiographs in the evaluation of cam-type femoroacetabular impingement. *Clin Orthop Relat Res* 2011;469:464-469.
17. Nepple JJ, Martel JM, Kim YJ, Zaltz I, Clohisy JC. Do plain radiographs correlate with CT for imaging of cam-type femoroacetabular impingement? *Clin Orthop Relat Res* 2012;470:3313-3320.
18. Jackson TJ, Stake CE, Trenga AP, Morgan J, Domb BG. Arthroscopic technique for treatment of femoroacetabular impingement. *Arthrosc Tech* 2013;2:e55-e59.
19. Byrd JWWT. Arthroscopic management of femoroacetabular impingement. *Oper Tech Sports Med* 2011;19:81-94.
20. Philippon MJ, Stubbs AJ, Schenker ML, Maxwell RB, Ganz R, Leunig M. Arthroscopic management of femoroacetabular impingement. *Am J Sports Med* 2007;35:1571-1580.
21. Tey M, Mas J, Pelfort X, Monllau JC. Arthroscopic treatment of hip chondral defects with bone marrow stimulation and BST-CarGel. *Arthrosc Tech* 2015;4:e29-e33.
22. Amenabar T, Piriz J, Mella C, Hetaimish BM, O'Donnell J. Reliability of 3 different arthroscopic classifications for chondral damage of the acetabulum. *Arthroscopy* 2015;31:1492-1496.
23. Ilizaliturri VM, Byrd JWT, Sampson TG, et al. A geographic zone method to describe intra-articular pathology in hip arthroscopy: Cadaveric study and preliminary report. *Arthroscopy* 2008;24:534-539.
24. Harris JD, Brand JC, Cote MP, Faucett SC, Dhawan A. The significance of statistics and perils of pooling. Part 1: Clinical versus statistical significance. *Arthroscopy* 2017;33:1102-1112.
25. Domb BG, El Bitar YF, Lindner D, Jackson TJ, Stake CE. Arthroscopic hip surgery with a microfracture procedure of the hip: Clinical outcomes with two-year follow-up. *Hip Int* 2014;24:448-456.
26. Mithoefer K, McAdams T, Williams RJ, Kreuz PC, Mandelbaum BR. Clinical efficacy of the microfracture technique for articular cartilage repair in the knee: An evidence-based systematic analysis. *Am J Sport Med* 2009;37:2053-2063.
27. Atilla HA, Luo DT, Stubbs AJ. Arthroscopic microfracture of hip chondral lesions. *Arthrosc Tech* 2017;6:e2295-e2299.
28. Mithoefer K. High-impact athletics after knee articular cartilage repair: A prospective evaluation of the microfracture technique. *Am J Sports Med* 2006;34:1413-1418.
29. Steadman JR, Briggs KK, Rodrigo JJ, Kocher MS, Gill TJ, Rodkey WG. Outcomes of microfracture for traumatic chondral defects of the knee: Average 11-year follow-up. *Arthroscopy* 2003;19:477-484.
30. Strauss EJ, Barker JU, Kercher JS, et al. Augmentation strategies following the microfracture technique for repair of focal chondral defects. *Cartilage* 2010;1:145-152.
31. Mithoefer K, Williams RJ, Warren RF, et al. The microfracture technique for the treatment of articular cartilage lesions in the knee. *J Bone Joint Surg Am* 2005;87:1911-1920.
32. MacDonald AE, Bedi A, Horner NS, et al. Indications and outcomes for microfracture as an adjunct to hip arthroscopy for treatment of chondral defects in patients with femoroacetabular impingement: A systematic review. *Arthroscopy* 2016;32:190-200.
33. Philippon MJ, Schenker ML, Briggs KK, Maxwell RB. Can microfracture produce repair tissue in acetabular chondral defects? *Arthroscopy* 2008;24:46-50.
34. Karthikeyan S, Roberts S, Griffin D. Microfracture for acetabular chondral defects in patients with femoroacetabular impingement. *Am J Sports Med* 2012;40:2725-2730.

35. Domb BG, Gupta A, Dunne KF, Gui C, Chandrasekaran S, Lodhia P. Microfracture in the hip. *Am J Sports Med* 2015;43:1865-1874.
36. Méthot S, Changoor A, Tran-Khanh N, et al. Osteochondral biopsy analysis demonstrates that BST-CarGel treatment improves structural and cellular characteristics of cartilage repair tissue compared with microfracture. *Cartilage* 2016;7:16-28.
37. Tahoun M, Shehata TA, Ormazabal I, Mas J, Sanz J, Tey Pons M. Results of arthroscopic treatment of chondral delamination in femoroacetabular impingement with bone marrow stimulation and BST-CarGel®. *SICOT J* 2017;3:51.

This is a post-peer-review, pre-copyedit version of an article published in *Knee Surgery, Sports Traumatology, Arthroscopy* journal. The final authenticated version is available online at DOI: https://doi.org/10.1007/s00167-020-06068-4

Promising radiological outcome after repair of acetabular chondral defects by microfracture augmented with chitosan-based scaffold: mid-term T2 mapping evaluation.

Mahmoud Fathy Tahoun, MD (1, 2)

Marc Tey, MD, PhD (2,4)

Inmacolada Ormazabal, MD (3)

Amro Saber Elsayed, MD (1)

Hatem Galal Said, MD, FRCS (5)

Joan Carles Monllau, MD, PhD (2)

(1) Dep. Of Orthopedics, Menoufia University, Egypt
(2) Dep. Of Orthopedics, Parc de Salut Mar, UAB, Spain
(3) Dep. Of Radiology, Hospital Universitari Dexeus, Spain
(4) Hip Unit, iMove Traumatologia, Clínica Mitrestorres, Spain
(5) Dep. Of Orthopedics, Assiut University, Egypt

Corresponding author:

Mahmoud Fathy Tahoun

mftahoon@hotmail.com

Hospital de l'Esperanca; Sant Josep de la Muntanya, 12, Postal Code 08024, Barcelona, Spain. Telephone: +34933674100

This is a post-peer-review, pre-copyedit version of an article published in *Knee Surgery, Sports Traumatology, Arthroscopy* journal. The final authenticated version is available online at DOI: https://doi.org/10.1007/s00167-020-06068-4

Abstract

Purpose: Radiological evaluation of the repair tissue produced after arthroscopic treatment of acetabular chondral lesions associated with femoroacetabular impingement (FAI) by the chitosan-based scaffold.

Methods: Patients with age of 18 - 55 years, clinical and radiological features of FAI, non-arthritic non-dysplastic hips were selected for arthroscopic treatment. Full thickness acetabular chondral defects were filled with chitosan-based scaffold material after microfracture. T2 mapping has been carried out for all patients after 24 months using a 1.5-T machine. Nine regions of interest (ROIs) were localized of 3 consecutive sagittal slices including the area of repair. T2 relaxation times of ROIs in the repair area have been compared with the corresponding posterior cartilage.

Results: Twenty-one patients; 17 men and 4 women underwent arthroscopic treatment of full-thickness acetabular chondral defects with mean size of 3.6 ± 1 cm^2 (range 2-6 cm^2), Zone 2 was affected in all cases while zone 3 was involved in 13 cases. T2 relaxation values were collected from 189 ROIs for quantitative analysis. Within the peripheral repair area, the mean T2 value was 49.1± 7.2 milliseconds (ms), while ROIs of the central repair area had mean T2 values of 50.2± 7.1 ms. Posterior cartilage showed mean T2 value of 46.2 ± 7.6 ms

Conclusion: Arthroscopic microfracture of large full thickness acetabular chondral defects with chitosan-based scaffold produced a homogenous repair tissue similar to the corresponding native cartilage of the same joint on quantitative T2 mapping at mid-term follow-up. Clinical relevance: Augmentation of the microfracture by chitosan-based scaffold is a promising modality for treatment of large full-thickness acetabular defects.

Level of evidence: Level IV.

This is a post-peer-review, pre-copyedit version of an article published in *Knee Surgery, Sports Traumatology, Arthroscopy* journal. The final authenticated version is available online at DOI: https://doi.org/10.1007/s00167-020-06068-4

Introduction:

Scaffold augmentation techniques have emerged to enhance the biomechanical properties of cartilage repair tissue after bone-marrow stimulation [11]. Chitosan-glycerol phosphate blood has previously shown to improve the quality of cartilage repair with a histological structure more similar to the native hyaline cartilage in animal models[14] as well as humans[15].

With increasing interest in cartilage repair, several magnetic resonance imaging (MRI) modalities have been advanced to provide high accuracy and reliability for evaluation of the articular cartilage and its repair techniques[2, 18, 22]. Delayed gadolinium-enhanced MRI of cartilage (dGEMRIC) and T2 mapping can detect early change in the cartilage matrix composition which precedes any structural damage of the cartilage [9]. T2 mapping assesses the degree of loss of collagen fiber orientation and subsequent increased mobility of water in the matrix[9, 12, 22]. Beside the safety of avoiding contrast injection and the advantage of faster scanning time, T2 mapping has been recommended for evaluation of cartilage repair because of its ability to estimate the restoration of articular zonal structure [8, 16].

Femoroacetabular impingement (FAI) is a common cause of acetabular chondral damage and osteoarthritis at the end stage [5, 10]. This study aimed at evaluating the repair tissue generated in the acetabular chondral defects associated with FAI after arthroscopic microfracture augmented by chitosan-based scaffold using cartilage-specific MRI method. Study population was hypothesized to exhibit favorable interpretation of the quantitative T2 values of the repair tissue in comparison to the native articular cartilage of the same joint.

Material & Methods

This work was conducted after fulfilling the rules of the Ethical Committee of Clinical Research of Hospital Universitario Quirón Dexeus, and obtaining a written informed consent from all participating patients. Between 2013 and 2015, 21 patients with full thickness acetabular chondral lesions associated with FAI have received arthroscopic treatment in the form of debridement and microfracture and application of chitosan-based material as a scaffold for the repair tissue. The patients have been candidates for this strategy of management by fulfilling the specific criteria; age of 18

- 55 years, with clinical and radiological features of FAI, no or mild radiological signs of osteoarthritis (Tönnis grade 0 or 1), no radiological signs of dysplasia (Wiberg angle <25, Tönnis angle > 10º).

Twenty-one patients, 17 men and 4 women, who met the selection criteria, were included in this study. Preoperative evaluation consisted of thorough clinical examination and radiographic assessment (measuring alpha angle, head-neck offset, lateral center edge angle of Wiberg and acetabular index angle of Tönnis). MR arthrography was routinely performed to detect the associated chondrolabral damage. By arthroscopic exploration, acetabular cartilage has been classified according to the Outerbridge and Beck's scores; patients with full-thickness acetabular cartilage lesion (Outerbridge IV or Beck's III, IV) were treated by full debridement and microfracture. Cartilage defect size was considered as either small (< $2cm^2$) or large (≥ 2 cm^2). The actual defect size was determined during arthroscopy after debridement. According to the available evidence at that time, defects < $2cm^2$ were effectively treated with microfractures only, while larger defects showed inferior long-term results. Thus, patients with small chondral defects (< $2cm^2$) were not included in the current study. According to the geographic zones of the acetabulum[7], Zone 2 was affected in all cases while zone 3 was involved in 13 cases.

After the standard microfracture, focal chondral lesions measured ≥ 2 cm^2 finally were supplemented by adding the chitosan-based material (BST-CarGel®). Labrum has been repaired for preexisting tear or reattached after acetabuloplasty indicated for pincer impingement. The peripheral compartment was addressed for femoroplasty. The capsule was closed by two or three sutures at the conclusion of the surgery. Partial weight-bearing with crutches and passive hip joint movements have been recommended for the patients from the first postoperative day, then gradually increased active exercises were allowed as tolerated, however, sports involving impacting or pivoting movements were avoided during the first year.

MRI studies were performed with a 1.5 Tesla Machine (Achieva; Philips; Netherland) 24 months after surgery. Studies included the following sequences: Axial fast-spin-echo (FSE) T2-weighted with fat saturation, Axial oblique FSE T1-weighted with fat

saturation, coronal FSE T2-weighted, sagittal FSE T2-weighted with fat saturation and sagittal fast spin-echo T1-weighted. MRI follow-up consisted of the T2 mapping and recording the T2 values of the cartilage repair tissue in comparison to the values of the healthy articular cartilage from the same joint. Nine regions of interest (ROIs) were localized manually at the acetabular articular cartilage of 3 consecutive sagittal slices including the area of repair. In each sagittal slice, two ROIs have been carefully drawn at different sites in the repair area anteriorly guided by reviewing the previously obtained preoperative MRA images and arthroscopic pictures, one of them close to the chondrolabral junction and the second one was more central. The third ROI was located at the apparently healthy posterior cartilage as a control for comparison with the repair area. MRI device software presents T2 values in 3 decimals; however, numbers were approximated to one decimal in the results for simplification. The T2 values from these ROIs were recorded and statistically analyzed. Images of all patients were evaluated by a single radiologist (I.O.) specialized in musculoskeletal radiology.

Statistical Analysis

To compare the repair cartilage with the corresponding normal cartilage in the same acetabulum, the average of T2 values from the three anterior ROIs was used as an assessment of the peripheral repair tissue. The same step was performed for the three central and three posterior ROIs to express the central repair and posterior normal acetabular cartilage respectively. Then, the mean value and standard deviation (SD) were calculated for each area in all patients. Shapiro-Wilk's test (p value> 0.05) and visual inspection of their histogram were conducted to assess data normality. Paired student t-tests were performed to compare the means of the peripheral and central repair areas with the posterior normal cartilage taking into account that $P < 0.05$ was considered statistically significant. Statistical analyses were performed using SPSS software version 22 (SPSS, Chicago, IL). Post-hoc analysis has been conducted which showed small sample size.

Results

The basic and demographic data of the patients regarding age, body mass index, Tegner activity level, and distribution of FAI morphology among cases are

demonstrated in Table 1. Arthroscopic procedures showed full-thickness chondral defects in the anterosuperior area of the acetabulum with mean size of 3.6 ± 1 cm^2 (range 2-6 cm^2).

T2 relaxation values were collected from 189 ROIs for quantitative analysis. Within the peripheral repair area, the mean quantitative T2 value was 49.1± 7.2 milliseconds (ms), while ROIs of the central repair area had mean relaxation T2 values of 50.2 ± 7.1 ms. The native posterior cartilage showed mean T2 value of 46.2 ± 7.6 ms (Table 2).

Discussion

The most important finding of the present study was that treatment of large full-thickness acetabular chondral defects with microfracture and chitosan-based scaffold resulted in a repair tissue with radiological features similar to the native hyaline articular cartilage over mid-term follow-up. Quantitative T2 relaxation analysis showed a non-significant difference between the peripheral area of the repair tissue (at the chondrolabral junction) and the native acetabular cartilage posteriorly. Also, a non-significant difference could be observed between the T2 values of the central area of the repair tissue (close to the center of the joint) and the native posterior acetabular cartilage. Specific evaluation of the peripheral area of the repair tissue is of great importance because it is more susceptible to shear forces during hip motions. A relatively wide range of T2 values was observed in the area of healthy posterior cartilage. This could be explained by the wide range of age of the patients (27-51 years) and the different MRI acquisition time (24 - 38 months). Other possibility is that the T2 records have been collected 2 years after the arthroscopic treatment; such long periods may involve change of the previous normal condition of the cartilage.

The value of T2 mapping for assessment of the acetabular cartilage in symptomatic FAI patients has been proved in different studies. According to Hesper et al[6], T2 values obtained from arthroscopically normal cartilage were significantly higher than the values of regions with cartilage degeneration. These results are consistent with Ellermann et al [3] who found a strong correlation between acetabular cartilage damage and decreased T2 values in patients with FAI symptoms.

Subchondral bone is one of the important parameters evaluated with cartilage repair methods [1, 4, 13]. Our technique considered careful protection of the subchondral bone during the microfracture procedure. This has been reflected on the MRI images obtained after 2 years which showed preserved integrity of the subchondral lamina with no edema, overgrowth or cyst formation. The radiological results of the current study go with the clinical outcomes previously reported in FAI patients received this technique for management of large focal chondral defect in non-arthritic, non-dysplastic hips[17, 23, 24]. In a clinical study, the arthroscopic combined treatment of microfractures and chitosan-based scaffold has maintained satisfactory clinical improvement on Hip Outcome Score, International Hip Outcome Tool 33, and Non-Arthritic Hip Score; in 91% of the patients at mean follow-up of 38.4 months[24].

The results of the current study are supported by similar studies conducted on patients with chondral lesions in the knee joint. In an extended multicenter randomized controlled trial, the treatment by BST-CarGel® has shown superior results over the microfracture only technique for chondral lesions in the knee joint regarding the MRI imaging and histologic analysis[15, 19, 20]. T2 mapping at 5 years showed significant difference between BST-CarGel® and microfracture only treated joints. The authors noted that T2 values of the BST-CarGel® group were always closer to the ipsilateral native cartilage T2 values measured in the same session. In another recent study by Steinwachs et al, non-significant change was observed between preoperative and postoperative T2 values after using BST-CarGel® with microfractures in the knee chondral defects[21]. The authors believe this was likely due to the physiological healing process as the images were obtained 6 months after surgery.

The current study has some limitations. Small sample size as showed the Post-hoc analysis. The time for T2 mapping follow-up was not the same for all patients (ranged from 24 to 38 months), so the expected changes in the repair tissue may differ among patients. The study did not include normal patients without FAI symptoms for comparison. Although the apparently normal posterior cartilage has been considered as self-control for comparison, but the minimum 2 years of follow-up may render this normal cartilage pathologic as a disease progression.

Repair of cartilage damage remains a great challenge to any joint preserving surgery. This study showed that patients with large full-thickness acetabular chondral defects, especially associated with FAI, can benefit from the combined treatment of microfracture and chitosan-based scaffold.

Conclusion

Combined arthroscopic microfracture and chitosan-based scaffold for treatment of large full-thickness acetabular chondral defects associated with FAI produced a homogenous repair tissue similar to the corresponding native cartilage of the same joint on quantitative T2 mapping at mid-term follow-up.

References

1. Chen H, Chevrier A, Hoemann CD, Sun J, Ouyang W, Buschmann MD (2011) Characterization of subchondral bone repair for marrow-stimulated chondral defects and its relationship to articular cartilage resurfacing. Am J Sports Med 39:1731–1740

2. Dhollander AAM, Huysse WCJ, Verdonk PCM, Verstraete KL, Verdonk R, Verbruggen G, Almqvist KF (2010) MRI evaluation of a new scaffold-based allogenic chondrocyte implantation for cartilage repair. Eur J Radiol 75:72–81

3. Ellermann J, Ziegler C, Nissi MJ, Goebel R, Hughes J, Benson M, Holmberg P, Morgan P (2014) Acetabular Cartilage Assessment in Patients with Femoroacetabular Impingement by Using T2* Mapping with Arthroscopic Verification. Radiology 271:512–523

4. Flanigan DC, Harris JD, Brockmeier PM, Lathrop RL, Siston RA (2014) The effects of defect size, orientation, and location on subchondral bone contact in oval-shaped experimental articular cartilage defects in a bovine knee model. Knee Surgery, Sport Traumatol Arthrosc 22:174–180

5. Ganz R, Leunig M, Leunig-Ganz K, Harris WH (2008) The etiology of osteoarthritis of the hip: An integrated mechanical concept. Clin Orthop Relat

Res 466:264–272

6. Hesper T, Neugroda C, Schleich C, Antoch G, Hosalkar H, Krauspe R, Zilkens C, Bittersohl B (2018) T2*-Mapping of Acetabular Cartilage in Patients With Femoroacetabular Impingement at 3 Tesla: Comparative Analysis with Arthroscopic Findings. Cartilage 9:118–126

7. Ilizaliturri VM, Byrd JWT, Sampson TG, Guanche CA, Philippon MJ, Kelly BT, Dienst M, Mardones R, Shonnard P, Larson CM (2008) A Geographic Zone Method to Describe Intra-articular Pathology in Hip Arthroscopy: Cadaveric Study and Preliminary Report. Arthroscopy 24:534–539

8. Imaging H, Zanetti M, Pfirrmann CW a., Sutter R, Zanetti M, Pfirrmann CW a. (2012) New Developments in Hip Imaging. Radiology 264:651–667

9. Jazrawi LM, Alaia MJ, Chang G, Fitzgerald EF, Recht MP (2011) Advances in magnetic resonance imaging of articular cartilage. J Am Acad Orthop Surg 19:420–429

10. Kaya M, Suzuki T, Emori M, Yamashita T (2016) Hip morphology influences the pattern of articular cartilage damage. Knee Surgery, Sport Traumatol Arthrosc 24:2016–2023

11. Kon E, Roffi A, Filardo G, Tesei G, Marcacci M (2015) Scaffold-Based Cartilage Treatments: With or Without Cells? A Systematic Review of Preclinical and Clinical Evidence. Arthroscopy 31:767–775

12. Lattanzi R, Petchprapa C, Ascani D, Babb JS, Chu D, Davidovitch RI, Youm T, Meislin RJ, Recht MP (2014) Detection of cartilage damage in femoroacetabular impingement with standardized dGEMRIC at 3T. Osteoarthr Cartil 22:447–456

13. Madry H, van Dijk CN, Mueller-Gerbl M (2010) The basic science of the subchondral bone. Knee Surgery, Sport Traumatol Arthrosc 18:419–433

14. Marchand C, Chen G, Tran-Khanh N, Sun J, Chen H, Buschmann MD, Hoemann CD (2012) Microdrilled Cartilage Defects Treated with Thrombin-Solidified Chitosan/Blood Implant Regenerate a More Hyaline, Stable, and

Structurally Integrated Osteochondral Unit Compared to Drilled Controls. Tissue Eng Part A 18:508–519

15. Méthot S, Changoor A, Tran-Khanh N, Hoemann CD, Stanish WD, Restrepo A, Shive MS, Buschmann MD (2016) Osteochondral Biopsy Analysis Demonstrates That BST-CarGel Treatment Improves Structural and Cellular Characteristics of Cartilage Repair Tissue Compared With Microfracture. Cartilage 7:16–28

16. Rehnitz C, Kupfer J, Streich NA, Burkholder I, Schmitt B, Lauer L, Kauczor HU, Weber MA (2014) Comparison of biochemical cartilage imaging techniques at 3T MRI. Osteoarthr Cartil 22:1732–1742

17. Rhee C, Amar E, Glazebrook M, Coday C, Wong IH (2018) Safety Profile and Short-term Outcomes of BST-CarGel as an Adjunct to Microfracture for the Treatment of Chondral Lesions of the Hip. Orthop J Sport Med 6:1–6

18. Robinson P (2012) Conventional 3-T MRI and 1.5-T MR arthrography of femoroacetabular impingement. Am J Roentgenol 199:509–515

19. Shive MS, Stanish WD, McCormack R, Forriol F, Mohtadi N, Pelet S, Desnoyers J, Méthot S, Vehik K, Restrepo A (2015) BST-CarGel® Treatment Maintains Cartilage Repair Superiority over Microfracture at 5 Years in a Multicenter Randomized Controlled Trial. Cartilage 6:62–72

20. Stanish WD, McCormack R, Forriol F, Mohtadi N, Pelet S, Desnoyers J, Restrepo A, Shive MS (2013) Novel Scaffold-Based BST-CarGel Treatment Results in Superior Cartilage Repair Compared with Microfracture in a Randomized Controlled Trial. J Bone Joint Surg Am 95:1640–1650

21. Steinwachs M, Cavalcanti N, Mauuva Venkatesh Reddy S, Werner C, Tschopp D, Choudur HN (2019) Arthroscopic and open treatment of cartilage lesions with BST-CARGEL scaffold and microfracture: A cohort study of consecutive patients. Knee 26:174–184

22. Surowiec RK, Lucas EP, Ho CP (2014) Quantitative MRI in the evaluation of articular cartilage health: Reproducibility and variability with a focus on T2

291 mapping. Knee Surgery, Sport Traumatol Arthrosc 22:1385–1395

292 23. Tahoun M, Shehata TA, Ormazabal I, Mas J, Sanz J, Tey M (2017) Results of
293 arthroscopic treatment of chondral delamination in femoroacetabular
294 impingement with bone marrow stimulation and BST-CarGel ®. Sicot-J 3:51

295 24. Tahoun M, Tey M, Mas J, Abd-Elsattar Eid T, Monllau JC (2018) Arthroscopic
296 Repair of Acetabular Cartilage Lesions by Chitosan-Based Scaffold: Clinical
297 Evaluation at Minimum 2 Years Follow-up. Arthroscopy 34:2821–2828

298

299

N	21	
male %	17 (81%)	
female %	4 (19%)	
Age	39.4 ± 6.8 yrs.	(27 - 51)
BMI	23.5 ± 2.3 kg/m^2	(20- 28)
Tegner level	6 ± 1	(3 -10)
Follow up	31.3 ± 4.6 m	(24- 38)
CAM-type FAI	14 (67%)	
Mixed-type FAI	7 (33%)	
Acetabular cartilage lesion:		
size	3.6 ± 1 cm^2	(2 - 6)
zone 2	21 (100%)	
zone 3	13 (62%)	

Table 1: Demographic patient data. Values are n (%) or mean ± standard deviation (range). BMI, body mass index; FAI, femoroacetabular impingement

	Normal posterior cartilage	**Repair cartilage**		
		Peripheral	**Central**	**Global**
Mean (ms)	47.1	49.1	50.2	49.8
SD	7.6	7.3	7.2	7.0
Range	36.6 - 69.2	38.5 - 60	37.8 - 64.7	38.2 - 60.8
p-value		n.s. *	n.s. *	n.s. *

Table 2: T2 values (ms=milliseconds) obtained from the normal posterior cartilage and the areas of repair tissue (peripheral, central and global) expressed in mean, standard deviation (SD) and range. Comparisons between the normal and repair cartilage areas are illustrated by the p-value (< 0.05 is statistically significant). *= non-significant (n.s.)

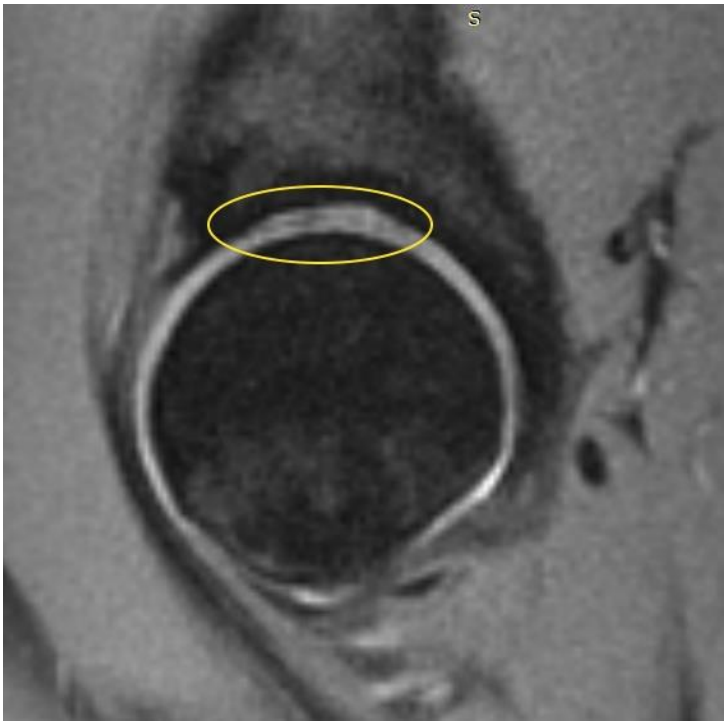

Figure 1: Preopertive MRA image of right hip with acetabular chondral delamination. Sagittal T2 image showing inverted oreo sign

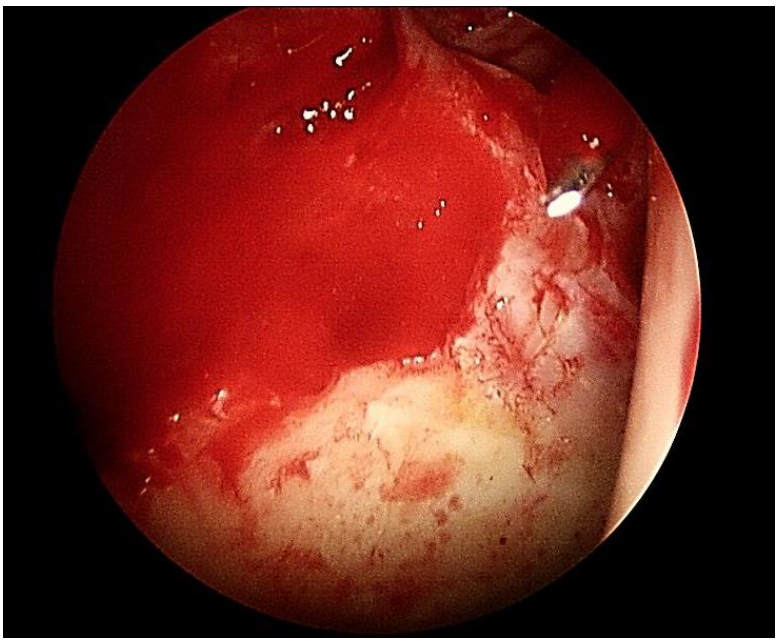

Figure 2: Intraopertive arthroscopic picture of right hip with acetabular chondral defect. The defect is covered with scaffold-blood mixture

This is a post-peer-review, pre-copyedit version of an article published in *Knee Surgery, Sports Traumatology, Arthroscopy* journal. The final authenticated version is available online at DOI: https://doi.org/10.1007/s00167-020-06068-4

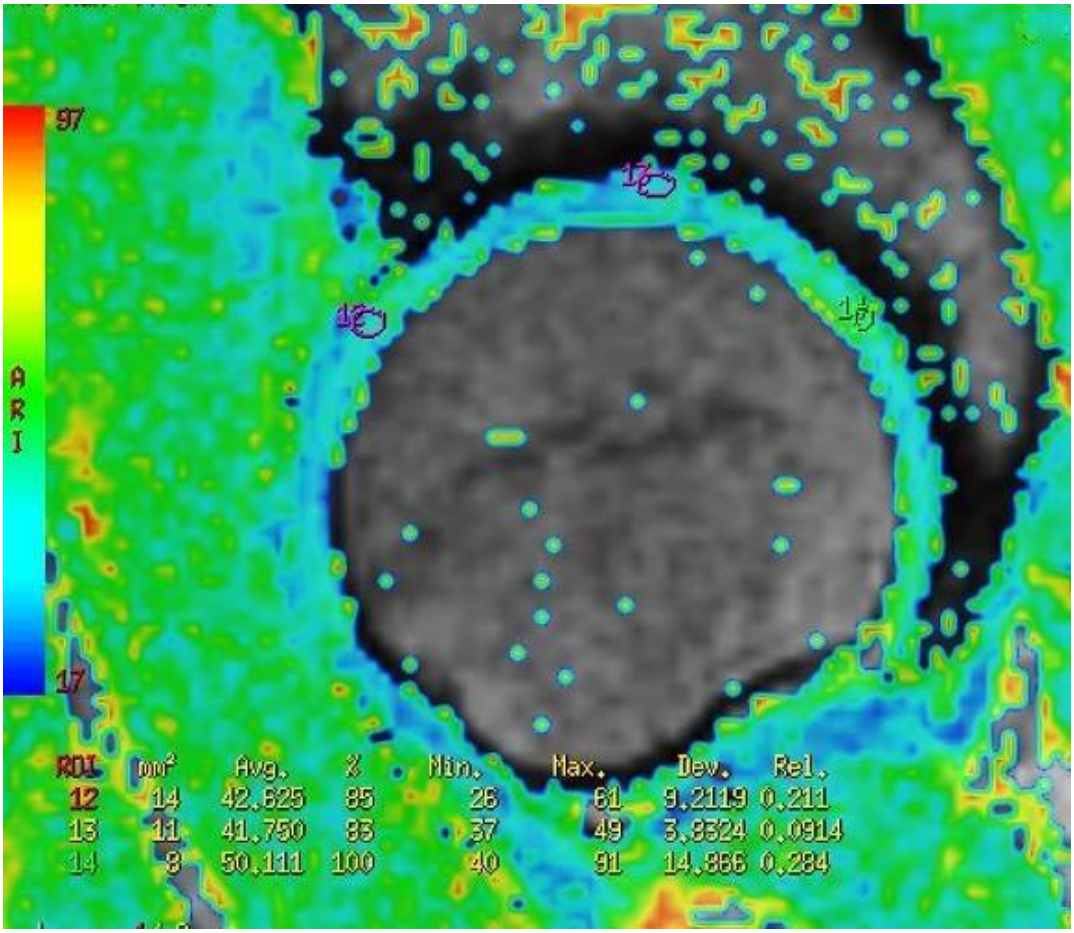

Figure 3: Postopertive MRI study of right hip with acetabular chondral delamination after treatment with chitosan-based scaffold . Sagittal T2 mapping image with 3 ROIs and corresponding T2 values.